



**MARISA CÉLIA DA  
SILVA RESENDE DA  
COSTA**

**Estudo de azulejos do século XIX e  
desenvolvimento de réplicas**

**Study of 19<sup>th</sup> century wall tiles for technical replicas  
development**









**MARISA CÉLIA DA  
SILVA RESENDE DA  
COSTA**

**Estudo de azulejos do século XIX e desenvolvimento  
de réplicas**

**Study of 19<sup>th</sup> century wall tiles for technical replicas  
development**

Tese apresentada à Universidade de Aveiro para cumprimento dos requisitos necessários à obtenção de grau de Doutor em Engenharia Civil, realizada sob a orientação científica da Doutora Ana Luísa Lomelino Velosa, Professora Auxiliar do Departamento de Engenharia Civil da Universidade de Aveiro e coorientação do Doutor Paulo Barreto Cachim, Professor Associado do Departamento de Engenharia Civil da Universidade de Aveiro e do Doutor João Paulo Coroado, Professor Coordenador do Instituto Politécnico de Tomar.



## **o júri**

presidente

**Professor Doutor Domingos Moreira Cardoso**

Professor Catedrático do Departamento de Matemática da Universidade de Aveiro

**Professor Doutor Fernando Joaquim Fernandes Tavares Rocha**

Professor Catedrático do Departamento de Geociências da Universidade de Aveiro

**Doutor João Manuel Caldas de Oliveira Mimoso**

Investigador Principal com Habilitações do Laboratório Nacional de Engenharia Civil

**Doutora Maria do Rosário da Silva Veiga**

Investigadora Principal com Habilitações do Laboratório Nacional de Engenharia Civil

**Doutora Ana Luísa Pinheiro Lomelino Velosa**

Professora Associada do Departamento de Engenharia Civil da Universidade de Aveiro

**Doutor João Paulo Pereira de Freitas Coroado**

Professor Coordenador do Instituto Politécnico de Tomar

**Doutora Eduarda Maria Martins Moreira da Silva Vieira**

Professora Auxiliar da Escola de Artes Universidade Católica Portuguesa



With love to the memory of  
my parents and all other life  
time masters.



## **Acknowledgments**

No man stands alone and the present work is the product of my friends and good people I meet on the way kind help and support. Besides learning about Portuguese cultural patrimony, the present work reminded me the precious value of friendship and kindness as divine forms of love.

I thank to the project Azulejar and Geobiotec for the financial support.

I thank Doctor Ana Luísa Velosa, Doctor Paulo Cachim and Doctor João Coroado for their precious orientation and teaching.

I thank ACRA, in the person of Doctor Isabel Ferreira, all the samples supplied for the present study, together with their technical sheets, concerning building localization and degradation conditions. I also thank Isabel Ferreira her kind teaching and friendship.

I thank Maria João Bastos, Celeste Azevedo, João Carlos Graça and Doctor Iuliu Bobos for their goodwill and kindness.

I thank Professor Doctor Celso Gomes, a lifetime master.

I thank Professor Doctor Fernando Rocha for all his support, understanding, human sensitivity and respect, making most of the research done in the present work possible.

I thank to my good friends, Cristina Sequeira, Marta Ferro, Manuela Jorge, Cristina Rosete, Odete Cartaxo, Paula Torres, Susana Olhero, Liliane Ribeiro, Tiago Silva, which supported me with friendship and technical help.

I thank to my husband, my daughter and my sister for their constant understanding and love.



**palavras-chave**

fachada, azulejo século XIX, patologias, matérias-primas, réplicas

**resumo**

O principal objectivo deste trabalho foi sistematizar características físico-químicas dos azulejos para conservação e restauro de fachadas azulejares da cidade de Ovar, pertencentes à fase produtiva da semi-industrialização e industrialização dos finais do século XIX inico do século XX, de forma a produzir réplicas técnicas para recolocação nos locais de fachada com lacunas de azulejo.

Além de se ter criado uma base de dados sobre estes materiais, formularam-se réplicas para os corpos cerâmicos calcários e *pó de pedra*, sugerindo matérias-primas e grau de moagem para a sua formulação, pressão de prensagem, ciclo e temperaturas máximas de cozedura conferindo-lhes características técnicas para que estas possam ser aplicadas lado a lado com os azulejos seculares, sem que perturbem a unicidade técnica da fachada.

Investigaram-se duas das patologias mais recorrentes que afectam o vitrado: destacamento por cristalização de sais e fendilhamento. A primeira afecta a perda da parte pictórica do azulejo, atirando-o para uma remoção compulsiva da fachada aquando da sua intervenção para conservação restauro. A segunda permite-nos compreender possíveis compromissos técnicos feitos no passado.



**keywords**

facade, 19<sup>th</sup> century wall tile, pathology, raw-materials, replicas.

**abstract**

The main objective of this work was to systematize physic-chemical characteristics of tiles removed for conservation and restoration of façades in the city of Ovar, belonging to the productive stage of semi industrialisation and industrialisation in late 19<sup>th</sup> century beginning of 20<sup>th</sup> century, in order to produce technical replicas to be used in façades gaps.

Besides creating a database on these materials with an inexistent extension in Portugal, it was also achieved the lab production of replicas for ceramic bodies of calcitic tiles and *pó de pedra*, suggesting raw materials and its particle size, pressing pressure, maximum temperatures and firing cycle, assuring technical characteristics so that they can be applied alongside the secular tiles without disturbing the technical harmony behaviour of the facade.

Two of the most recurrent pathology affecting the glaze were investigated: glaze detachment promoted by salts crystallization and crazing. The first affects the loss of the tile waterproof decoration, throwing it to a compulsory removal of the facade at its intervention for restore and conservation. The second allows us to understand possible technical commitments made in the past.



## List of Publications

---

1. Bonding layer between glaze and ceramic body in 19/20<sup>th</sup> century Portuguese tiles  
Marisa Costa, A.L. Velosa, P. Cachim, A.B. Lopes, M. Ferro  
13<sup>th</sup> Euroseminar on Microscopy Applied to Building Materials  
14-18 June 2011, Ljubljana, Slovenia.  
ISBN: 978-961-90366-6-2
2. Exterior wall tiles pathologies.  
Marisa Costa, P. Cachim, A. L. Velosa  
Patorreb 2012 – 4<sup>o</sup> Congresso de patología e rehabilitación de edificios  
12-14 April 2012, Santiago de Compostela, Spain  
ISBN: 978-84-96712-49-2
3. Raw materials of Portuguese ceramic tiles produced in Oporto region in late 19<sup>th</sup> early 20<sup>th</sup> century.  
Marisa Costa, P. Cachim, J. Coroado, A.L. Velosa  
Azulejar 2012 – Conservação de Revestimentos Azulejares em Fachadas  
10-12 October 2012, University of Aveiro, Portugal  
ISBN: 978-989-98041-1-1
4. Definition of Firing temperature of XIX century tiles  
Marisa Costa, P. Cachim, J. Coroado, A.L. Velosa  
EMAC 2013 – European Meeting on Ancient Ceramics  
19-21 September 2013, University of Padua, Italy
5. Ancient wall tiles- The importance of the glaze/ceramic interface in glaze detachment  
Marisa Costa, P. Cachim, J. Coroado, F. Rocha, A. Velosa  
Materials Science – Paper accepted for publication  
ISSN: 1392-1320



## Contents

---

List of Figures .....	v
List of Tables .....	ix
Glossary .....	xi
Chapter 1 .....	1
Introduction.....	1
1.1 Foreword.....	3
1.2 Research Objectives .....	4
1.3 Structure of the thesis .....	5
References .....	7
Chapter 2.....	9
Bibliographic review.....	9
2.1 The tile - Concepts.....	11
2.2 Historical framing.....	11
2.2.1 Introduction of tile in Portugal .....	11
2.2.1.1 Alicatado .....	12
2.2.1.2 Corda-seca technique .....	13
2.2.1.3 Aresta (or Cuenca) technique.....	13
2.2.1.4 Majolica technique.....	15
2.2.1.5 Semi-industrial tiles .....	17
2.3 The tile in Portugal .....	20
2.3.1. National manufacturing units that supplied tiles for 19 <sup>th</sup> century facades .....	23
2.3.2 Ceramic body types and their raw materials .....	29
2.3.3 Glaze types. Glaze raw materials .....	33
2.4 Tiles processing .....	35
References .....	44
Chapter 3.....	49
Materials and methods .....	49

3.1 Materials .....	51
3.1.1 Raw materials used.....	51
3.1.1.1 Kaolin.....	51
3.1.1.2 Quartz sand .....	53
3.1.1.3 Ball clay .....	54
3.1.1.4 Calcite .....	55
3.1.1.5 Talc .....	56
3.2.2 Samples used.....	57
3.2 Methods .....	59
3.2.1 Samples in powder .....	59
3.2.1.1 X-ray diffraction – XRD .....	60
3.2.1.2 X-ray fluorescence - XRF .....	64
3.2.1.3 Fourier-Transformed infrared spectroscopy - FTIR .....	66
3.2.1.4 Thermogravimetry (TGA) and Differential Scanning Calorimetry (DSC) .....	69
3.2.1.5 Particle size distribution.....	69
3.2.2 Techniques that require samples without glaze and tile back .....	71
3.2.2.1 Dilatometry .....	71
3.2.2.2 Calcination tests .....	72
3.2.3 Entire tile observation techniques .....	73
3.2.3.1 Scanning Electron Microscopy and Energy Dispersive Spectroscopy - SEM and EDS .....	73
3.2.3.2 Optical microscopy .....	74
3.2.3.3 Porosimetry .....	75
3.2.3.4 Water absorption.....	76
3.2.3.5 Water absorption coefficient due to capillary action .....	77
3.3 Replicas pallets preparation.....	78
References .....	79
Chapter 4.....	81
Results and discussion .....	81
4.1 Introduction to experimental work .....	<b>83</b>
4.2 19 <sup>th</sup> century tiles characterization .....	86
4.2.1 Ceramic body .....	86
4.2.1.1 X- ray diffraction analysis .....	88

4.2.1.2 X-ray fluorescence analysis .....	91
4.2.1.3 Thermal Gravimetric Analysis and Fourier Transformed Infrared Spectroscopy .....	92
4.2.1.4 Calcination tests .....	97
4.2.1.5 Microstructure .....	100
4.2.1.6 Water absorption percentage.....	103
4.2.1.7 Water absorption coefficient due to capillary action and pore size determination .....	104
4.2.1.8 The importance of the glaze/ceramic body interface in glaze detachment caused by salt crystallization .....	106
4.2.1.9 Ancient tiles raw materials proposal.....	118
4.2.2 Lead glazes of the studied samples .....	121
4.2.2.1 – Optical microscope results of the glazed layer .....	126
4.2.2.2 SEM/EDS values .....	130
4.2.2.3 SEM - images of lead-tin glazes .....	133
4.2.2.4 – Experimental determination of linear expansion coefficient ( $\alpha$ ) of the ceramic bodies .....	135
4.2.2.5 - Theoretical discussion of the expansion coefficient ( $\alpha$ ) of the ancient glazes .....	136
4.3 Pathology and risk factors of the tile facades from late 19 <sup>th</sup> early 20 <sup>th</sup> century .....	140
4.3.1 Glaze detachment in old ceramic wall tiles – The influence of mortar binder ....	146
4.4. Replicas preparation and analysis.....	167
4.4.1 Contemporary tiles used in restoration.....	167
4.4.1.1 Sample 1 characterization .....	168
4.4.1.2 Sample 2 characterization .....	171
4.4.2 Ceramic body replicas suggestion.....	174
4.4.2.1 Calcitic ceramic body .....	175
4.4.2.2 <i>pó de pedra</i> ceramic body.....	178
4.4.3 Glazing of new tiles – procedure for adequate performance .....	180
References .....	184
Chapter 5.....	195
Conclusions.....	195
5.1 Conclusions .....	197

5.2 Future work.....	201
----------------------	-----

## List of Figures

---

Figure 1 - Wall tiles and pavement alicatado Sintra's Palace (Sintra 2013) .....	12
Figure 2 - Tiles produced with corda seca technique. Sintra's Palace (Sintra 2013) .....	13
Figure 3 - Example of tiles produced with aresta technique. Sintra's Palace (Sintra 2013)....	14
Figure 4 - Relief tile with grape leaves - Sintra's Palace (Sintra 2013) .....	14
Figure 5 - Tiles arrangement for firing (Aveiro 2008) .....	15
Figure 6 - Tripod marks after glaze firing (Aveiro 2008).....	15
Figure 7 - Polychromatic majolica. Panel of Odivelas Convent (Gomes 2011).....	16
Figure 8 - An example of transfer-print from the nineteenth century (Harvey 2010) .....	17
Figure 9 - An example of a metal plate used in the lithographic decoration process at Sacavém (author' photograph).....	18
Figure 10 - Example of a manual tile press (Prostes 1907).....	18
Figure 11 - Press atelier (year 1900) in the French factory Paray-le-monial created by Paul Charnoz in 1877 (Charnoz 2010).....	19
Figure 12 – Aleluia's factory (Aveiro) wind mill in 1911 (Aleluia 1955) .....	22
Figure 13 – Tile production by dry process (Aleluia 1955).....	22
Figure 14 – Example of facade with “listelo” and decorative tiles.....	23
Figure 15 – Geographic location of some of Porto most important tile factories of the 19 <sup>th</sup> century Image of the Douro River separating Porto from Vila Nova de Gaia (Soeiro, Alves et al. 1995). .....	28
Figure 16 - SEM image of a kaolinitic aggregate formed by stacking octahedral lamellar crystals of kaolinite (Senna 2008).....	32
Figure 17 - Engraving of the atelier of the presses at Sacavém in 1932 (author' photograph)36	
Figure 18- Tile image where colour difference of the ceramic body due to firing atmosphere is evident (author' photograph).....	37
Figure 19 - Scheme of a circular kiln used at Fábrica de Louça de Sacavém (author' photo) 40	
Figure 20- Interior of the kiln, the firing room (author' photo).....	40
Figure 21 – The remaining of a cone firing control (author' photo) .....	41
Figure 22 - Typical example of cones behaviour to temperature .....	42
Figure 23– Photo of a Buller ring of high temperatures (author' photo).....	42
Figure 24 – Example of <i>gazettes</i> for tile firing (author' photo).....	43
Figure 25- Existing kaolin in Portugal (Velho, Gomes et al. 1998) .....	52

Figure 26 – kaolin XRD.....	52
Figure 27 – Quartz sand XRD .....	53
Figure 28 – Ball clay XRD .....	54
Figure 29 – Calcite XRD .....	55
Figure 30 – Talc XRD.....	56
Figure 31 – Fast agate mill.....	60
Figure 32 – Electro-magnetic spectrum (Rigaku).....	60
Figure 33 – X-ray spectrum of a molybdenum tube at different KV settings (Rigaku) .....	61
Figure 34 – Characteristic radiation (Rigaku) .....	62
Figure 35 – Condition for diffraction of X-ray (Rigaku).....	63
Figure 36 – Press used to make pressed pallets .....	64
Figure 37 - Panalytical's spectrometer, Axios model .....	65
Figure 38 – Bruker Tensor 27 FTIR spectrometer.....	67
Figure 39 – Axial and angular deformation types (Nakamoto 1970) .....	68
Figure 40 – Sedigraph 5100.....	71
Figure 41 - Netzsch- DIL 402 PC dilatometer (GmbH 2005) .....	72
Figure 42 – One of the ceramic industrial kilns used .....	72
Figure 43 – Resin mounted sample for surface polishing .....	74
Figure 44 – Hitachi SU-70 high-vacuum scanning microscope .....	74
Figure 45 – Optical microscope Leica EZ4HD .....	75
Figure 46 - X-ray diffraction maxima of a calcitic ceramic body .....	90
Figure 47 – X-ray diffraction maxima of a <i>pó de pedra</i> ceramic body .....	91
Figure 48 – TGA of P89 sample .....	93
Figure 49 – TGA from P127 sample.....	93
Figure 50 – TGA from P133 sample.....	94
Figure 51 - Sample 24 FTIR spectrum .....	95
Figure 52 – P24 XRD maximum diffraction, presenting calcite and portlandite .....	96
Figure 53 - XRD of P24 after calcination at 1040°C where calcite and portlandite main diffraction maximums are not found.....	97
Figure 54 – Aspect of P104 over-fired sample at 1150°C .....	98
Figure 55 – X-ray diffraction maxima of P104 fired piece .....	99
Figure 56 – X-ray diffraction pattern after P104 piece being calcined at 1150°C.....	100
Figure 57 - P10 ceramic body and glaze.....	101
Figure 58 – P89 ceramic body ang glaze, a closer look.....	101

Figure 59 - P10 ceramic body heterogeneities .....	102
Figure 60 – P89 ceramic body with salt crystals .....	102
Figure 61 – P133 ceramic body with salt crystals .....	103
Figure 62- Typical pore size distribution assessed in the studied samples. <i>pó de pedra</i> the curve on the left and calcitic body on the right.....	105
Figure 63 – An example of <i>pó de pedra</i> and calcitic ceramic bodies water absorption due to capilar action curves .....	106
Figure 64 – SEM image of interface glaze/ceramic body of a contemporary tile (HC).....	113
Figure 65 – HC interface glaze/ceramic body closer look.....	113
Figure 66 – Volume of mercury intrusion data in 3 samples (P127, HC and P133) .....	115
Figure 67 – A SEM cut view where can be seen a fracture beneath the glaze of P133.....	116
Figure 68 – Salts beneath the glaze of P133 .....	116
Figure 69 – EDS of the crystals marked in Figure 5.....	116
Figure 70 – A SEM view of the surface that suffered from glaze detachment.....	117
Figure 71 – Example of crazing suffered by all <i>pó de pedra</i> tiles’ glazes.....	128
Figure 72 – Example of an opaque glaze in a perpendicular view .....	129
Figure 73 – Example of a calcitic tile with double glaze layer.....	130
Figure 74 – Sum up of the value of Si, Pb, K, Ca, Al and Na in the studied glazes.....	132
Figure 75 – Tin oxide cristalization in an opaque glaze (P24) .....	134
Figure 76 - P10 SEM glaze surface observation where chemical attack can be seen .....	134
Figure 77 - SEM observation of the upper part of the P133 tile, were once the glaze was. Instead, salt crystals can be seen.....	135
Figure 78 – Tiles with pores and associated pathology .....	141
Figure 79 – Example of glaze crazing (on the left side) and glaze detachment by glaze crazing (on the right).....	142
Figure 80 – Example or glaze crazing provoked by persistent humidity .....	142
Figure 81 - Colour detachment due to a poor colour/glaze thermal expansion coefficient adjustment .....	143
Figure 82– Examples of tile perimeter glaze detachment .....	144
Figure 83 – Examples of lack of mortar/tile adherence .....	144
Figure 84 – Example of glaze detachment caused by salt crystallization .....	145
Figure 85 – Example façade and tile suffering from glaze detachment .....	146
Figure 86 – Efflorescence and crypto-florescence example (Scherer 1999).....	148

Figure 87 – Polarized optical microscope microphotographs of: a)Santa Pudia limestone (SP), b)Fraga limestone (CF), c)Bonar dolostone (DB), d)travertine from Albox (TA), e)Uncastillo sanstone (AU), f)Villaviciosa sanstone (AV)(E.Molina, G.Cultrone et al. 2011).....	150
Figure 88 - Mercury intrusion porosimetry data (continuous line) of studied samples by Molina (E.Molina, G.Cultrone et al. 2011).....	151
Figure 89 - Mercury intrusion porosimetry of some of the old tiles studied .....	152
Figure 90 - Glaze detachment in the tile borders caused by salt crystallization.....	153
Figure 91 – P24 XRD, where calcite and portlandite main diffraction maximums can be seen .....	159
Figure 92 – P89 ceramic body with numerous calcium crystallizations .....	162
Figure 93 – EDS of the crystals .....	162
Figure 94 – Crystallized salts in the ceramic body/glaze interface, provoking structural rupture .....	163
Figure 95 – Path of destruction made by salt ascension .....	164
Figure 96 – Microstructure of a tile never used .....	165
Figure 97 – Sample 1 XRD.....	168
Figure 98 – Sample 1 microstructure.....	170
Figure 99 – Sample 1 glaze and ceramic body SEM observation. Sample in fracture.....	170
Figure 100 – Old tile glaze and ceramic body SEM observation. Sample in fracture.....	171
Figure 101 – Sample 2, XRD.....	172
Figure 102 – Samples 2 microstructure .....	173
Figure 103 – Calcitic replicas firing curve .....	176
Figure 104 – Sample 2 glaze fracture due to cutting .....	180
Figure 105 – Engobe and glaze thickness seen by optical microscope .....	182

## List of Tables

---

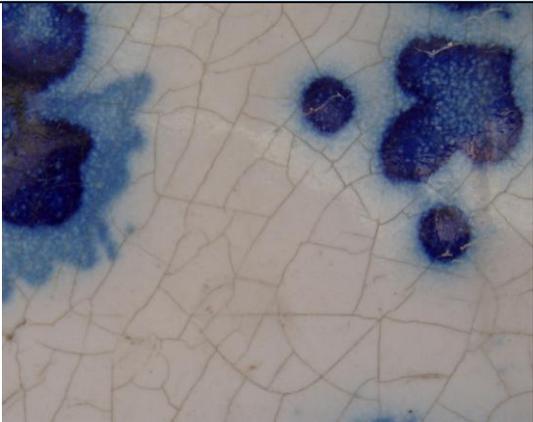
Table 1- Chronology of tile in Portugal (Azulejo 2012).....	20
Table 2- Some of the most important Portuguese factories of XIX century .....	24
Table 3 – Chemical results obtained by Lepierre to A.A.Costa and J.P.Valente tiles (Lepierre 1899) .....	31
Table 4 -Chemical compositions of white glazes from 17 <sup>th</sup> century (Coentro 2011).....	34
Table 5- Calorific power of some combustible materials (Tabelas 2010).....	39
Table 6 – Kaolin XRF values.....	53
Table 7 – Quartz sand XRF values .....	54
Table 8 – Ball clay XRF values .....	55
Table 9 – Calcite XRF values .....	56
Table 10 - Talc XRF values .....	57
Table 11 – Tile references, pictures and production units of the studied samples .....	57
Table 12– Typical high temperature crystalline phases present in the samples under study ..	89
Table 13 – Chemical analysis data of the studied samples, obtained by XRF .....	92
Table 14 – P89, P127 and P133 weight losses analyses from TGA data .....	94
Table 15 – Calcination results of some calcitic samples .....	98
Table 16 - Water absorption percentage of the 26 studied samples .....	104
Table 17 - Values for water absorption coefficient due to capillary action.....	106
Table 18 – Tile pictures and references .....	108
Table 19 – SEM images of the glaze, interface area and ceramic body of the studied samples .....	109
Table 20 – EDS wt% values of the chemical elements present in the glaze, interface and ceramic body of the studied samples .....	110
Table 21 – Elementary EDS photos of P133 (Al, Na, K) .....	111
Table 22 – Average interface values observed in the analysed samples .....	112
Table 23 – Water absorption of the studied samples .....	114
Table 24 – Summary of the observations made by optical microscope in the samples glazes .....	127
Table 25 – EDS area analyses (wt %) obtained in 14 of the studied samples .....	131
Table 26 – Linear expansion coefficient of 6 samples of ancient ceramic bodies .....	136
Table 27 – Appen oxide factors (Renau 1994) .....	137

Table 28 – Comparing theoretical glaze $\alpha$ with experimental ceramic bodie’s $\alpha$ .....	138
Table 29 – Some average weather values in Oporto from 1901 to 1990 (Ferreira 2009) .....	154
Table 30 - Some Ovar’s average weather data from 2007 to 2011(Monteiro 2012).....	155
Table 31 – Samples pictures and references .....	157
Table 32 – XRF of the main oxides of the studied samples .....	160
Table 33 – Water absorption of tile samples before and after calcinations at 1000° C .....	161
Table 34 - Sample 1 XRF values .....	169
Table 35 – Sample 1, water absorption due to capillary action and percentage .....	169
Table 36 – Sample 2 XRF values .....	172
Table 37 - Sample 2, water absorption due to capillary action and percentage.....	173
Table 38 – Chemical analysis data of the raw materials used in the replicas preparation.....	175
Table 39 – Results of the studied samples and replicas after firing.....	177
Table 40 – Analytical results of the stoneware replicas after firing at 1235°C .....	179
Table 41 – Sample 3 ceramic body and glaze results .....	181

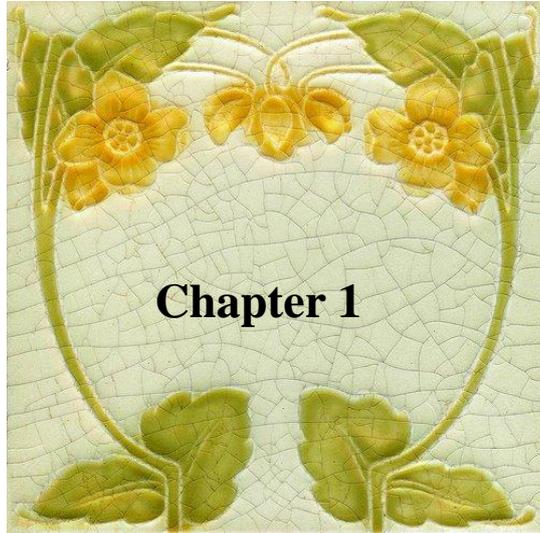
# Glossary

Glossary	Definition	Photographic examples
<p>Tiles's back face</p>	<p>It is the tile part that stays in contact with the mortar, opposite face of the glazed one</p>	
<p>Ceramic body</p>	<p>The porous body that is under the glaze</p>	
<p>Glaze</p>	<p>The visible part of the tile when placed in the wall. It is characterized by the gloss, water proof capacity and colour. Holds the decoration pattern</p>	
<b>Production defects</b>		
<p>Ceramic body bending</p>	<p>The ceramic body is not completely flat presenting bending due to production problems (pressing, drying or glaze tensioned)</p>	

<p>Crater</p>	<p>Very big pin holes and less numerous</p>	
<p>Crack</p>	<p>Ceramic body separation. Pressing, drying or firing defect.</p>	
<p><b>Panel defects</b></p>		
<p>Glaze detachment</p>	<p>The glaze comes out leaving the ceramic body exposed</p>	
<p>Tile detachment</p>	<p>Tile separation from the holding mortar</p>	

<p>Tile lacunae</p>	<p>Tiles fell down after tile detachment</p>	
<p>Structural crack</p>	<p>Cracks on the tiles provoked by the building structural movements</p>	
<p>Staining</p>	<p>Stains promoted by the presence of micro-organisms that lie under the transparent glaze</p>	
<p>Mix Factors</p>		
<p>Glaze crazing</p>	<p>The glaze cracks due to stresses between the glaze and the ceramic body. This can be due to a bad thermal expansion coefficient agreement between them or by moisture expansion of the ceramic body.</p>	





## **Introduction**

---



## 1.1 Foreword

The use of tiles (whether inside or outside the buildings) is almost a brand in Portuguese historic architecture, expressing a national taste for colour and for the picturesque. Its widespread use since the late 19<sup>th</sup> century transformed the country into a huge open-air museum, which now displays all sorts of pathology needing multidisciplinary technical intervention.

The tiles applied on the outside of buildings, subjected for more than a century to the rigors of weather variations, suffer from specific pathology of porous materials (Flatt 2002, E.Molina, G.Cultrone et al. 2011, Santos, Vaz et al. 2012). In this way, there is a vast field of work in art conservation and restoration, which up to now has often been performed without a proper backup of scientific knowledge. This study should encompass knowledge of the materials subjected to weathering during tens of years, compatibility between old and new materials and suitability of new materials to weathering exposure.

Tile manufacture in Portugal began in the 16<sup>th</sup> century. At this time tiles were totally manufactured and thus only affordable to the clergy, royalty or nobility. From this time until the beginning of semi-industrialization, which took place in the second half of the 19<sup>th</sup> century, the Portuguese tiles were hand painted, usually with figurative themes frequently of colossal dimensions. With the price reduction possible by semi-industrial and industrial production, their use became possible for the medium and high classes who started its widespread use in houses' facades as aesthetic and lasting solutions.

Although Portugal has been one of the most active countries in Europe in the use of tiles, little is known about the technical outlines of this production. A slight analysis is not enough to deeply evaluate the materials that resist the passing of time, and there is need of the application of laboratory technologies to formulate hypotheses and seek explanations in the context of art history, in its more technical aspects, as well as in the decision of the methodologies to be used in interventions of preservation of old materials.

A literature survey reveals that it normally deals with historical-artistic considerations covering only the features and chemical-mineralogical nature of the glassy surface. There are some historical studies such as those performed by Leão (Leão 1999) Veloso (Veloso 2009), Ana Domingues (Domingues 2003), Isabel Ferreira (Ferreira 2009), but on manufacturing process and factories, considerations were only found in Mariz (Ferreira 2009) and Fernandes (Fernandes 2008). In studies performed by Thais (Sanjad, Rômulo Simões et al. 2004) and

Cristiane (Silva, Silva et al. 2006) chemical and mineralogical studies of ceramic body in a small number of semi-industrial period of Portuguese tiles applied in Brazil can be found, with a proposal of some of the raw materials and of a very wide range of probable firing temperatures. In these works there is no information about the source of tiles (productive area, country, and factory). Clearly the most exhaustive work on the chemical characteristics of late 19<sup>th</sup> century tile production in Portugal belongs to Lepierre (Lepierre 1899) .

The awareness of the importance of the restoration of the built heritage is increasingly urging for lasting technical answers that do not contribute to the de-characterization of buildings nor to the emergence of serious pathological manifestations by promoting the acceleration of the deterioration of pre-existing elements (Veiga and Aguiar 2002). Therefore, it is necessary to produce technical replicas to replace the missing or destroyed tiles, adapted to the existing buildings.

Considering the importance and the lack of knowledge existing in this field, several experimental techniques were used aiming to fully characterize chemical composition (x-Ray fluorescence - XRF, Scanning Electron Microscopy with Energy Dispersive Spectroscopy – SEM/EDS) crystalline phases (x-Ray diffraction -XRD, Fourier Transformed Infrared Spectrometry - FTIR), microstructure (SEM/EDS), porous network (water absorption coefficient due to capillary action, pore size determination by mercury intrusion and percentage of water absorption), thermal linear expansion coefficient (dilatometry), salt crystallizations (Thermal Gravimetric Analysis - TGA, SEM/EDS, XRD, FTIR) and glazing technology (optical microscope).

## **1.2 Research Objectives**

The present work has the main aim of obtaining ceramic bodies' technical replicas with physical and chemical characteristics similar to those of old ceramic bodies' tiles. The tiles used for this study come from the city of Ovar facades, a city already aware of the value of this heritage. The tiles provided are mostly of the facades of the homes of the middle or upper-middle classes, from the factories of Vila Nova de Gaia (A.A.Costa and J. Pereira Valente). Some of the studied tiles are not branded and so were classified as belonging to an unknown production unit.

With the results of the systematic study of the physical and chemical characteristics of 19<sup>th</sup> century northern factories A.A Costa, J. Pereira Valente and of some northern unbranded tiles the aim of this research was to:

1. understand the composition of the ceramic bodies and differences among them;
2. suggest the ceramic body raw materials possibly used at the time;
3. characterize the glazes used in the 19<sup>th</sup> century northern factories A.A Costa, J. Pereira Valente and some northern unbranded tiles, as well as that from a Sacavém tile. Based on this characterization, suggest causes of glaze crazing, a common pathology;
4. attain a deeper insight on calcite crystallization in the ceramic as there are calcite crystals in the ceramic bodies, the provenance of which is not clear;
5. propose actual raw-materials, their grinding level as well as their percentages in the ceramic body, pressing pressure and firing enthalpy so that ceramic body technical replicas can be produced. In the present work, replicas of the ceramic body are considered as being nowadays produced ceramic bodies with crystalline phases, chemical composition, water absorption percentage and water absorption due to capillary rise, as similar as possible from the old tiles. It is believed that if old ceramic bodies' technical characteristics are achieved, replicas will have a harmonious behaviour with the rest of the tiles in the façade preventing further unnecessary degradation that inadequate replicas might cause.

### **1.3 Structure of the thesis**

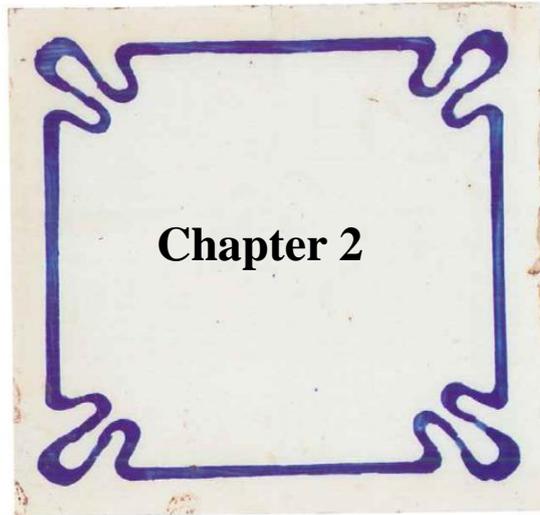
This dissertation is structured in five chapters. Chapter 1 presents a brief introduction to the thesis, the research objectives and the thesis structure. Chapter 2 provides a literature review and some technical considerations related to tile production. The analytical techniques used in the research are described in Chapter 3. The outcome of all the analytical work performed to attain the proposed objectives and its discussion can be seen in Chapter 4. The overall conclusions of the research work and future directions are presented in Chapter 5.

There is a second volume in the present thesis containing the characterization files for each of the studied tiles, including building photos, location, facade pathology and all the analytical results obtained. This work is in Portuguese as its aim is to serve the practical work performed at ACRA, as consulting data and provide a wider basis of knowledge in terms of ceramic tiles' characteristics.

## References

- Domingues, A. M. P. (2003). António Almeida da Costa e a Fábrica de Cerâmica das Devesas. Master, Universidade do Porto.
- E.Molina, G.Cultrone, E.Sebastián and F.J.Alonso (2011). "The pore system of sedimentary rocks as a key factor in the durability of building materials." Engineering Geology 118: 110-121.
- Fernandes, I. M. (2008). A Fábrica de Louça de Miragaia. Instituto dos Museus e da conservação. Lisboa.
- Ferreira, L. M. (2009). O azulejo na arquitectura da cidade do Porto [1850 - 1920]. Caracterização e intervenção. Doutoramento, Universidade do País Vasco.
- Ferreira, M. I. M. (2009). Azulejos tradicionais de fachada em Ovar contributos para metodologia de conservação e restauro. Ovar, Camara Municipal de Ovar.
- Flatt, R. J. (2002). "Salt damage in porous materials: how high supersaturation are generated." Journal of crystal growth 242: 435-454.
- Lepierre, C. (1899). Estudo chimico e tecnologico sobre cerâmica portugueza moderna, Imprensa nacional. Lisboa
- Leão, M. (1999). A cerâmica em Vila Nova de Gaia. Edições Manuel Leão. Gaia
- Sanjad, T., A. Rômulo Simões, M. Mendonça de Oliveira and W. A. d. M. Costa (2004). "Caracterização mineralógica de azulejos de Salvador e Belém dos séculos XVI, XVII e XIX." Revista Esc. Minas 57(4).
- Santos, T. P., M. F. Vaz, M. L. Pinto and A. P. Carvalho (2012). "Porosity characterization of old Portuguese ceramic tiles." Construction and Building Materials 28: 104-110.
- Silva, C. P. d., M. F. Silva and R. S. Angelica (2006). Azulejos históricos europeus produzidos no final do século XIX e início do século XX: caracterização mineralógica e química de biscoitos. XVII seminário de iniciação científica da UFPA. Brasil.
- Veiga, R. and J. Aguiar (2002). "Revestimentos de paredes em edifícios antigos." Cadernos de edifícios - LNEC 2.
- Veloso, A. J. d. B. (2009). Azulejos semi-industriais de fachada. I. Almasqué. Curso de história do azulejo - Cinco séculos de presença em Portugal. Museu Nacional do Azulejo. Lisboa





## **Bibliographic review**

---



## **2.1 The tile - Concepts**

The tile is a building material and decorative element composed by two types of materials: the ceramic body and the glaze. Due to the presence of the glaze, this wall coating material not only is very durable and needing low maintenance but it also allows an aesthetic utilization.

Tiles can be differentiated by the body ceramic type and by the type of glaze and decoration.

Typically tiles were produced by bi-firing process. Bi-firing consists in a first firing of the ceramic body and a second firing, at a lower temperature than the first, to fire the glaze. The first firing was done to promote gaseous releases associated with the raw materials of ceramic body constituents' decomposition, in order to decrease the amount of glass defects, in particular the emergence of pinholes and lack of brightness and to provide mechanical strength and porosity necessary for the application of the glaze. The second firing, usually made a few tens of degrees below the first firing, was necessary to promote the glazing, its adherence to the ceramic body and adherence of the possible existing colours of the decoration to the glaze.

## **2.2 Historical framing**

### **2.2.1 Introduction of tile in Portugal**

Archaeology gives the possible hypotheses about the occurrence of utensils and artefacts in humankind's existence. Although it is already possible to date the findings that belonged to our ancestors, there are possibly still many issues to discover and maybe it is not still known exactly where and when the tile art began. However it is known that tiles oldest pieces, found until now, date back to five thousand years BC. These findings in excavations in Egypt were used in tile murals. Until the 6th century A.C. the Assyrians and the Babylonians manufactured bricks and painted tiles with colourful figures. In about 600 of our era the Arabs also adopted such methods, upgrading them with a new technique that was the

application of lustre with different colours of metallic aspect. It was the Arab invasion of Spain that introduced tiles manufacture and use in buildings and this then spread across Europe (Veloso 2009).

It was by the hand of the King D. Manuel (late 15<sup>th</sup> century) that the use of the wall tiles was initiated in Portugal, after a journey he made to Spain. This monarch imported Spanish-Moorish tiles and decorated his residence, Sintra National Palace, in a similar fashion as the used in the neighbouring country. Portugal imported tiles until the mid 16<sup>th</sup> century, when tile workshops were created (Sintra 2013).

### 2.2.1.1 Alicatado

*Alicatado* is the oldest technique applied in Portugal. It was imported to be used for the first time in Portugal, at Sintra's Palace. The ceramic body was hand-moulded and each tile was monochromatic. The geometric forms used at the time, were achieved by cutting the tiles with different colours, with different sizes and geometric shapes and grouping pieces together. The name of this technique is due to the cutting process, as it was done with the help of a pair of pliers (*alicatado* process) (Sintra 2013).

This technique was popular in the 16<sup>th</sup> and 17<sup>th</sup> centuries, but was replaced by other techniques because its application not only required the craftsman to follow the order to the place of its application but it was also a very slow process (Gomes 2011). Figure 1 shows two examples of tiles produced under the explained technique.

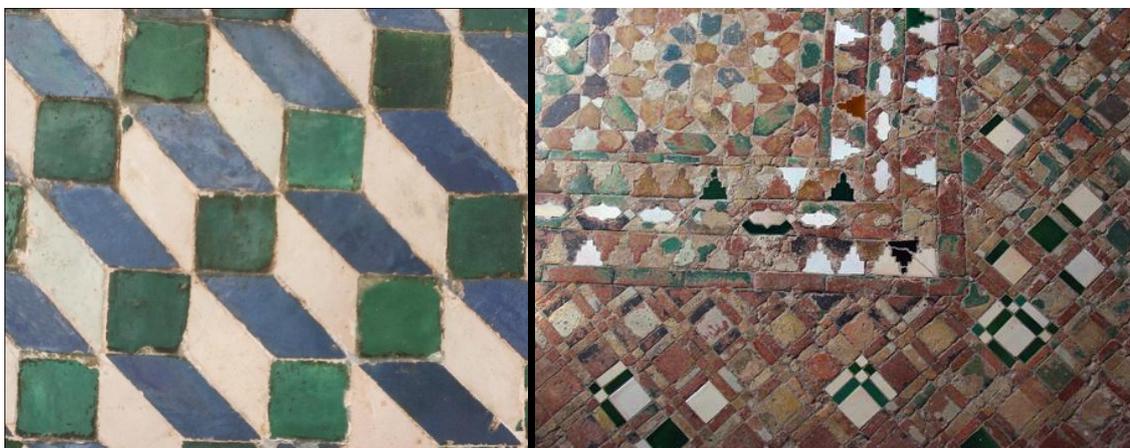


Figure 1 - Wall tiles and pavement alicatado Sintra's Palace (Sintra 2013)

### 2.2.1.2 Corda-seca technique

Corda-seca technique is a technique amply used in the late 15<sup>th</sup> century, early 16<sup>th</sup> century. This technique consists in the engraving of the design in the wet ceramic by making grooves that were filled in with manganese mixed with a fat, ensuring the separation of the different water soluble colours, during application and firing (Gomes 2011). Figure 2 depicts an example of *corda seca* technique imported from Spain to Sintra Palace.

This technique almost always presented a mechanical barrier separating the different areas of the different colour glazes (Veloso 2009). The main producers of this kind of tile in the Iberian Peninsula were Seville, Valencia, Malaga and Toledo (Sintra 2013)(Sintra 2013)(Sintra 2013)(Sintra 2013).



Figure 2 - Tiles produced with corda seca technique. Sintra's Palace (Sintra 2013)

### 2.2.1.3 Aresta (or Cuenca) technique

In Aresta (or Cuenca) technique the separation of colours was done by engraving the design on the wet ceramic body with the help of a wooden or metal mould, leaving the defined design lines in the form of edges (aresta in Portuguese). The edges allowed, as in *corda seca*, the separation of the coloured glazes during firing (Figure 3). *Aresta* technique was the logical step after *corda seca* allowing price reduction because it permitted higher production quantities, but also allowed more freedom in the type of design (Gomes 2011) .



Figure 3 - Example of tiles produced with *aresta* technique. Sintra's Palace (Sintra 2013)

This technique was used in Portugal, where a very creative variant was used. This creation (called the relief tile) consists of a pattern with grape leaves in relief (Figure 4). There are also rare examples with metallic reflection achieved after a third firing of an alloy of silver and bronze (Veloso 2009).



Figure 4 - Relief tile with grape leaves - Sintra's Palace (Sintra 2013)

*Corda seca* and *aresta* tiles techniques of the late 15<sup>th</sup> century and early 16<sup>th</sup> century, remained in History under the name *mudejares*, Hispanic- Arab or Hispano-Moorish. During the sixteen century they were imported in large quantities to Portugal and applied in churches and palaces.

This technique requires a homogeneous and stable ceramic body which, after a first firing (*chacote*), is covered with a slip of glaze. For the second firing (already with the glaze

applied) the tiles were placed horizontally in the kiln, built in small pottery tripods as in Figure 5.



Figure 5 - Tiles arrangement for firing (Aveiro 2008)

These tripods marked three points in the glaze, clearly seen in Figure 6, important nowadays in the evaluation of authenticity.



Figure 6 - Tripod marks after glaze firing (Aveiro 2008)

#### **2.2.1.4 Majolica technique**

At the end of the 16<sup>th</sup> century decisive technological progress known by the name of *majolica* emerges (example in Figure 7). In this revolutionary process, direct painting on the white tin glazes with metallic colours became possible, without the use of physical separators between the colours, which was a process that delayed and turned the production process more expensive (Gomes 2011) .



Figure 7 - Polychromatic majolica. Panel of Odivelas Convent (Gomes 2011)

Produced in the form of various objects such as tableware, vases, sculptures and tiles, the majolica ceramic body underwent a first firing to ensure technical performance and achieving porosity and mechanical strength achieved in order to absorb the glaze slip and resist decoration application.

The white glaze was composed by tin, silica, lead and sodium carbonate . The opacity and the whiteness of these glazes was due to the tin oxide particles spread in the glaze (Coentro 2011).

In the 15<sup>th</sup> century, Florence became the main producer of majolica, combining the technical advances of the Renaissance with a renewal of aesthetic modelling and decoration.

In Portugal, the glazes and metallic oxides raw materials for the decorations were usually imported from the United Kingdom (Leão 1999, Ferreira 2009).

### 2.2.1.5 Semi-industrial tiles

It was the British who established the dividing line between the craft processes and the semi-industrial and industrial era. In 1758 an invention by John Sadler was responsible for the first production revolution by making decoration process by the called *transfer printing*. The name of this technique, still used nowadays, derives from the process of transferring the decoration from a copper plate to paper and then to the tile surface.

Using available handmade white tin glazed delftware tiles, John Sadler applied the newly developed method of printing on ceramics to tiles. This printing method allowed for an image engraved onto a copper plate or cut from a wood block to be transferred to a tile using paper or a glue bat. The image could then be fired at a relatively low temperature for a very brief time (15 minutes). This method had the obvious advantage of hastening production both in decoration and firing. However, since the decoration was placed atop the tin glaze it was subsequently much less durable and subject to wear (Harvey 2010).

Once Sadler states “without the aid or assistance of any person or persons, did, within the space of six hours, to wit, betwixt the hours of nine in the morning and three in the afternoon of the same day, print upwards of twelve hundred earthenware tiles of different patterns, at Liverpool aforesaid, and which as these dependents have heard and believe, were more in number and better and neater, than one hundred skilful pot painters could have painted in the like space of time in the common and usual way.” (Van Lemmon p.127) (Harvey 2010).



Figure 8 - An example of transfer-print from the nineteenth century (Harvey 2010)

In 1830 the British discovered another printing process using copper plates applying the colours directly to the tile: the lithographic process (Figure 9). But at this point the tile was still hand moulded, not having the necessary quality and its long production time was holding back the productivity achieved by the new decorations techniques.



Figure 9 - An example of a metal plate used in the lithographic decoration process at Sacavém (author's photograph)

Another English accomplishment was made in Herbert Minton's factory in Stoke-on-Trent (England) that in 1835 first to use the mechanical pressing of tiles, bringing tile production to a new era: the serial production (Ferreira 2009). These presses were manual, as in Figure 10.



Figure 10 - Example of a manual tile press (Prostes 1907)

The pressing process allowed the transition from a hand-moulded piece using a ceramic composition in a plastic state (with a mouldable consistence) that needed several hours to dry to a fast and more reliable process. The drying process of the hand-moulded technique was a sensitive process by itself as binding and cracks were common defects. The pressing technology used what was called the “dry process” as the ceramic paste had very low water content (nowadays 5 to 6% of water content is normally used), needing a small amount of time to dry before the first firing process. The “dried paste” was used in powder form.

Pressing allowed the production of thinner tiles with even thickness and the introduction in the tile’s back face of the name of the production unit, permitting its unequivocal provenance. However, not all the pressed tiles were marked, leaving many questions on provenance without answers.

In 1873, again in the UK, the first steam tile press was used in the Maw & Company factory. Using steam in tile production allowed massive production, reducing tile prices.



Figure 11 - Press atelier (year 1900) in the French factory Paray-le-monial created by Paul Charnoz in 1877 (Charnoz 2010)

In Figure 11 the moulds in the foreground are those in which the “dried” paste (powder) was placed, before undergoing compression in the presses that can be seen in the background of the image (Charnoz 2010).

## 2.3 The tile in Portugal

Tile manufacture started in Portugal in mid 16<sup>th</sup> century, when the first majolica workshops were created.

In the process of the reconstruction of Lisbon after the 1755 earthquake, Marquês de Pombal gave encouragement to tile production and in an attempt to rationalize its production, implanted in the pre-industrial plan. From 1832 until mid-1865 ten new ceramic factories were created (Lepierre 1899).

Table 1 displays a summary of tile production development in Portugal.

Table 1- Chronology of tile in Portugal (Azulejo 2012)

Time	Historical data	Techniques/Styles
End 15 <sup>th</sup> cent./begin. 16 <sup>th</sup> cent.	D. Manuel contacts directly with Seville and tile becomes widely used in Portugal.	<i>Aresta ou Cuenca</i>  <i>Esgrafitado</i> : use of nail or stylus for writing decorative motifs on the dark glaze down until the ceramic body.  <i>Relevo</i>
16th cent. (1 <sup>st</sup> half)	Initiation of tile production in Portugal.	<i>Majólica</i>
17 <sup>th</sup> cent. (1 <sup>st</sup> half)		The most used colours: yellow and cobalt blue on white. Also the orange brown (iron oxide); olive green and brown tones and purple (manganese oxide).
17 <sup>th</sup> cent.	Portuguese production increased: Lisbon as the largest national	More rich and varied palette: use of green (copper) and manganese

Time	Historical data	Techniques/Styles
(2 <sup>nd</sup> half)	ceramic centre.	(called "côr de vinho").  Cobalt blue and purple-manganese tiles, imported from Holland.
End 18 <sup>th</sup> cent./ begin. 19 <sup>th</sup> cent.	D. Maria Period	Combination of industrial and craft techniques. Printing: brush painting, through waxed paper cut outs applied on the glazed tile.
19 <sup>th</sup> Century	Creation of 3 production centres: Lisbon, Porto and Aveiro – responsible for the intensive production of tiles.	Mechanical pressing: ceramic paste pressed in moulds
20 <sup>th</sup> Cent. (1 <sup>st</sup> half)	Widespread use of tile	<i>Arte Nova</i>

At the end of the 19<sup>th</sup> century industrialized production techniques are introduced in Portugal through British influence. The tiles are no longer manually produced at casts and the ceramic body becomes mechanically pressed in manual presses through a mould that gives the desired shape, making them thinner and allowing marking on the back surface of the tile the brand of the producer. Firstly, the production of the ceramic body of the tile was pressed in manual presses passing slowly through water and wind power presses up to steam presses (already in the 20<sup>th</sup> century). Before steam, tile factories used water power from rivers or wind power (as in Figure 12) to move the production machinery.

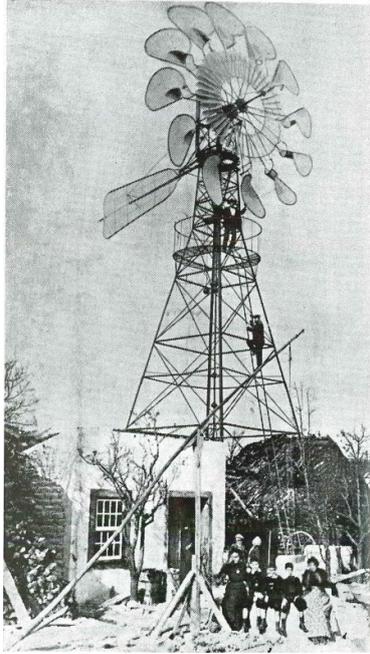


Figure 12 – Aleluia’s factory (Aveiro) wind mill in 1911 (Aleluia 1955)

In the early 20<sup>th</sup> century Portuguese ceramics factories were faced with two problems: competition from foreign ceramic products (United Kingdom and France) and technological backwardness, reflected in the type of machinery used as in Portugal slow processes still prevailed while the steam machine proliferated abroad (Aleluia 1955).

A.A. Costa was the first factory in Portugal to have production based on steam (Portela 2004).

Figure 13 shows an example of a motorized grinding machine and tile press in 1922, used in Aleluia factory.

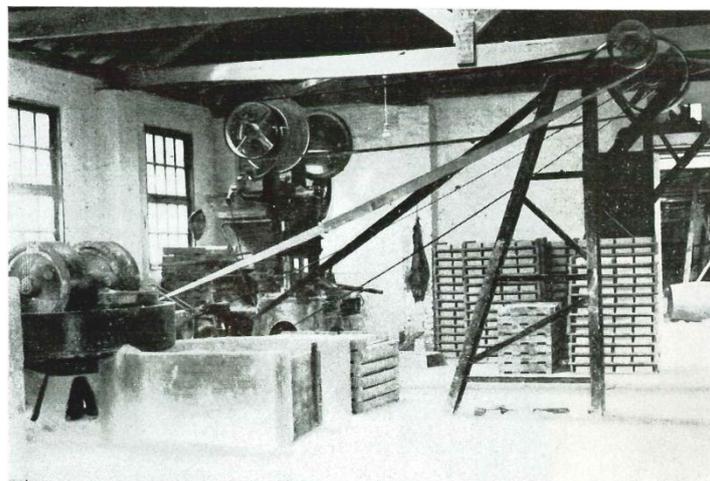


Figure 13 – Tile production by dry process (Aleluia 1955)

From the mid 19<sup>th</sup> century with the decline of tile manufacturing costs promoted by industrialization, their use becomes more accessible. Many factories in Portugal produced tiles, a fashionable construction material at the time. This ended in an economic crisis in the 1920's related to excess offer, forcing the prices down (Aleluia 1955) and submerging many factories in deep economic crisis.

### 2.3.1. National manufacturing units that supplied tiles for 19<sup>th</sup> century facades

The beginning of tile industrialization process in Portugal is not extensively studied nor documented. The historical information available (Lepierre 1899, Cordeiro 1996, Leão 1999, Portela 2004, Fernandes 2008, Ferreira 2009, Ferreira 2009, Sacavém 2009) is often contradictory, and technical issues are very scarce and fragmented.

Several cities in Portugal are a very instructive example of this cultural reality, bringing us an immense collection of facades with tiles. With an extremely wide set of tiles from so many centuries of production, still very little is known about the technical characteristics of the Portuguese tiles.

The industrial tile is characterized by opposition to the handmade by being thinner, with even height, with the back of the tile marked and less heterogeneities in the ceramic body and glaze. The common size of the analysed tiles is 14 x 14 cm for the decorative tile which usually occupies most of the facade and the “listelo” (or border) with 14 x 7 cm as in Figure 14.

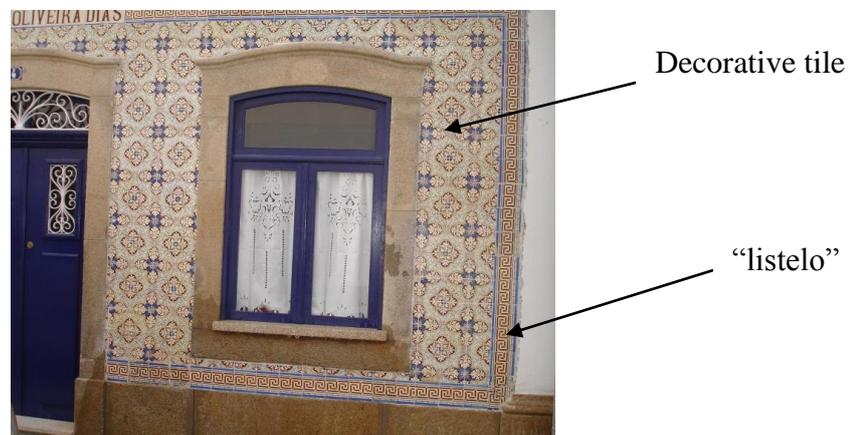


Figure 14 – Example of facade with “listelo” and decorative tiles

The decoration could be made by lithography or transfer printing. The glaze could be opaque or transparent with engobe if the ceramic body presented some colour (calcareous ceramic bodies) or only transparent glaze if the ceramic body was white (pó de pedra ceramic bodies).

Some of the most important Portuguese factories of semi-industrial and industrial era, are shown in Table 2 (Lepierre 1899, Aleluia 1955, Amadori and Ruffinelli 2009, Ferreira 2009) taking into account their production time and other relevant data.

Table 2- Some of the most important Portuguese factories of XIX century

Foundation date/ closure	Factory name	Brief history
1832 to 1930	Roseira (Lisbon)	The family Rosinska or Rosenska came from Samkt-Gallen, in Bohemia, to Lisbon in order to install itself as a tableware manufacturer. The golden period of the factory was in the second half of the 19 <sup>th</sup> century due to a recognition of the national value of tiling as a form of decorative art by D. Fernando II, by ordering the reproduction and recreation of Portuguese traditional tiling models to Pena Palace .The factory also produced some "artistic", figurative tiling, marked with "R", an initiative of João Roseira, which begin to be known and characterized as their production.
1849 till today	Viúva Lamego (Lisbon)	It was founded in 1849, by António da Costa Lamego. Only in 1863 began manufacturing faience and tiles, devoting itself previously to red clay tableware manufacture. In the field of tiling it rivalled with Sacavém factory in designing patterns for tile facades. Nowadays it only uses hand painting and mechanically finished.

Foundation date/ closure	Factory name	Brief history
1850 to 1994	Sacavém (Lisbon)	<p>The factory was probably founded in 1850, although it is common thought that its production only started in 1856. The factory became one of the main industries of the Lisbon area. Always with a strong connection to England (Stoke-on – Trent) due to the origin of its owners it had good ease of transport products and to import technology from that country. Closed in 1994, by judicial declaration of bankruptcy.</p>
1905 till today	Aleluia (Aveiro)	<p>João Aleluia left Fonte Nova Factory with 4 others workers and founded in 1905 the Aleluia Factory at Aveiro. At this time, the company was devoted, in particular to the manufacture of household wares and tiles on a small scale.</p> <p>In 1917 it acquired modernized equipment, with the goal of achieving the highest level of production. In 1922 it adopted the manufacture of tiles using the dry method.</p> <p>It is still working in wall and floor tile massive production.</p>
1766 to 1920	Massarelos (Porto)	<p>It was founded by Manuel Duarte Silva in Massarelos (Porto). At the beginning it produced pieces according to the French taste, and marked them with the letter P. or with the inscription “PORTO”.</p> <p>In 1873 started tile production. The production of this factory is especially known in the second half of the 19<sup>th</sup> century, by a large amount of standard tiles in relief that coated many Porto facades. In 1920 it closed due to a fire.</p>

Foundation date/ closure	Factory name	Brief history
1784 to 1930	Santo António Vale Piedade (Porto)	<p>Located in Vale Piedade in Vila Nova de Gaia, it was founded by the Genovese Jerónimo Rossi, Sardenha vice-consul in Porto. It had an initial period of great industrial development in the manufacture of relief faience, in competition with English ware.</p> <p>Continued to renew itself and the labour until about 1930, when closed.</p>
1840 to 1985	Carvalhinho (Porto)	<p>Founded in 1840 it operated until almost the present day. The first installation of the factory was in the chapel of Senhor do Carvalhinho, which gave rise to the name of the factory.</p> <p>In 1906 the factory expanded and renewed the technical part becoming able to improve production quality and outcome.</p> <p>In 1923, following German and English ceramic factories models, a new factory is installed, equipped with the most modern technological equipment of the time: ceramic body preparation machines, hydraulic presses for the automated manufacture of tiles and tunnel kiln.</p> <p>In 1930, due to major financial difficulties it joined the Real Fábrica de Sacavém of great prestige at the time. In 1965 became independent of the English factory, closing permanently in the mid-80s by indebtedness and decay.</p>

Foundation date/ closure	Factory name	Brief history
1865 to 1980	A.A.Costa (Devesas) (Porto)	<p>Founded in 1865 by António Almeida Costa at Quinta das Devesas, Vila Nova de Gaia, near the railway station.</p> <p>In 1881 it employed 180 individuals, and in 1897 the number of workers rose to 700.</p> <p>Wrongly linked to the end of artistic ceramics and the beginning of industrial ceramics, Devesas ceramic factory knew admirably how to merge the two realities, becoming one of the most important factories in the country.</p> <p>It had a railroad that connected the various workshops, a steam-driven nora to deliver the products to the drying warehouses, as well as a lift.</p> <p>For these reasons, the industrial complex of Devesas and its produced pieces are an important cultural legacy. The factory only closed fully in 1980 but since 1915 its decline was noticeable and permanent.</p>
1884 to 1969	José Pereira Valente	<p>Factory founded by J. Pereira Valente, an ancient A.A. Costa employee, in Vila Nova de Gaia.</p> <p>During its existence it changed its name for three times</p> <p>1884 – 1904, José Pereira Valente  1904 – 1915, José Pereira Valente e Filhos  1915 – 1969, Valente e Moreira</p> <p>In 1980 the factory building burned down.</p>

The present work will focus on the production of Porto/Vila Nova de Gaia because besides being the most productive industrial area of the country in terms of the amount of tiles produced it was undoubtedly the industrial group that coated most Northern Portuguese facades. Also, from these factories are all the samples (but one) used in this work, provided by ACRA (Atelier Conservação e Restauro de Ovar).

Ana Margarida Domingues in her master's thesis (Domingues 2003) transcribed from ancient texts about the aforementioned factories that; "produce a weekly amount of immense work, of which a part is used in the city necessities and its neighbourhood, and the other part is intended for exportation, both to all the lands of the North and South of the Kingdom, as for the Islands, and the Empire of Brazil”.

In addition to the large number of existing factories in Porto region by the end of the XIX century, their size was considerable for the time. Reports from that time show, for example, Santo António do Vale da Piedade factory (produced faience and *pó de pedra* ware, vases, decorative figures and tiles) employed "more than one hundred people daily", while A.A.Costa factory (produced statues, tiles, decorative dishes) had more than 500 people (Domingues 2003).

The existing factories labouring in Porto metropolitan area in the 19<sup>th</sup> century can be seen in Figure 15 in a geographic representation of Porto positioning the most important factories at the time (Fábricas , Lepierre 1899, Soeiro, Alves et al. 1995, Amadori and Ruffinelli 2009, Ferreira 2009)

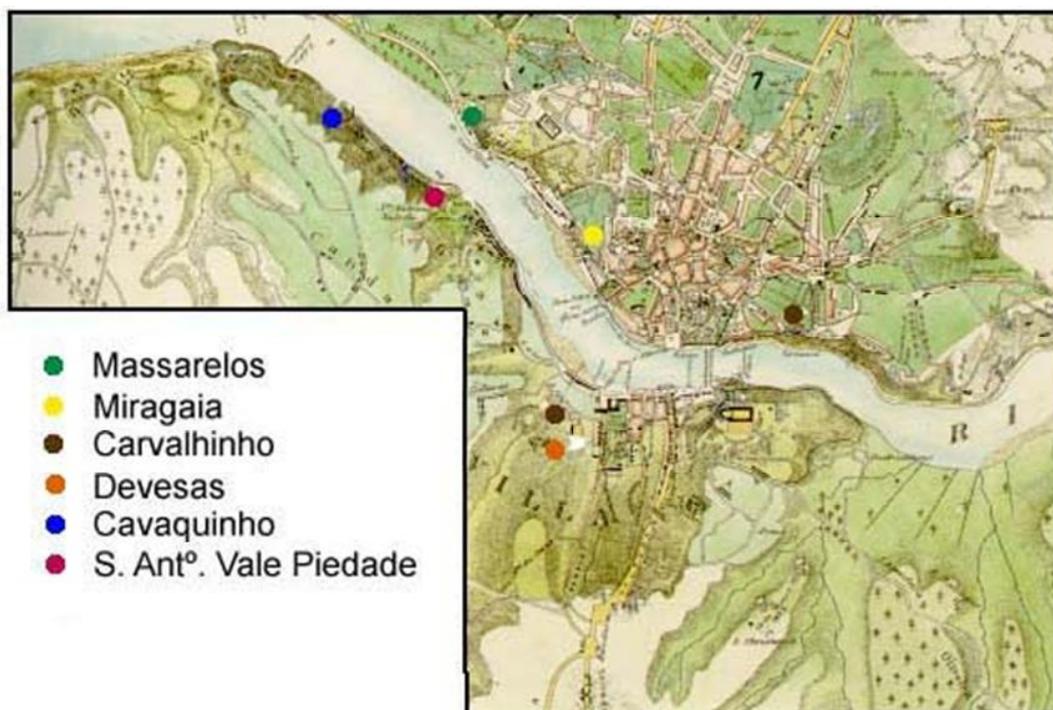


Figure 15 – Geographic location of some of Porto most important tile factories of the 19<sup>th</sup> century Image of the Douro River separating Porto from Vila Nova de Gaia (Soeiro, Alves et al. 1995).

Miragaia (1775 to 1852) and Cavaquinho (1768 to 1860) factories only produced tableware and closed before the Portuguese industrial era. Cavaquinho was the first Portuguese factory to use *pó de pedra* ceramic body technology to ware production (Cavaquinho 1999).

Due to the fact that almost all big factories of tiles that participated in the facades coating of Portuguese and Brazilian buildings in the late 19<sup>th</sup> century and early 20<sup>th</sup> century suffered great fires destroying any records or machinery that could give clues to scholars, almost no information is available today.

### 2.3.2 Ceramic body types and their raw materials

In the past, the technological know-how was in the hands of the masters and the progress of the plant depended on them. Due to their mobility between factories in pursuit of a better salary or working conditions, it is not strange that technologies were similar within the same region, as well as the formulas of the ceramic bodies, glazes and decorations.

Since the 16<sup>th</sup> century that the tile ceramic body was calcitic (Ferreira 2009) although it is quite possible that raw materials might have suffered adjustments along the passing of the years with the accumulation of experience and foreign influences.

In the second half of the 18<sup>th</sup> century, Wedgwood, an English Potter, formulated a new composition for faience by mixing clay without iron oxide with finely ground quartz sand and then firing this mixture until the ceramic body presented no porosity producing the called stoneware. In Portugal some production units used an adaptation of the English formula to low temperature so that the fired ceramic body presented white colour but porosity far from zero. In this way, instead of simple clay (or mixture of clays) factories that introduced this technical novelty began to use a mixture of clays without iron with very fine ground quartz (called the *pó de pedra*) (Leão 1999). Depending on the ceramic body composition, the first firing was done at temperatures ranging from 1000°C to 1300°C. The result was a white ceramic body, which dispensed the tin glaze oxide as a background for the purposes of decoration. After decorated, the ceramic body was coated with a transparent lead glaze and the firing of the assemblance was done at a temperature between 900°C and

1200°C (Leão 1999). This technical change decreased the manufacture cost as the very expensive tin was not used (Cordeiro 1996, Amadori and Ruffinelli 2009).

From the interventions already made to facades, it is known that in the beginning of the 20<sup>th</sup> century, the Northern facades were coated by two kinds of tile ceramic bodies: the calcitic ceramic bodies and the *pó de pedra*.

While the calcitic ceramic bodies probably had as raw materials kaolinitic clays, quartz, talk (or dolomite) and calcite and have a dull yellowish colour, the *pó de pedra* ceramic bodies probably only had quartz and kaolin as raw materials, presenting a very white ceramic body.

Tile raw materials have to be undoubtedly connected to the history of their manufacturing technique. In the 19<sup>th</sup> century a wide path regarding manufacturing techniques had already been drawn. It is in this period that the tile was produced industrially, forcing a technological adaptation of the ceramic body and glaze. In this way, it can be found the logical evolution of the raw materials: more refined and an optimization of mixtures of materials in order to provide a higher quality and reproducibility of the finished product.

The ceramic body composition of the tiles of late 19<sup>th</sup> century early 20<sup>th</sup> century is rather unknown, as there are almost no studies about this subject (Cordeiro 1996, Ferreira 2009). Lepierre gives us a clue about the Porto ceramic factories composition saying that the glazed faience, covered with an opaque tin glaze, was obtained by mixing clay used for small sculptures (not plastic, containing iron and calcium, in order to obtain greater fusibility) with sand and marls (mixture of calcite, clay minerals, with traces of quartz), responsible for calcium introduction, which was essential as practice showed at the time (Lepierre 1899). Other raw materials were used to optimize the ceramic body for the processing technology and firing temperatures. Balances would have to be made between materials that gave mechanical resistance, decreased distortion, and fluxes such as calcite (Leão 1999).

The chemical analysis performed by Lepierre on tile fragments of the two production units more studied in the present work (A.A.Costa and J. Pereira Valente), are shown in Table 3.

Table 3 – Chemical results obtained by Lepierre to A.A.Costa and J.P.Valente tiles (Lepierre 1899)

Production unit	Colour	SiO <sub>2</sub>	Al <sub>2</sub> O <sub>3</sub>	Fe <sub>2</sub> O <sub>3</sub>	CaO	MgO	Alcalis
A.A. Costa	yellowish	44.7	19.5	4.0	30.2	1.2	0.4
J.V. Pereira	yellowish	50.7	24.4	3.3	15.9	2.9	1.9

The clays raw material, commonly called *barros*, are aluminium silicates more or less hydrated and with different colorations, depending on the oxides contained. Thus, the more pure, the more its colouring is closer to white, being kaolin its purest form (kaolinite), composed almost exclusively of silica, alumina and water (Si<sub>2</sub>Al<sub>2</sub>O<sub>5</sub>(OH)<sub>4</sub>) (Gomes 1986).

Clays can be defined in different ways. For the ceramist clay is a natural material which acquires plasticity when in contact with a certain amount of water; for the petrologist, it is an aggregate easily fragmented, almost always of very fine mineral particles not identifiable to the naked eye; for the sedimentologist it is a definition of particle size of all sediment in prevailing equivalent spherical diameter particles less than or equal to 2 µm, to give just a few examples (Gomes 1986, Vasconcelos 2008). As a concept with more generalized acceptance, clay is considered a natural product which has the so called clay minerals as basic composition with equivalent spherical diameter less than 2 µm, containing also other minerals and in some groups also containing organic matter. The clay minerals are mainly formed by the elements O, Si, Al, H, Fe, Mg, Ca, K and Na and in their ionic state can combine in fifty series. The non-clay minerals exist in the form of some silicates, carbonates, phosphates, oxides, hydroxides and sulphates. The types of clay minerals are distinguished by the chemical composition and structural organisation (Gomes 2002).

It is the laminar structure of the clay minerals that binds to water molecules acquiring the necessary plasticity for the workability of the ceramics in different kinds of technical processing.

The first clays used in calcareous tiles had high levels of various impurities including iron oxide which gave inhomogeneity and coloration to the ceramic body. For this reason, the most common colouring of this ceramic body at the time is a buff red, making it necessary to cover the ceramic body surface with a white opaque glaze, so the decoration colours could be visible and the final aspect could be harmonious.

It is thought that with the evolution of quality parameters, kaolinitic clays started to be used, as a more pure raw material with white colouring when fired. Kaolinitic clays mainly consist of clay minerals of the kaolinite group ( $\text{Al}_2\text{Si}_2\text{O}_5(\text{OH})_4$ ) (Vasconcelos 2008). A kaolinitic aggregate can be seen in Figure 16.

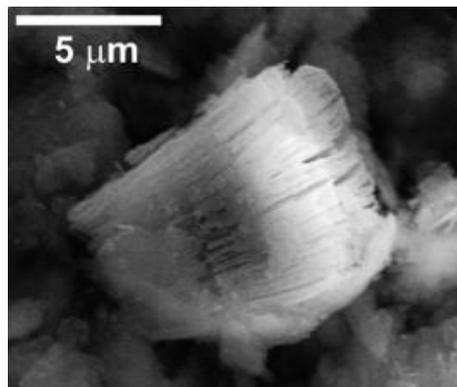


Figure 16 - SEM image of a kaolinitic aggregate formed by stacking octahedral lamellar crystals of kaolinite (Senna 2008).

Among historical references, there is some controversy about clays provenance that fired in white (or light coloured) for Porto tile's industry (Leão 1999, Ferreira 2009). However, for the some Portuguese geologists that question is very clear, due to the vast deposit of excellent quality of kaolin which extends from the Porto until Albergaria-a-Velha (Vasconcelos 2008). In Porto area, kaolin deposits are known and exploited for a long time (Coelho 2006, Vasconcelos 2008). In her Master's thesis, Maria Cristina Vasconcelos (Vasconcelos 2008) states the existence of the so-called "ceramica portuense" that since the 18<sup>th</sup> century was distinguished by the brightness and quality of its ceramic body due to the region's kaolin. This work also mentions that all the great Porto factories from late 19<sup>th</sup> century, beginning of the 20<sup>th</sup> century were users of this local raw material (Santo António do Vale de Piedade, Carvalhinho, Devesas factories, among others) (Vasconcelos 2008). In his work from 1898, Lepierre (Lepierre 1899) analysed 440 Portuguese clays leading him to consider that Portugal had good quality clays. Lepierre wrote that, A.A. Costa (Devesas factory, one of the northern most important factories of his time) used raw materials exploited and composed by the factory itself. From these considerations it is thought that the white clays used in the Northern factories came from the North of Portugal, rich in good kaolin and clays (Vasconcelos 2008).

It is known, however, that for the Sacavém factory the kaolin came from England (Sacavém 2009). However, in the Portuguese industrial world, Sacavém was a different unit because it was owned by English, with masters either English or trained in England (Stoke-on-Trent). According to engineer Clive Gilbert, a founder's descendant and employee at the end of Sacavém labouring time, it was cheaper to import all the raw materials from England than to make them come from the North of Portugal to Sacavém (near Lisbon) (Sacavém 2009).

Quartz is introduced in the ceramic body in order to give rigidity, and shape stability in the drying and firing process. It also plays a very important role in the liberation of gases from the ceramic body firing due to raw materials' decomposition.

The alkaline feldspars promote a decrease in melting temperature of quartz and of the clay body ceramic constituents, promoting the transformation of a glassy phase that confers increased mechanical strength and durability to the tile. Calcite, talc and dolomite also have a role in lowering the firing temperature of the ceramic composite (Gomes 2002). The introduction of talc not only helps the pressing process and increases the fired mechanical strength, but also diminishes the fired ceramic body expansion due to moisture. Calcite and talc are also used to make the ceramic body look whiter (Renau 1994).

The clays that fired white (cream) used in the production of ceramic tile bodies usually do not contain carbonates, so the addition of calcite was required, as a promoter of open porosity, mechanical resistance, dimensional stability during firing and essential to ensure a thermal coefficient of expansion compatible with the lead glaze of used at the time (Lepierre 1899, Albero, Porcar et al. 1991).

### 2.3.3 Glaze types. Glaze raw materials

One definition of glass can be “an over cooled liquid, obtained by the fusion of inorganic oxides, that is cooled until room temperature without facing crystallization” (Materials 1945, Renau 1994, Fernandes 2012). Technically, there are three very important features of the glass that must be considered. Firstly, as glass is non-crystalline, it cannot be described as a chemical unit cell that repeats itself periodically in space. Secondly, as glass is an over cooled liquid, it is in a state of non-equilibrium that depends on its composition and

thermal history. Thirdly, the non-equilibrium state of the glass means that it takes a long time to approach equilibrium state (Fernandes 2012). The glass can be transparent, opaque, colourless or coloured. Mechanically it is hard but brittle and presents a conchoidal fracture (Fernandes 2012).

In the ceramic tiles glaze compulsory elements have to be present: *glaze structural producers*, *net modifiers* and *net stabilisers* (Navarro 1991, Renau 1994, Alaimo, Bultrini et al. 2004). *Glaze structural producers* have the general chemical formula of  $RO_2$ ,  $RO_3$ ,  $R_2O_5$  (most common is  $SiO_2$ ) formed by structural units that don't repeat at regular distances from each other, forming an uneven net with random organization. *Net modifiers* are the elements that occupy the net holes, making the net bonds weaker, promoting the glaze fusion at lower temperatures. The most frequent *net modifiers* used are: Li, Na, K, Ca, Mg, Ba, Sr, Pb and Zn. The *net stabilizers* promote stability to the amorphous state of the glaze, avoiding its crystallization. The general chemical formula for *net stabilizers* is  $R_2O_3$ , being  $Al_2O_3$  the most important one (Renau 1994).

Recent studies of glazed 17<sup>th</sup> century glazed tiles made by  $\mu$ -EDXRF and EDS, showed that the samples tested had the following chemical compositions (Table 4) (Coentro 2011):

Table 4 -Chemical compositions of white glazes from 17<sup>th</sup> century (Coentro 2011)

	SiO <sub>2</sub>	PbO	K <sub>2</sub> O	SnO	Na	Al <sub>2</sub> O <sub>3</sub> , CaO
%	58 a 72	18 a 32	3,5 a 10	1,6 a 7,1	< 2,5	traces

All the 19<sup>th</sup> early 20<sup>th</sup> century tiles had lead glazes. The advantages of using lead glazes are known since remote times. It is known that around 2000 BC the first formulation of glazes with copper and lead was studied (Fonseca 2000). Among the advantages of using lead as *net modifier* is the low melting point, high brightness, transparency and ability to be mixed with oxides that give colour and/or opacity (Molera, Pradell et al. 2001).

According to different sources (Molera 1999, Fernandes 2008, Coentro 2011), opacified lead glazes with tin oxide were made by firstly fritting the lead with the tin that was

later added to silica and heated until the mixture attained complete fusion. In order to be used, the frit was grinded to a very thin powder and added to water to form a slurry (Senna 2008).

The transparent lead glazes from the 19<sup>th</sup> century, used in white bases of *pó de pedra* had as constituents lead oxide, sand, and marine salt, as there was no longer need for opaque glazes (Leão 1999).

The raw materials of the glazes (tin, lead, sodium carbonate and potassium carbonate) and decoration (prints and pigments) were imported via maritime routes from England, the Netherlands and France (Ferreira 2009).

## 2.4 Tiles processing

*“Whoever studied the history of ceramic industry in Portugal – since the company’s history and of their periods of operation, to manufactured products passing through the technology that was used- in particular in the Porto region, knows the difficulties that exist to access sources, as almost all of the factories have disappeared a long time ago, their files have not been preserved, the official documentation available is extremely scarce or even non-existent and, in addition to all these obstacles, in the historical literature that has been published there are many inaccuracies and errors ...” (Cordeiro 1996).*

As stated by Lopes Cordeiro there is not much that may be said about ceramic processing from late 19<sup>th</sup> and early 20<sup>th</sup> century. All the considerations that will be made are due to the personal experience in the contemporary tile industry and gathering of some information given by collected pictures.

It is believed that the quantities of raw materials contained in the formulation of the masters responsible for production should be quantified by elements of volume or number of shovels, due to the high cost of weighing material at the time and the fact that there are some formulas of glazes and ware ceramic bodies from early 20<sup>th</sup> century with quantities expressed in number of mugs.

As today, the hardest raw materials would have to be ground to a fine powder, so that the reactions during firing would give the final product with the desired physical characteristics. The grain sizes used for ground materials, like sand, calcite and feldspars are

unknown, and it is only known that the final porosity as well as the mechanical resistance also depend on this parameter. The smaller the grain sizes, the higher the reactivity of materials with temperature promoting greater amount of liquid phase in the same composition. To these ground raw materials clays were added, previously diluted in water (to homogenize and remove the undesired materials by sieving or by decanting). It is unknown how each factory prepared the ceramic body but it is known that the conformation process of the tile was made by pressing and that this technology used, and still uses, an almost dry ceramic powder (with more or less 6% of moisture). If the components mixture and grinding was performed in a wet process or by a humid process, it is not clearly known.

The pressing process being manual or assisted by mechanical strength issue is not clearly answered in the available literature. It is believed that the mass-produced tiles at the beginning of the 20<sup>th</sup> century would already be processed using mechanical presses. An example of a pressing atelier in Sacavém factory in 1932 can be seen in Figure 17.



Figure 17 - Engraving of the atelier of the presses at Sacavém in 1932 (author' photograph)

After the ceramic body was pressed, regardless of its preparation method, it still had some moisture that needed to be extracted. The drying was performed gradually and at low temperature (typically between 25 and 40° C), after which the tile was ready for the first firing. During firing, and depending on the enthalpy supplied to the composite ceramic body, the constituent minerals underwent structural changes, in volume, until they reached kinetic balance. These transformations were usually associated with a volumetric shrinkage, accompanied by a structural rigidity that translated into a greater mechanical resistance and lower porosity but with greater suction capacity.

After firing, the colour and uniformity of colour depends on iron, titanium oxide or manganese content and oxygen content and its distribution in the atmosphere of the kiln. The yellow-ochre colour usually indicates high levels in CaO + MgO. Clays with carbonates fire between 1000° C and 1100° C with the yellow-ochre colour (Gomes 2002).

In the ceramic composite with clays with an iron oxide percentage higher than 1%, the colour difference between the peripheral parts and the inside of the tile was often displayed as yellow-red on the outside and yellow-ochre on the inside, due to the lack of oxygenation of the inside of the tile, so that the valence +3 iron in the form of hematite transforms into valence iron +2 in FeO (example Figure 18).



Figure 18- Tile image where colour difference of the ceramic body due to firing atmosphere is evident (author' photograph)

In order to achieve a complete transformation of the raw materials into the desired sintering technical characteristics for a given chemical/mineralogical composition, it is very important to ensure that the maximum temperature is achieved as well as the isothermal plateau at this temperature. But, not least important is the heating rate to achieve the maximum temperature. The use of more moderate maximum temperatures implies gradual temperature rise to ensure that the reactions of the transformation processes are complete and a good sintering is reached. In the 19<sup>th</sup> century, due the cost of firing raw materials, for their low calorific power and because a lot of time was lost waiting for kilns cooling periods, tile producers had all the interest to take their firing to the lowest possible temperature. So, it is thought that the heating of the sintering mass would be done gradually, providing greater activation energy of grain growth than the activation energy for densification, as expressed by the formula:

$$dp/dt \propto 1/T \exp (- Q/ RT )$$

Where:  $\rho$  - Densification;

$t$  - Time;

$T$  - Maxima temperature;

$Q$  – Activation energy

$R$  – Perfect gases constant

$\alpha$  – proportional to

Slow and gradual heating and cooling are essential so that, in the intervals of temperature at which the ceramic body suffers stronger dilation or contraction, there is no rupture of the piece. Typically rapid volume changes happen on heating and cooling at 573° C with the reversible transformation of quartz  $\alpha \leftrightarrow \beta$ , between the 900°C and 1050°C, when the structure suffers greater shrinkage due to reorganization of the clay minerals.

There are no historical elements that can give certainties which type of kilns were used to fire tiles in Porto region in the beginning of the semi-industrialization period. It is

thought that the combustible material had to be woody or mineral (coal). Table 5 gives the calorific power of some combustible materials so that the probable amount of combustible material needed for each firing cycle can be understood.

Table 5- Calorific power of some combustible materials (Tabelas 2010)

Combustible materials	Calorific power [Kcal/Kg]
Wood	2 000 a 4 000
Coal	6 000 a 7 500
Natural gas	8 000 a 10 000
Propane	11 900 a 22 000
Butane	11 800 a 28 300

By the calorific power of wood and coal, it can easily be understood that the kiln heating probably was done at very slow rate needing many hours to achieve the maximum firing temperature.

In Figure 19 a kiln used in the Fábrica de Louças de Sacavém is outlined, in which all kinds of manufactured products (tiles, tableware, sanitary ware) were fired. The combustion area was beneath the ground of the firing room.

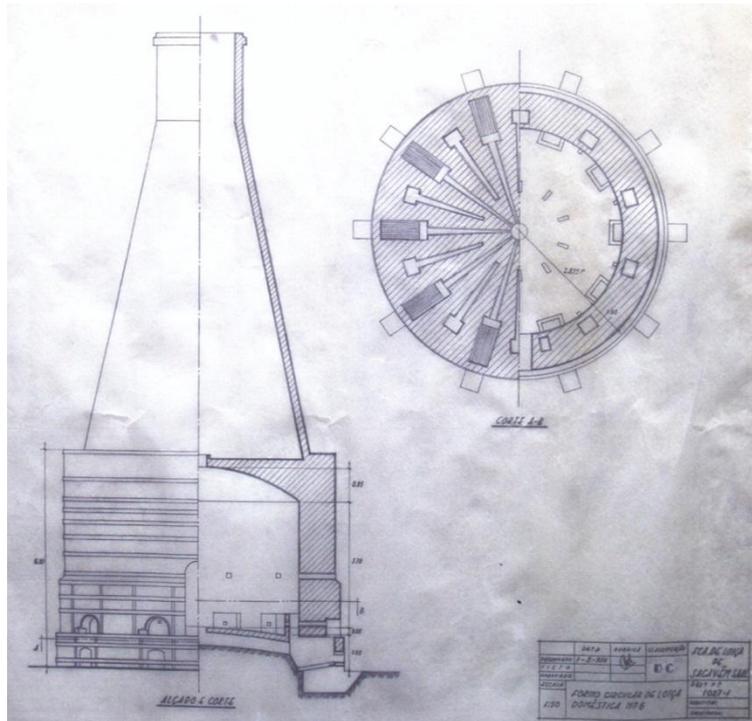


Figure 19 - Scheme of a circular kiln used at Fábrica de Louça de Sacavém (author' photo)



Figure 20- Interior of the kiln, the firing room (author' photo)

On the left bottom of Figure 20 tableware *gazettes* used to protect the ware from the kiln smoke can be seen; they also enabled piling of ceramics until considerable heights, as it can be inferred by the charge/discharge ladder height. Analysing the same figure we can easily understand the existence of large thermal gradients as well as oxygen gradients

between the firing pieces near the walls and next to the floor, and the top placed in the centre of the kiln. In a technical point of view, it is believed that it would be improbable that two similar firing cycles would be possible due to the variation of the combustible material, speed at which it was put to burn, amount of ceramic inside the kiln, its thermal inertia, oxygen content on combustion, among others. Consequently it is expected to be found, in the same factory and at the same production time, fluctuations in the amount of crystalline phases present that may not be associated with differences in formulation or dosage error, but to changes in firing enthalpies.

Since ancient times the maximum firing temperature control was made visually, being the master consulted to verify the colour of refractory material or colour inside the kiln, using the "colour and brilliance pyrometer" experience of radiation of the materials under the heat of the flames. Later, in a technological giant step, pyrometric cones were invented by Josiah Wedgwood (England) in 1782. But it was Hermann Mow in 1886 that developed the cones bringing them up to the modern era. Its marketing must have begun around 1896. The cone consists of ceramic material the composition of which defines the softening temperature of each cone (each cone has a number associated with its softening temperature). The cones do not give a firing temperature, but the time integration with the temperature, the so-called equivalent temperature. Three to four cones with different softening temperature were placed together in a support (Figures 21 and 22) and placed in a kiln entrance for easy visualization. With the flexion of the right cone, the combustion material was suspended as firing reached the maximum temperature. The kiln temperature would be considered as being the one between the cone less flexed and the one that remained standing.



Figure 21 – The remaining of a cone firing control (author' photo)



Figure 22 - Typical example of cones behaviour to temperature

In a more technologically advanced phase, the so-called Buller rings (Figure 23) appeared using the principle that to a ring (ceramic) retraction corresponds a certain temperature. Like the pyrometric cones, Buller rings give the integration time/temperature of firing.



Figure 23– Photo of a Buller ring of high temperatures (author' photo)

After the first firing, the ceramic body had good enough porosity and mechanical resistance to absorb the glaze slip. The glaze was applied in liquid form, with a density and viscosity normally factory-specific, although always within certain narrow limits. The application was made by curtain or partial dip, avoiding tarnishing the back of the tile so that it didn't glue to the refractory while firing. The adherence of the glaze to the biscuit was made possible by the ceramic body porosity, which absorbed the water from the glaze slip creating a deposit of the slip solid particles constituents on the biscuit surface with a thickness that, after firing, was less exuberant by densification caused by the fusion.

After the glaze and decoration application, the pieces were fired in *gazettes* (Figure 24) so tiles would not touch each other or the holding system, as in Figure 5.



Figure 24 – Example of *gazettes* for tile firing (author' photo)

During glaze firing, liquid phase is formed due to the presence of fluxes and lead low melting point. This liquid phase penetrates the surface pores of the ceramic body, reacting in a depth which is composition, sintering time and temperature dependent. The magnitude of this layer of great importance is given by the equation of time/temperature that allows, or not, the diffusion of elements between the glaze and the ceramic body (Kopar 2007). The atmosphere and pressure of the kiln as well as a balanced thermal curve to allow the degassing smooth and effective are primary factors for the quality and appearance of the glaze.

## References

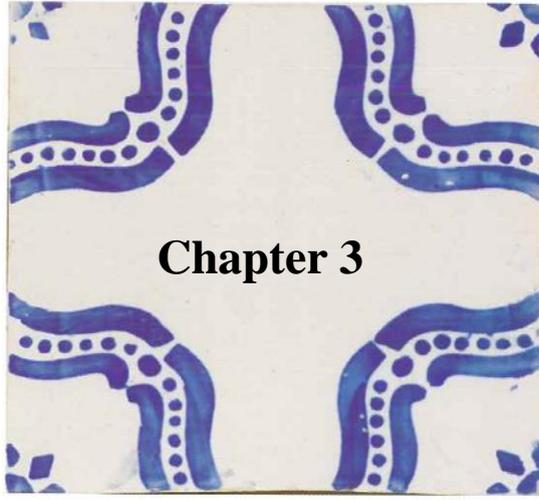
- Alaimo, R., G. Bultrini and G. Montana (2004). "Microchemical and microstructural characterization of medieval and post-medieval ceramic glaze coating." Applied Physics A 79: 263-272.
- Albero, J. L. A., V. B. Porcar, A. B. Fuentes and J. E. E. Navarro (1991). Defectos de Fabricación de Pavimentos y Revestimientos Cerámicos. Instituto Cerâmico de Valência. Valência
- Aleluia, F. (1955). História da Fábrica Aleluia - 1905 – 1955. Fábrica Aleluia. Aveiro
- Amadori, M. L. and L. Ruffinelli (2009). Azulejos: historical-technical notes and conservation problems. International seminar "conservation of glazed ceramic tiles. Research and practice". Laboratório Nacional de Engenharia Civil. Lisboa.
- Aveiro, Museu da Cidade (2008). "15x15" Aveiro - a essência colorida do azulejo. Câmara Municipal de Aveiro. Aveiro
- Azulejo, M. d. (2012). "<http://mnazulejo.imc-ip.pt/Data/Documents/Cronologia%20do%20Azulejo%20em%20Portugal.pdf>." Retrieved Novembro 2012.
- Cavaquinho, F. (1999). "[http://www.portoxxi.com/cultura/ver\\_folha.php?id=19](http://www.portoxxi.com/cultura/ver_folha.php?id=19)." Retrieved Fevereiro 2011.
- Charnoz, I. M. P. (2010). "<http://ventsumorvan.org/pdfs/pdfs/vdm-0773.pdf>." Retrieved Janeiro 2011.
- Coelho, A. M. S. (2006). Depósitos de caulino associados a faixas de fracturação: Geologia, morfotectónica e georecurso. Mestrado, Universidade de Aveiro.
- Coentro, S. X. (2011). Estudo da camada pictórica na azulejaria portuguesa do século XVII. Mestrado. Laboratório Nacional de Engenharia Civil. Lisboa.
- Cordeiro, J. M. L. (1996). As fábricas portuenses e a produção de azulejos de fachada (Sécs.XIX-XX). Divisão de Património Cultural.

- Domingues, A. M. P. (2003). António Almeida da Costa e a Fábrica de Cerâmica das Devesas. Master, Universidade do Porto.
- Fernandes, H. A. G. d. R. (2012). Development of lithium disilicates based glass-ceramics. Doutoramento. Universidade de Aveiro.
- Fernandes, I. M. (2008). A Fábrica de Louça de Miragaia. Instituto dos Museus e da Conservação. Lisboa.
- Ferreira, L. M. (2009). O azulejo na arquitectura da cidade do Porto [1850 - 1920]. Caracterização e intervenção. Doutoramento, Universidade do País Vasco.
- Ferreira, Maria Isabel (2009). Azulejos tradicionais de fachada em Ovar contributos para metodologia de conservação e restauro. Ovar, Camara Municipal de Ovar.
- Fonseca, António Tomás (2000). Tecnologia do processamento cerâmico. Universidade Aberta. Lisboa
- Fábricas, C. <http://paginas.fe.up.pt/porto-ol/mlr/index.html> - Consultado em Novembro 2011.
- Gomes, C. (1986). Argilas o que são e para que servem. Fundação Calouste Gulbenkian. Lisboa
- Gomes, C. (2002). Argilas - aplicação na indústria. Dinterna. Lisboa
- Gomes, Jim Robert Puga (2011). Exemplos da Azulejaria dos Séculos XVI e XVII em Coimbra. Master, Universidade de Coimbra.
- Harvey, W. (2010). "A Brief History of Transfer Printed Tiles." [http://www.transcollectorsclub.org/bulletin\\_previews/articles/11\\_Winter\\_Spring\\_Printed\\_Tiles\\_feature\\_1.pdf](http://www.transcollectorsclub.org/bulletin_previews/articles/11_Winter_Spring_Printed_Tiles_feature_1.pdf). Retrieved Fevereiro 2011.
- Kopar, T., Ducman, Vilma (2007). "Low-vacuum SEM analyses of ceramic tiles with emphasis on glaze defects characterisation." Materials characterization 58: 1133-1137.
- Lepierre, C. (1899). Estudo chimico e tecnologico sobre cerâmica portuguesa moderna. Imprensa nacional. Lisboa
- Leão, M. (1999). A cerâmica em Vila Nova de Gaia. Edições Manuel Leão. Gaia

- Materials, T. A. S. f. t. (1945). C162 - Compilation of ASTM Standard Definitions. Philadelphia.
- Molera, J., T. Pradell, N. Salvadó and M. Vendrell-Saz (2001). "Interactions between clay bodies and lead glazes." Journal of American Ceramic Society 84: 1120-1128.
- Molera, J. (1999). "Evidence of Tin Oxide Recrystallization in Opacified Lead Glazes." Journal of American Ceramic Society 82: 2871-2875.
- Navarro, J. M. (1991). El Vidrio. Fundación Centro Nacional del Vidrio. Madrid
- Portela, A. M. (2004). "Devesas: As origens históricas da fábrica de cerâmica que mais marcou as fachadas de Ovar." Dunas 4: 61-72.
- Prostes, P. (1907). Indústria Cerâmica. Livrarias Aillaud et Bertrand. Paris.
- Renau, R. G. (1994). Pastas y Vidriados en la fabricación de pavimentos y revestimientos cerámicos. Faenza Editrice Ibérica, S.L. Espanha
- Sacavém, Museu. (2009). Porta aberta às memórias. Museu de Sacavém. Sacavém
- Senna, J. (2008). "Characterization of clays used in ceramic manufacturing industry by reflectance spectroscopy: an experiment in the São Simão ball-clay deposit, Brazil." Applied Clay Science 41(2-1): 85-98.
- Sintra, Parque Nacional (2013). "<http://pnsintra.imc-ip.pt/pt-PT/palacio/azulejos/ContentDetail.aspx>." Retrieved Janeiro 2011.
- Soeiro, T., J. F. Alves, S. Lacerda and J. Oliveira (1995). A Cerâmica Portuguesa - Evolução Empresarial e Estruturas Edificadas. Portugalia.  
<http://ler.letras.up.pt/uploads/ficheiros/3834.pdf>. 16: 203 - 287.
- Tabelas, p. c. (2010). "<http://betserpi-seguridadcontraincendio2.blogspot.pt/2010/06/materiales-solidos-poder-calorifico-en.html>." Retrieved Junho 2011.
- Vasconcelos, M. C. (2008). Caulino: das origens às aplicações. Master. Universidade de Aveiro.

Veloso, A. J. d. B. (2009). Azulejos semi-industriais de fachada. I. Almasqué. Curso de história do azulejo - Cinco séculos de presença em Portugal. Museu Nacional do Azulejo.





## Chapter 3

### Materials and methods

---



## **3.1 Materials**

### **3.1.1 Raw materials used**

Three criteria were considered for choosing the raw materials used to produce replicas. One was the possibility of a durable supplying, the second one the proximity to Oporto (the case of kaolin) and being Portuguese was the third criteria. The raw materials chosen were the ones, among some available samples of raw materials used in nowadays ceramic industry that gave better results. The search for Portuguese raw materials near Oporto is due to the conviction that the Oporto ceramic industries of the past used local raw materials. The only ceramic raw materials exploitation done nowadays near Oporto is the kaolin that is the reason why the rest of the raw materials are from other parts of the country.

#### **3.1.1.1 Kaolin**

Kaolin is a clay with high alumina content, small plasticity, it has white colour after firing and it is a highly refractory material (Renau 1994). Its utilization might be linked with the need to increase the ceramic body whiteness.

The kaolin chosen was Vialpo, kaolin extracted near Ovar (Outeiro, nº8 on Figure 25) because its exploitation is not far from Porto belonging to the same kaolin deposit as Porto kaolin's and is a well know ceramic raw material exploited since the 19<sup>th</sup> century.



Figure 25- Existing kaolin in Portugal (Velho, Gomes et al. 1998)

The kaolin XRD is as Figure 26 and XRF as Table 6.

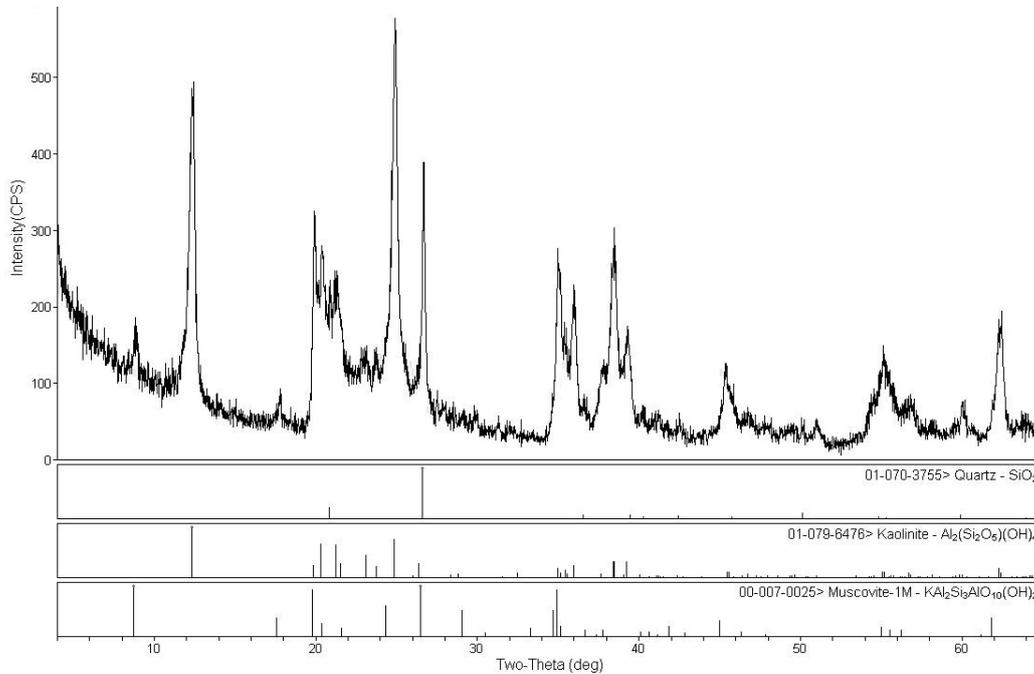


Figure 26 – kaolin XRD

Table 6 – Kaolin XRF values

	L.O.I.	Na <sub>2</sub> O	MgO	Al <sub>2</sub> O <sub>3</sub>	SiO <sub>2</sub>	K <sub>2</sub> O	Fe <sub>2</sub> O <sub>3</sub>
(%)	12,72	0,04	0,11	35,66	49,18	1,19	0,85

### 3.1.1.2 Quartz sand

Quartz is the predominant crystalline form of silica (SiO<sub>2</sub>). It is used as mechanical support that allows a faster drying with less drying cracks and reduces the ceramic body firing deformation.

The quartz sand, with reference RM 41K, from Sibelco- Rio Maior (n° 14 on Figure 27) was considered because it is a commercial sand exploitation specially used in the ceramic industry. Its XRD is as Figure 27 and XRF as Table 7.

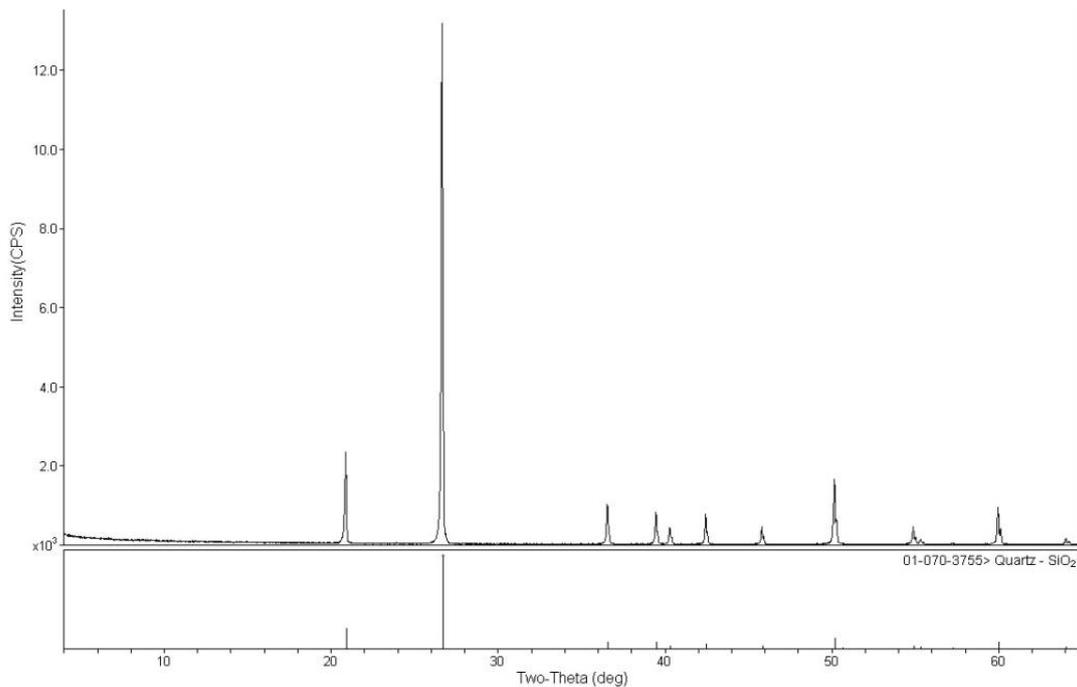


Figure 27 – Quartz sand XRD

Table 7 – Quartz sand XRF values

	L.O.I.	SiO <sub>2</sub>	Al <sub>2</sub> O <sub>3</sub>	Fe <sub>2</sub> O <sub>3</sub>
(%)	0,16	99,34	0,34	0,03

### 3.1.1.3 Ball clay

Ball clay was used with the reference BM-9 from Mário Moderno – Rio Maior, with XRD as Figure 28 and XRF as Table 8. It is a plastic clay giving to the ceramic body the ability to change its shape and maintain it without facing rupture.

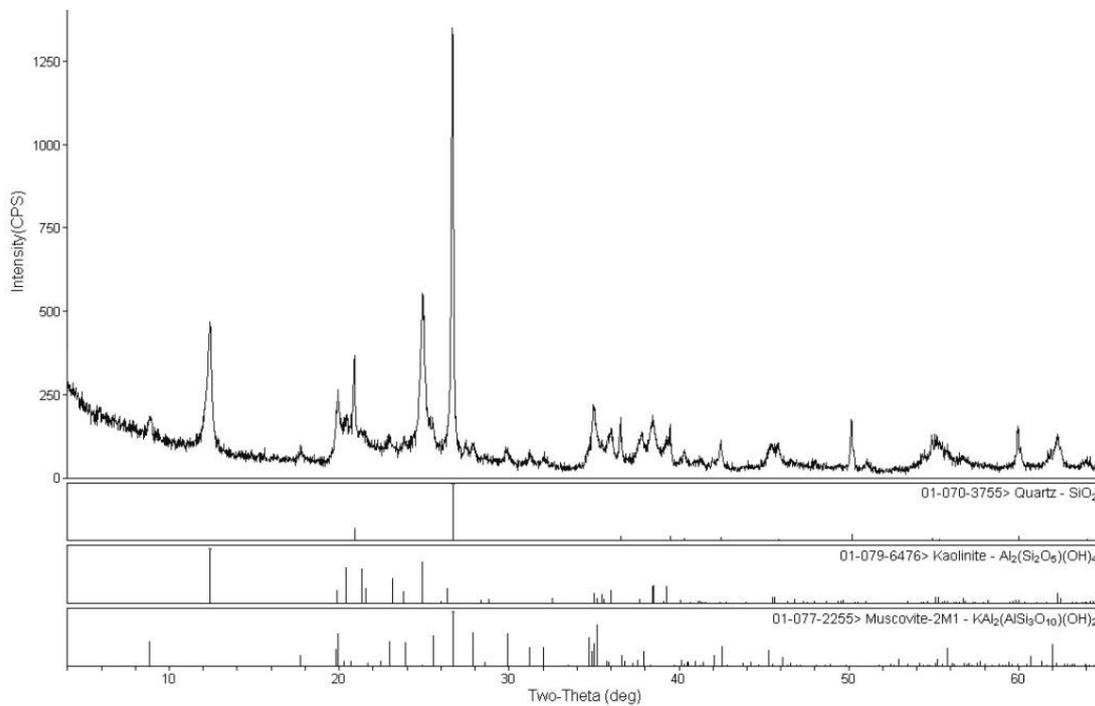


Figure 28 – Ball clay XRD

Table 8 – Ball clay XRF values

	L.O.I.	MgO	Al <sub>2</sub> O <sub>3</sub>	SiO <sub>2</sub>	K <sub>2</sub> O	Fe <sub>2</sub> O <sub>3</sub>
	11,41	0,48	28,50	55,14	1,46	1,64

### 3.1.1.4 Calcite

Calcite is used in order to obtain a porous ceramic body and as a flux, allowing to fire at lower temperatures. Calcite also has a ceramic body whitening ability (Albero, Porcar et al. 1991).

The calcite used is from Serra dos Candeeiros and it has no commercial designation as mining samples were used because commercial samples were not available. Its XRD is as shown in Figure 29 and its XRF results are displayed in Table 9.

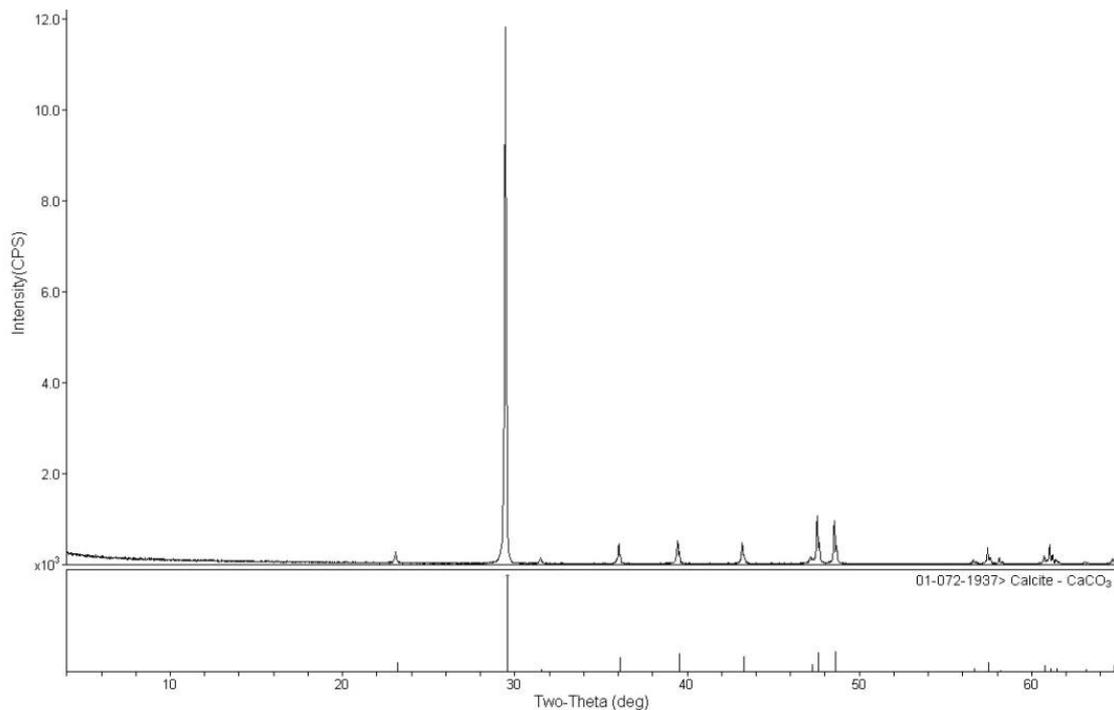


Figure 29 – Calcite XRD

Table 9 – Calcite XRF values

	<b>LOI</b>	<b>CaO</b>	<b>MgO</b>	<b>SiO<sub>2</sub></b>
<b>(%)</b>	38,36	60,91	0,29	0,28

### 3.1.1.5 Talc

Talc is a magnesium silicate with a laminar structure and flux ability that increases firing mechanical resistance. Talc is also used as a pressing additive (Albero, Porcar et al. 1991).

The talc used has as reference Mitalco C from the company Mitalco because it is a well-established product in the ceramic market.

In Figure 30 it can be seen the Mitalco C diffraction maxima and in Table 10 the chemical analysis done by XRF.

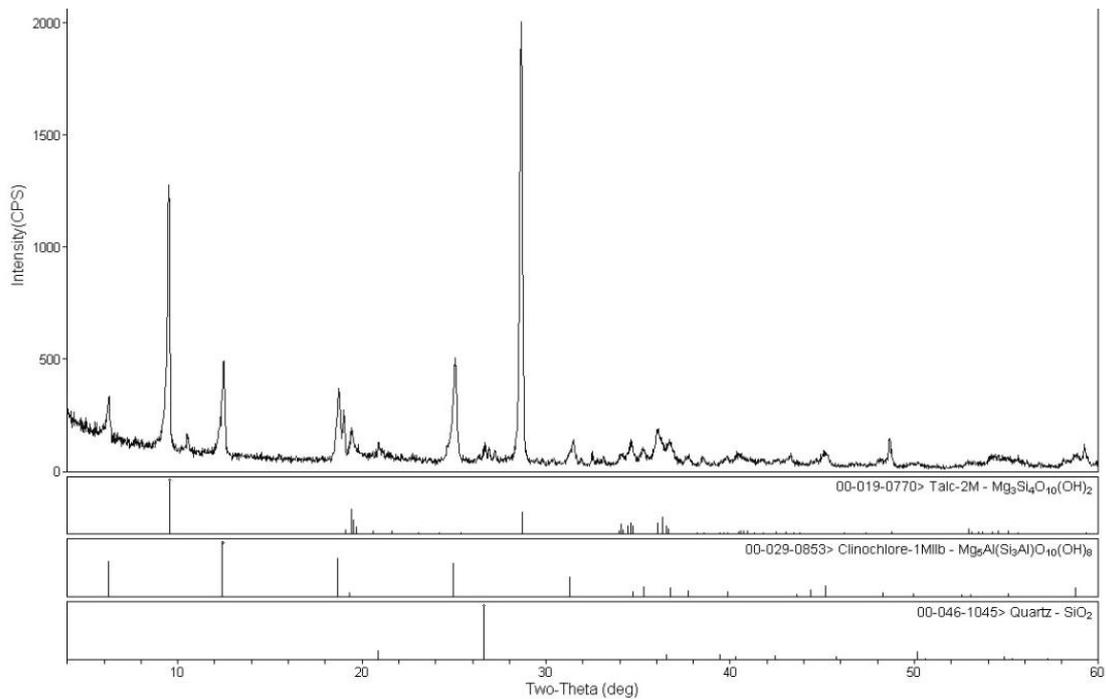


Figure 30 – Talc XRD

Table 10 - Talc XRF values

	LOI	SiO <sub>2</sub>	MgO	Fe <sub>2</sub> O <sub>3</sub>	Al <sub>2</sub> O <sub>3</sub>	CaO	Cr	TiO <sub>2</sub>	Ni
(%)	6,95	54,99	25,29	6,55	4,37	1,19	0,18	0,11	0,14

### 3.2.2 Samples used

The present study was made to tiles removed from facades that had been intervened for restoration purposes in Ovar. Twenty six glazed tiles of 14x14 cm were studied from which twelve are from the factory A.A.Costa, eight from J. Pereira Valente, one from a Lisbon factory Sacavém (14 x 6.5 cm) and five tiles with unknown production unit as in Table 11.

Table 11 – Tile references, pictures, production units and ceramic body type of the studied samples

Tile reference	Picture of the tile	Production unit	Ceramic body type
P8		Unbranded	calcitic
P9		A.A. Costa	calcitic
P10		J.P.Valente	calcitic
P14		Unbranded	calcitic
P18		Unbranded	calcitic
P19		J.P.V. e Filhos	calcitic
P20		J.P.V. e Filhos	<i>Pó de pedra</i>

P24		Unbranded	calcitic
P58		P.V.	calcitic
P59		A.A.Costa	calcitic
P66		A.A.Costa	calcitic
P78		A.A.Costa	calcitic
P87		Valente e Filhos Fab. loijas	<i>Pó de pedra</i>
P82		Valente, Lda	<i>Pó de pedra</i>
P89		A.A.Costa	calcitic
P98		J.P.V.	calcitic
P104		A.A.Costa	calcitic
P109		J.P.Valente	calcitic
P115		A.A.Costa	calcitic
P116		A.A.Costa	calcitic
P124		A.A.Costa	calcitic
P127		A.A.Costa	calcitic
P133		Unbranded	calcitic
P137		Sacavém	<i>Pó de pedra</i>

RJF229		A.A.Costa	calcitic
DA5		Valente e Filhos	<i>Pó de pedra</i>

## 3.2 Methods

The aim of knowing to be able to reproduce was this work guideline. To know is necessary to analyse through multiple analytical techniques that not only reveal the existing, but confirm or complement information previously obtained. In this chapter, all the analytical techniques used in the present study are presented as well as the reason for their choice.

### 3.2.1 Samples in powder

To enable the application of the selected techniques that require powder as analysing samples and to avoid materials mixing, the ceramic bodies from old wall tiles were separated from the remaining fragments of both glaze and mortar, using a mechanical petrographic cutting machine. After separation, the ceramic body was dried and milled in a fast agate mill (Figure 31) until a thin powder was obtained. This powder was used in X-ray diffraction, X-ray fluorescence, Fourier-Transform infrared spectroscopy and Thermogravimetry and Differential Scanning Calorimetry techniques. Particle size distribution was used for the replicas composite size characterization.



Figure 31 – Fast agate mill

### 3.2.1.1 X-ray diffraction – XRD

X-rays are used since the beginning of the 20<sup>th</sup> century as a way of crystalline phases identification (Fonseca 2000).

X-rays are a form of electro-magnetic radiation represented as “ $\lambda$ ”. These occur in the region of the electro-magnetic spectrum between 0.01 nm and 10 nm. This region is bounded on the short wavelength side by Gamma rays and on the long wavelength side by Ultra-Violet radiation (Figure 32). The X-ray wavelength is given in (nm) or, more commonly in the crystallographic world, in the older unit Angstrom ( $\text{\AA}$ ). Like all Electro-magnetic radiation, X-rays can be viewed both as waves and as particles (packets of energy, photons)

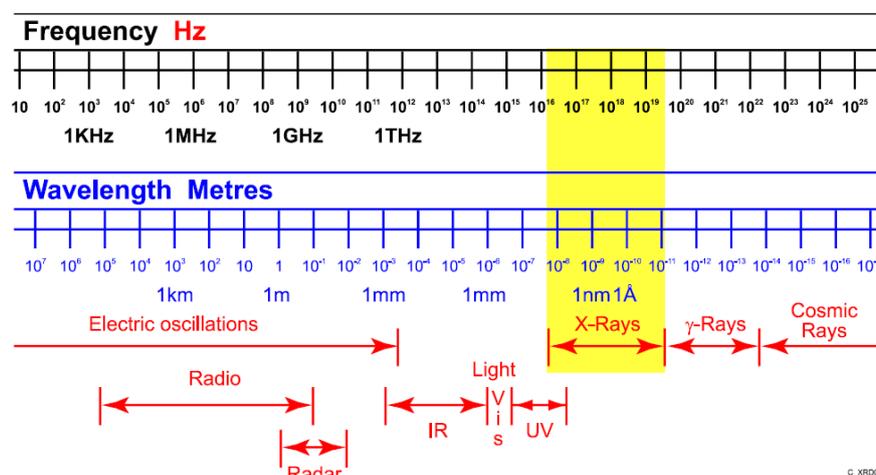


Figure 32 – Electro-magnetic spectrum (Rigaku)

X-rays can be generated when an atom is bombarded with high-speed electrons. The spectrum obtained, in the X-ray region of the Electro-magnetic spectrum is similar to that shown in Figure 32.

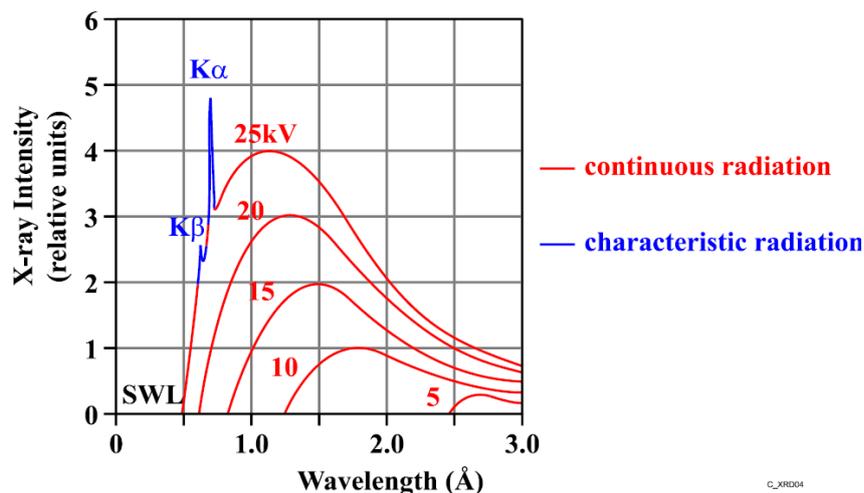


Figure 33 – X-ray spectrum of a molybdenum tube at different KV settings (Rigaku)

Figure 33 shows the spectrum of a Mo (molybdenum) tube at different tensions. The spectrum at lower tensions shows only a continuous band of X-rays but at a higher tension, 25 kV or higher, superimposed on this continuum, two discrete wavelengths appear the so-called characteristic lines. One of these characteristic wavelengths, usually the  $K\alpha$ , is used in X-ray diffraction.

When high-energy electrons strike the target (anode), orbital electrons can be removed from some of the target atoms. The removal of one or more electrons results in the atom becoming ionized. An ionized atom is in an unstable or excited state. One or more electrons within the atom will then move between the electron shells to stabilise the ionised electron. As the electron falls back to a lower electron shell, the atom emits an X-ray photon. The photon emitted is called after the shell towards which the electron will fall. Furthermore, there is a sub-division depending on the number of transition levels, where one level

transition will cause  $\alpha$  radiation (transition from L-shell towards K-shell will cause  $K\alpha$  radiation) a two level transition will cause  $\beta$  radiation and a three level transition  $\gamma$  radiation (Figure 34).

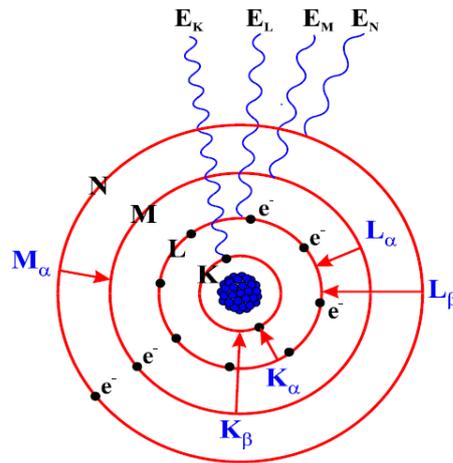


Figure 34 – Characteristic radiation (Rigaku)

A crystal is a solid with a regular and periodic arrangement and a natural shape of a polyhedron (Rigaku , Gomes 1979). Usually a crystal lattice is drawn as a set of parallel lines at a distance  $d$  where all atoms are situated in these planes. When a monochromatic beam falls onto a crystal lattice, a diffracted beam will only result in certain directions. As diffraction conditions, it is necessary that the waves emitted by the individual atoms are in phase with each other in the direction of detection. Other diffraction condition is that the incident beam, the diffracted beam and the normal to the reflecting surface all lie in one plane and the angle of the incident beam is the same as the angle of the diffracted one (Figure 35) (Rigaku , Gomes 1979).

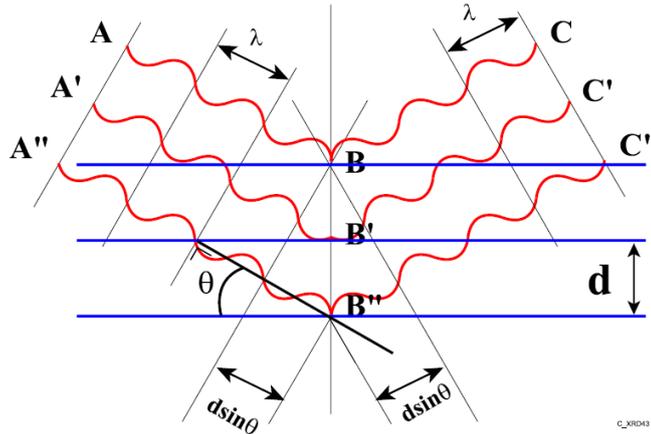


Figure 35 – Condition for diffraction of X-ray (Rigaku)

Bragg's law (fundamental equation of selective reflection) is fundamental for **d** calculation and is given by:

$$n\lambda = 2d \sin \theta$$

Where **nλ** is an integer wavelengths number, usually used number 1

**d** is the distance between the crystal lattice

One of the conclusions from Bragg's law is that the **d** value only depends on the unit cell parameters, but not of the atoms position in it (Gomes 1979).

X-ray diffraction of non-oriented powders was performed with a Rigaku Geigerflex D/max – C series apparatus, which uses  $\text{Cu}\alpha$  radiation with  $\lambda = 1.544 \text{ \AA}$  obtained under 40 kV/30 mA, and a scanning speed of  $3^\circ/\text{min}$  between  $4$  and  $80^\circ 2\theta$ . The phase identification was made by JADE 9 program using International Centre of Diffraction Data Powder Diffraction Files (ICDD PDF).

### 3.2.1.2 X-ray fluorescence - XRF

The X-ray fluorescence spectrometry (XRF) is a technique that allows the analysis of chemical elements atomic number greater than 9, in concentrations between 100% and few ppm (Gomes 1979).

XRF is not an absolute analytical method and the concentration of a given element is determined by comparing the intensity of the radiation emitted by an element in the sample, with the intensity of the radiation emitted by the same element existing in known quantity in a standard sample, attaining a relative accuracy of 0.1% to 0.3% (Rigaku).

When the sample atoms are irradiated by high energy photons X, electrons are ejected in photon form which creates some orbital vacancies; converting the atoms into unstable ions. To return the atom to its initial stable state, the orbital vacancies are filled by electrons from outer orbitals. Such transition, characteristic for each element, is accompanied by an emission of a secondary photon with energy equal to the energy difference between the initial and final levels. This phenomenon is known as fluorescence.

Pressed pallets were made with the ceramic body powder in a 4 cm diameter mould, containing 10 g of sample. The same press was used to press tiles replicas (Figure 36).



Figure 36 – Press used to make pressed pallets

The pallets were examined with an X-ray fluorescence (XRF) Panalytical's spectrometer, Axios model, having one Rh rod (Figure 37).



Figure 37 - Panalytical's spectrometer, Axios model

Experimental procedure for pressed discs:

- With the sample previously ground in an agate mill, it is dried at 110°C during 12 hours;
- To 10.0 g of dried sample is mixed 5 gouts of 2% Moviol (alcohol binder);
- The mixture is pressed to 15 ton in a 4 cm diameter mould;
- The analysis is performed.

The loss on ignition (L.O.I.) or weight loss on ignition is expressed as a percentage, whereas the weight lost by the sample after the test (thermal test), comparing the burned weight sample with the weight of the dry sample. The loss on ignition is due to volatile loss. The experimental procedure for L.O.I, given in percentage, is:

$$\text{L.O.I.} = (p_1 - p_2 / p_1) \times 100$$

- Weighing 1.5g ( $p_1$ ) of the sample in powder already dried at 110°C to a porcelain holder;
- Fire the sample at 1100°C during 3 hours;
- When cold, weigh the sample powder ( $p_2$ )

### 3.2.1.3 Fourier-Transformed infrared spectroscopy - FTIR

The Fourier Transformed Infrared Spectroscopy (FTIR) was used to evaluate the molecular vibrations in-plans related to mineral phases identified previously by XRD.

The selected samples were mixed with a KBr matrix in an equivalent proportion of 1:200, namely: 1 mg of grinded sample was mixed with 200 mg of KBr. This mixture has been carefully homogenised in an agate mortar. The powder obtained was put into a metal mould and subjected to a maximum pressure of 10 tons, under vacuum. A pressed disk of 13 mm diameter and 1 mm thick was obtained which was analysed perpendicularly to the infrared beam causing the molecular vibration of the constituents.

A Bruker Tensor 27 FTIR spectrometer in absorbance mode (Figure 14) was performed in the range 4000 - 400  $\text{cm}^{-1}$  wavenumber, equipped with a DTGS (deuterated triglycine sulphate) single plate detector (Figure 38).

The interaction of electromagnetic radiation with materials or chemical compounds was studied by spectroscopic techniques, applied to the energy levels of molecules. Typically, the vibrational transitions of the infrared electromagnetic spectrum are situated in the following three regions:

- a) Close infrared (harmonic region) from 12.500 a 4.000  $\text{cm}^{-1}$  wavenumber.
- b) Medium infrared (vibration-rotation infrared region) from 4.000 to 200  $\text{cm}^{-1}$  wavenumber.
- c) Remote infrared (rotation region) from 200 to 10  $\text{cm}^{-1}$  wavenumber.

The chemical bonds of the crystalline phases or chemical compounds have specific vibration frequency, which correspond to vibrational levels of the molecule. The infra-red spectra are produced by different modes of vibration and rotation of a molecule.

A vibrational mode in the infrared spectrum is promoted by the absorption of the incident energy, it is essential that there is dipole momentum change during the vibration. The vibration of two similar atoms against each other, such as oxygen or nitrogen atoms in their molecules, does not cause change of electrical symmetry, or dipole momentum of the molecule; these molecules do not absorb in infrared region.

In normal modes of vibration of a molecule the main participants of the vibration will be two atoms linked by a chemical bond. These vibrations have frequencies which depend primarily of the masses of the atoms that vibrate and the constant of the force of the bond between them. The frequencies are also slightly affected by other atoms bonded to the two vibrant atoms.



Figure 38 – Bruker Tensor 27 FTIR spectrometer

Molecular vibrations can be classified by axial deformation (or stretching) and angular deformation (bending) that can be symmetrical or asymmetrical. The angular vibrations can also be classified in- or out-of- plan.

The vibrational excitation is provided by periodic variation of electric dipole in the molecule during the vibrations; the energy transfer occurs by the interaction of oscillating dipoles with the oscillatory electric field of infrared radiation as long both vary in the same frequency. Only under these conditions the alternating electric field of incident radiation interacts with the molecule causing the observed spectra. It is important to note the existence of diatomic molecules homo- and hetero-nuclear because only the latter will produce vibrational absorption spectra. Molecules like  $O_2$ ,  $H_2$  among others are homo-nuclear and so will not produce the spectrum because there is no difference in the energy levels of the atoms. The spectrum is not only related with the energy levels but also with the types of vibrations present in the sample during their interaction with radiation. There are different types of vibrations. Basically, molecular vibrations can be classified into two types: vibration of axial

deformation (stretching) and angular deformation (bending). The axial deformations, or stretching, are radial oscillations of the distances between the nuclei while the angular deformation involves changes of the angles between the bonds or, as in asymmetric deformation mode off plan, changes in the angle between the bond containing plane and a reference plane.

The axial deformation types present in the studied crystal-chemical structures are axial and angular type (Figure 39). The axial deformation can be symmetrical or asymmetrical.

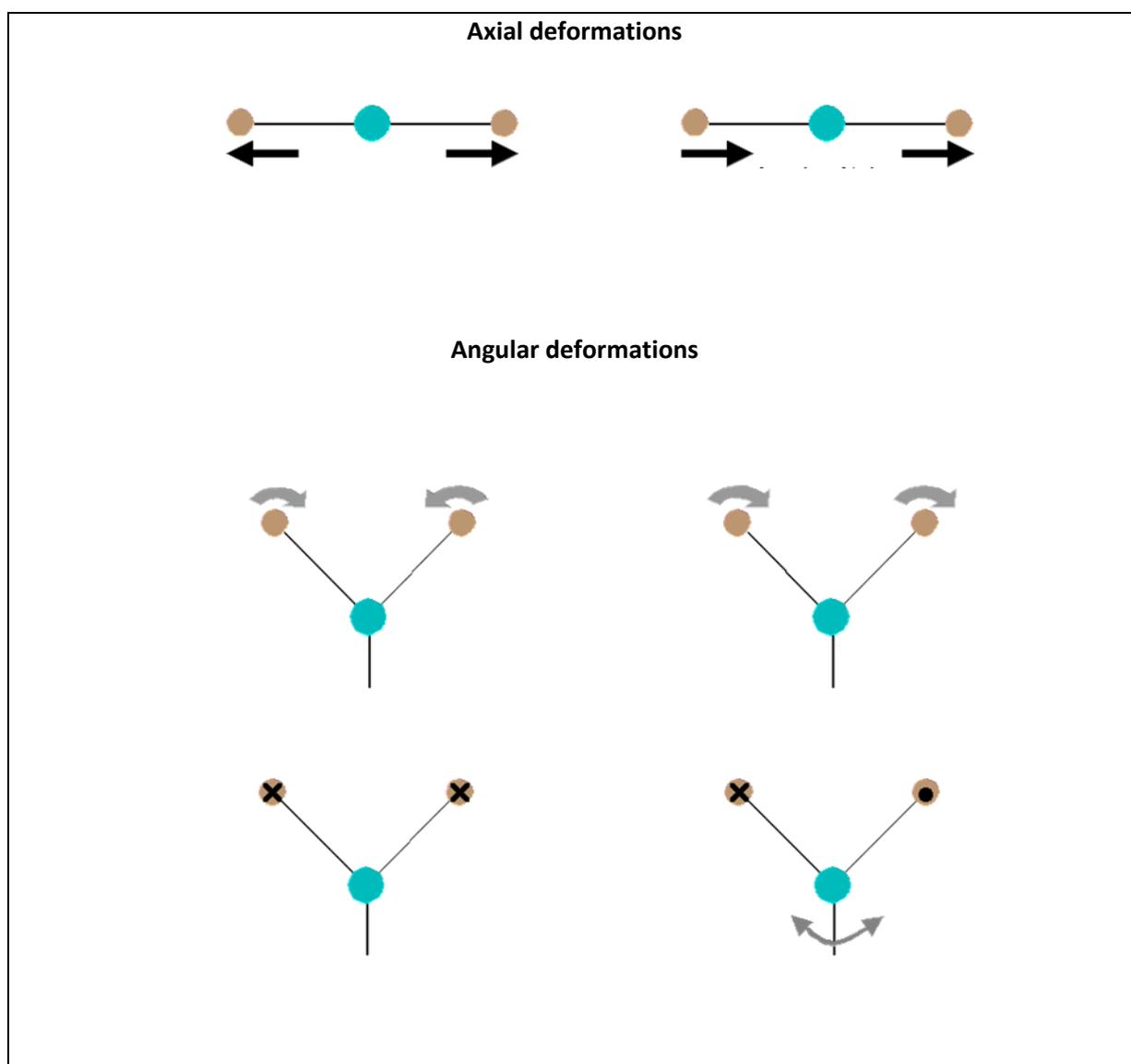


Figure 39 – Axial and angular deformation types (Nakamoto 1970)

The infrared spectra were obtained for representative samples previously characterized by x-ray diffraction. The identification of molecular vibrations in-plans took into account the position and type of axial deformation in relation to the chemical complexes representing the mineral phases that characterizes the selected samples.

#### **3.2.1.4 Thermogravimetry (TGA) and Differential Scanning Calorimetry (DSC)**

Simultaneous thermal analyses (TGA/DSC) measurements were carried out to characterize the mass change and energetic transformations of the sample during its heating. Thermal analyses (TGA and DSC) allow for the detailed determination kinetics and transformation features at temperatures that cause weight and energy variation. The thermal analysis apparatus used was a Netzsch STA 409 C. This system was equipped with a thermogravimetric-differential scanning calorimetry sensor, and aluminium crucibles were used for the tests.

In the present work differential scanning calorimetry was used to measure phase transition. This technique measured the energy required to keep both sample and reference at the same temperature along the defined heating curve. When the sample suffers a phase transition, whether the process is exothermal or endothermal, the apparatus measures the necessary heat to maintain both the sample and the reference at the same temperature.

The measurements were carried out between room temperature and 1100°C in a dynamic air atmosphere at a heating rate of 10°C/minute.

#### **3.2.1.5 Particle size distribution**

The sedimentation size analysis is based upon the fact that the measured equilibrium velocity of a particle through a viscous medium, can be related to the size of the particle by Stoke's law (Micrometrics 1995, Lima and Luz 2001):

$$D = Kv^{1/2} \text{ [}\mu\text{m]}$$

Where

$$K = \left[ 18 \frac{\eta}{(\rho - \rho_0)g} \right]^{1/2}$$

$D$  - is the diameter of the spherical particle (or its equivalent spherical diameter);

$v$  - is its equilibrium sedimentation velocity;

$\rho$  - is the particle density;

$\eta$  - fluid medium viscosity;

$\rho_0$  – fluid medium density;

$g$  – is the acceleration of gravity.

In practice, truly spherical particles are seldom found so it is universally accepted to specify the size of non-spherical forms in terms of a sphere of the same material that would have the same sedimentation velocity. In this case, it is usually used the term “equivalent spherical diameter”.

Data on the sedimentation velocity of suspended particles is usually obtained by measuring the concentration of particles remaining in suspension as a function of time. A dilute dispersion of the fine particle sample is stirred to render it homogeneous and then allow sedimentation without disturbing. By Stoke’s law a particle of diameter  $D$  will settle a distance  $h$  in time  $t$  according to the equation:

$$D = K \left( \frac{h}{t} \right)^{1/2} \text{ [}\mu\text{m]}$$

The particle size analyser used was the SediGraph 5100 (Figure 40) that is able to identify particles up to 0.1  $\mu\text{m}$  by combining the particle falling rates method and the amount of X-ray absorption by the suspension method.



Figure 40 – Sedigraph 5100

### 3.2.2 Techniques that require samples without glaze and tile back

Dilatometry and calcination tests were performed in some of the samples under study. To these tests, the glaze and the back of the tiles were cut off to avoid material interference in the results.

#### 3.2.2.1 Dilatometry

Linear thermal expansion is the dimensional variation of the tested specimen (glaze or ceramic body) with temperature increase and decrease. This dimensional variation has its cause in the thermal vibrations of the tested material. For linear expansion coefficient, a high-temperature Netzsch- DIL 402 PC dilatometer was used (Figure 41). The dilatometer system includes a graphite furnace, an alumina protective tube and a sample holder, and it allowed measurements to be carried out between room temperature and 1200°C under static oxidizing conditions. The system was calibrated using an alumina standard prior to the samples tests.

The samples of the ancient ceramic bodies were cut to 25 mm long and 5 mm thick stripes and were submitted to a heating rate of 10°/ min from 30° until 400° C. Calculations were performed by the apparatus software.



Figure 41 - Netzsch- DIL 402 PC dilatometer (GmbH 2005)

### 3.2.2.2 Calcination tests

Calcitic samples calcination was performed in small ceramic body pieces in two different tunnel industrial kilns ( Figure 42) in oxidation atmosphere: one with a 180 minutes cycle and 1180° C as set point (1150° C ring temperature) and another with a 300 minutes cycle and 1100° C as set point (1100° C ring temperature). *Pó de pedra* samples were calcinated in the kiln with 1150°C ring temperature and also in another with 360 minutes cycle and 1380°C as set point (1360°C ring temperature). The cycles and temperatures used was not a personal choice but it was what was available in the ceramic industry where the tests could be made.

The ceramic bodies pieces were weighed, colour checked and measured before and after re-firing. XRD analyses were performed before and after calcination to verify weight loss, contraction due to sintering and phase changes.



Figure 42 – One of the ceramic industrial kilns used

This sort of test can give information about the first firing suffered by the ceramic body. If the calcinated sample suffers no alteration with a new firing, it means that it was originally fired at a similar temperature; if anything changes (except the weight) it means that the original firing was made under a lower enthalpy.

### 3.2.3 Entire tile observation techniques

In several analytical techniques pieces of the entire tile constituents were used; glaze, ceramic body and ceramic back, after a proper mortar cleaning. These techniques were SEM, SEM/EDS, optical microscope, porosimetry, water absorption percentage and water absorption due to capillary action.

#### **3.2.3.1 Scanning Electron Microscopy and Energy Dispersive Spectroscopy - SEM and EDS**

For SEM/EDS two kinds of sample preparations were required, considering what was intended to be obtained as information. For mapping of elements, polished samples were required, while for structural observations fractured tiles were used.

To enable the visualization of glaze/ceramic body interface, vertical cuts with 1.5 cm length and 0.5 cm height were made in the tile with a sharp mechanical cutting machine, obtaining the simultaneous observation of the glaze, glaze/ceramic body interface and ceramic body. The samples were mounted in resin (Figure 43) and polished with 30, 15, 9, 6, 3 and 1  $\mu\text{m}$  diamond pulp until a smooth surface was obtained. Due to the fact that samples of ceramic body suffer easy degradation in the polishing process, in some samples it was not possible to obtain an even surface.



Figure 43 – Resin mounted sample for surface polishing

A high- vacuum scanning electron microscope (SEM) Hitachi SU-70 (Figure 44) with 1 nm resolution was used, equipped with energy-dispersed spectroscopy (EDS) Bruker Quantax 400 with the feature of less than 133 eV energy resolution . An acceleration voltage of 15 kV was used for observation and imaging and 30 kV for qualitative and quantitative element mapping.



Figure 44 – Hitachi SU-70 high-vacuum scanning microscope

### 3.2.3.2 Optical microscopy

To enable the visualization of glaze/ceramic body assemblance in order to identify different typologies of glazing (the presence of engobe under the glaze coating, glaze degree

of opacification), perpendicular fractures to the glaze surface were made and visualized in an optical microscope Leica EZ4HD (Figure 45). It is a microscope with a magnification range from 8x to 35x with an object field diameter of 5.7 to 25 mm and a working distance of 100 mm. The microscope used allows images visualization and recording in a PC.

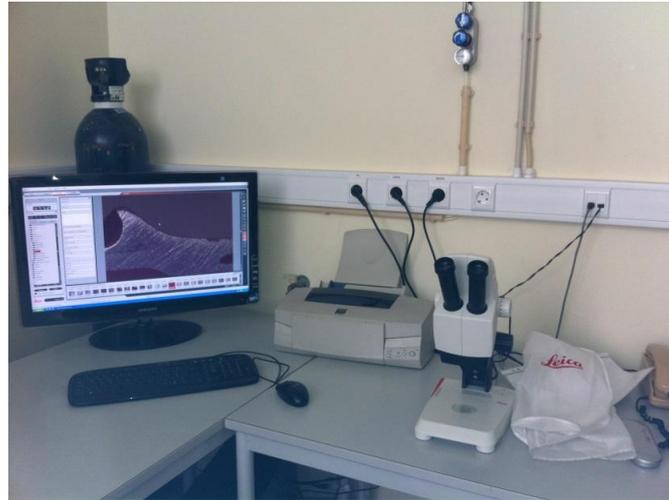


Figure 45 – Optical microscope Leica EZ4HD

### 3.2.3.3 Porosimetry

The open pores size and its distribution in the porous network, influence most of the properties of ceramic materials as the mechanical strength, thermal conductivity, thermal shock resistance, among others. The porous network besides being very useful to facilitate the penetration of mortar binder in the ceramic body, improving adhesion is a moisture input channel to the structure of the ceramic body when applied.

The mercury porosimetry provides, among others, the average value of the pore size, total pore area and density of the material. It is often used for the study of porous materials with pore size greater than 50nm because it is very efficient for pores from nano size until some hundred microns(Rigby and Edler 2002).

Mercury is used because at room temperature, it does not react with most of the materials and also for its high surface tension which makes it nonwetting. In order for mercury to penetrate into pores, an external pressure is applied so as to overcome the surface

tension of mercury and the radius of curvature formed between mercury and solid particle. The imposed pressure and pore size are usually related in this method through Washburn's equation (Rigby and Edler 2002):

$$p = - \frac{2\gamma \cos \theta}{r}$$

Where:

$p$  is the necessary pressure to force mercury into the pores [MPa]

$\gamma$  is the surface tension

$\theta$  is the contact angle

$r$  is the pore radio [nm]

Washburn's equation is applicable to cylindrical pores which is not always the case in the materials studied, because often the pore is wide in the interior and narrow on the exterior (bottle-neck type) trapping mercury inside. Another approach of this essay is to estimate the contact angle between mercury and the pore wall using the approximate value of 130°, knowing, however, that this angle varies with the sample nature (Carvalho 2002).

The equipment used was the AutoPore IV Micrometrics Mercury Intrusion Porosimeter which operates at a pressure range between 0.003 and 227 MPa thus allowing the intrusion of mercury in pores of diameter of 5.5 nm to 360 µm.

#### **3.2.3.4 Water absorption**

Glazed tiles were tested to determine water absorption according to EN ISO 10545-3: Determination of water absorption (Qualidade 2004). The tiles samples were dried in an oven adjusted to 110°C until constant mass was achieved (48 hours). Each tile was weighed in a balance with an accuracy of 0.02% and the mass of the tested specimens and each value was

recorded as  $m_0$ . After that the samples were put into boiling water, with no contact between them, for two hours. After two hours, the heat source was removed and the samples stayed immersed until the water cooled to room temperature (4 hours). A cloth was wetted and wrung out by hand and placed in a flat surface where each sample was lightly dried in each side. After light drying, each sample was weighed and its results were recorded as  $m_1$ . For each tile sample, the water absorption, expressed as a percentage of the dry mass, was calculated using the equation:

$$\text{Water absorption \%} = \frac{m_1 - m_0}{m_0} \times 100$$

In which:  $m_0$  is the dried sample weight

$m_1$  is the wet sample weight

### **3.2.3.5 Water absorption coefficient due to capillary action**

The water absorption coefficient due to capillary action was tested based in the EN 1015-18 standard with modification as this standard is used for hardened mortar.

The tiles samples used had 14 x 7 cm with 6 mm thickness. Firstly they were dried at 110°C until constant mass (48 hours), after each sample was weighed in a balance accurate to 0.02%, the mass of the tested specimens and each value was recorded as  $M_0$ . A tray large enough to contain several samples at the time was prepared with a geotextile on its bottom. It was filled with water so the samples would be immersed in one face by 2mm. After dipping the samples in the water they stayed there for, 2, 3, 4, 5, 10 and 15 minutes test intervals. The upper limit of time adopted in the trial was 15 minutes, since after that the ceramic body was completely saturated due to its small thickness.

After each dipping time, the sample was light cleaned and weighed ( $M_1$ ) after which it was returned to the water to complete the immersion time.

The coefficient of water absorption is by definition equal to the slope of the straight line linking the representative point of weight obtained in the different time dipping intervals. The equation used to calculate water absorption coefficient due to capillary action,  $C$ , was:

$$C = \frac{M1 - M0}{A \sqrt{\Delta t}} \quad [kg/m^2 \cdot h^{\frac{1}{2}}]$$

Were:

$A$  is the dipped sample area [m]

$\Delta t$  is the difference of each dipping times [h]

### 3.3 Replicas pellets preparation

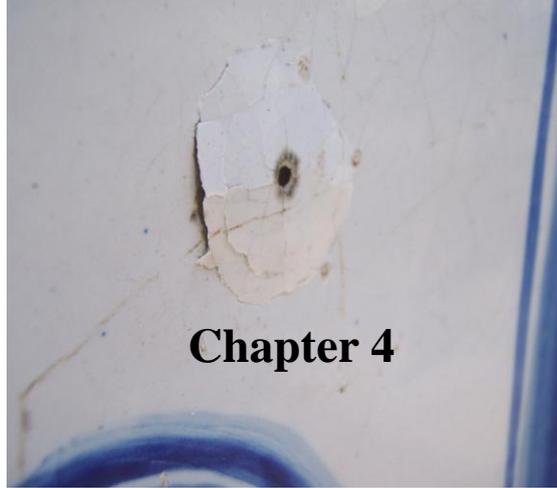
The raw materials were completely dried and the grinding of the quartz and calcite was made in a fast agate mill (Figure 31). To control the milling evolution, a Sedigraph 510 Micrometrics apparatus was used. After achieving the desired particle size, slurry with the quantities of each raw material to be tested was made to guarantee homogeneity in the distribution of all the raw materials. The slurry was dried and crushed until a fine powder was obtained. 10 grams of this composite was weighed and pressed in the lab press and mold in Figure 36. The mould produces pellets with 4 cm of diameter and several pressing pressures were tested as it was one of the variables to be studied as it highly influences the ceramic body porosity.

The pellets were fired in an electrical laboratory furnace with the capacity to reach 1300°C with a controller allowing designing all the heating steps (other variable to be studied as it influences mineralogical phases to be developed as well as microstructure features of the ceramic body).

## References

- Carvalho, Maria Arlete (2002). Expansão por humidade de materiais cerâmicos de construção. Master. Universidade de Aveiro.
- Fonseca, António Tomás (2000). Tecnologia do processamento cerâmico. Universidade Aberta. Lisboa.
- GmbH, N.-G. (2005). "Improving zircónia ceramics through thermoanalytical characterization." [http://www.netzsch-thermal-analysis.com/us/industries-branches/ceramics-glass.html?tx\\_solr%5Bpage%5D=3&tx\\_solr%5Bfilter%5D%5B0%5D=industryCategory%3ACeramics%20%26%20Glass](http://www.netzsch-thermal-analysis.com/us/industries-branches/ceramics-glass.html?tx_solr%5Bpage%5D=3&tx_solr%5Bfilter%5D%5B0%5D=industryCategory%3ACeramics%20%26%20Glass) Retrieved May 2013.
- Gomes, C. F. (1979). Raios X no estudo de materiais. Universidade de Aveiro.
- Lima, R. M. F. and J. A. M. Luz (2001). Análise granulométrica por técnicas que se baseiam na sedimentação gravitacional: Lei de Stokes. Revista Escola de Minas. Ouro Preto - Brasil, Scielo Brasil. 54, nº2.
- Micrometrics (1995). SediGraph 5100 Operation manual. Micrometrics.
- Nakamoto, K. (1970). Infrared Spectra of Inorganic and Coordination Compounds. New York.
- Qualidade, I. P. (2004). EN ISO 10545-3. Determination of water absorption of open porosity 10545-3.
- Rigaku SuperQ Version 3.0. Reference Manual - XRD Theory, Rigaku.
- Rigby, S. and K. Edler (2002). "The influence of mercury contact angle, surface tension, and retraction mechanism on the interpretation of mercury porosimetry data." Journal of Colloid and Interface Science 250: 175-190.
- Velho, L., C. Gomes and C. Romariz (1998). Minerais Industriais: geologia, propriedades, tratamentos, aplicações, especificações, produção e mercado. Universidade de Aveiro.





## Chapter 4

## Results and discussion

---



## 4.1 Introduction to experimental work

The objective of the present work is focused on the **old tile ceramic body** characterization to replicate it and on the old tile glaze characterization. Although the glaze is the part of the tile that is more evident when the tile is applied on the wall, it is the ceramic body that is the structural element becoming, in the aim of the present work, the element to be understood and replicated although both entities are important. If on the one hand the ceramic body confers the mechanical support, on the other hand it is the glaze, besides its aesthetical importance, that gives the tile waterproof ability, higher chemical and physical durability. Therefore, the experimental work is divided into three main subjects: **old tiles ceramic body** and glaze characterization, risk factors and linked tile pathology characterization, suggestion for ceramic body technical replicas. Firstly, the determination of the technical characteristics of the old tiles under study was performed in order to create a basis for a proposal of a new product with technical characteristics as similar as possible to those of the old tiles, but trying to avoid technical non-conformities, such as crazing glaze, of the latter.

**Analytical techniques** such as **XRD, XRF, FTIR, TGA, SEM/EDS**, mercury pore intrusion, water absorption due to capillary rise and water absorption percentage tests **were undertaken to characterize the ceramic bodies**. The samples' **glazes were studied with SEM/EDS and optical microscopy**.

In this study the first step taken was the **old ceramic bodies' characterization** by **XRD** and XRF, in order to have a work basis for the selection of raw materials and to achieve a basis for the determination of proportions to be used. **The mineralogical phases present in XRD** were important as a clue to understand which **chemical elements tiles** were produced with and at **which temperature production** processes took place. Much has been written about the mineralogical and structural modifications suffered by clays when subject to fire transformation action as well as the main crystalline phases that appear when mixing up to 3 oxides and which are defined in phase diagrams (Konta 1995, Lee, Kim et al. 1999, M.M.Jordán, Boix et al. 1999, M.P.Riccardi, B.Messiga et al. 1999, Benedetto, R.Laviano et al. 2002, Gomes 2002, Trindade and al 2008, Baccour 2009, M.S.Tite 2009), one might think that being in the presence of a given crystalline phase would undoubtedly give the right answer to the question of the firing temperature of the object in question. That is not always

true, especially when the system composition is more complex than a mixture of 3 oxides as different mixtures of oxides can give different phase transformation temperatures. The challenge takes expression when, as in the case of tiles, there is a wide variety of oxides cohabiting in the array of the original ceramic body. Under these conditions, only the experimental trial leads to some answers.

The genesis and relative amount of phases in a tile ceramic body depends on the **raw materials** used and enthalpies provided during firing. These elements are the ones **responsible for the ceramic body thermal expansion coefficient** as well as for the moisture expansion behaviour, that is why its importance to be replicated. The tile component that was subjected to a more rigorous approach was calcite as it was not clear that the quantity analysed in the old tiles was only due to the tile raw materials or also due to an exterior income. In this case, the salt intrusion causing pathology misleads the real tile calcium content. Reaching the **raw ceramic body composition** is a complex task as the original raw materials are unknown and new raw materials with other oxide percentage content have to be used with similar final results.

To reach a technical replica with the same water behaviour as that of the ancient tiles, it is important to prevent faster degradation of the other tiles when applied together in the façade. Porosity determination, water absorption by capillary action, porosimetry and water absorption percentage were performed in the old ceramic bodies to better characterize them and to adjust replica's raw materials particle size, pressing pressure and firing cycle. Porosity is manufacturing process dependent as raw materials type and their particle size distribution, as well as pressing pressure are very important parameters for size and amount of the porous network.

The glaze/ceramic body interfaces of the old tiles were studied, together with a contemporary tile, to evaluate chemical diffusion as a way of understanding the glaze firing temperature, together with its importance in the glaze detachment pathology. It is expected that the chemical interpenetration between the two bodies is greater, the higher the temperature of the glaze firing temperature. It was expected that the larger the interface, the more resistant to glaze detachment the tile would be.

The harmony of a facade is given by its appearance. Glaze crazing is a common pathology spread in facades of nineteenth century tiles, almost transmitting an idea that glaze crazing characterizes most of these products. This idea should not prevail as many of the

ancient tiles do not present glaze crazing revealing a well-established knowledge on how to produce and apply adequately.

After the ceramic body characterization it became necessary to **characterize the glaze**, regarding both glazing techniques and chemical composition. These were subjected to analysis trying to establish glaze crazing factors. Glazing techniques versus compositions, ceramic body type and thermal expansion coefficients were the main factors attended to in this study. Crazing was also analysed taking into account glazing technique and glaze chemical composition.

A hypothesis is presented, based on results from all the studied samples, for a probable cause why *pó de pedra* tile glazes suffer from glaze crazing, and why all the tin glazes in calcitic ceramic bodies presented no crazing. From the present work it may be inferred that glaze crazing existed while new production techniques were not mastered. One cannot forget that before the existence of analytical apparatus like the dilatometer, knowledge was acquired on a trial and error basis.

Degradation motives or risk factors for the integrity of tiles are several. In the present study some of them are pointed out but a special focus is given to glaze detachment risk factors. The importance of the degradation impact of salts crystallization near the glaze/ceramic body interface was studied.

Glaze detachment was studied further because is a well visible pathology and, at the same time, it is an exterior water penetration means to the facade contributing to its faster degradation. To have an idea of the importance of this pathology in the 19<sup>th</sup> century facades, a street of Ílhavo, a town near Aveiro, with 54 houses with tile facades was subjected to statistics analysis. The conclusion taken was that 33.3% of the facades suffered from glaze detachment, becoming the most significant pathology of the tiles in the street in question. From other observations in other towns one gets the certainty that glaze detachment is the most severe pathology in seaside towns (other realities are not studied by the author).

Two contemporary tiles used in restoration as material basis for pictorial replicas (replicas where only the colour and type of drawing is alike to the old ones) were studied to evaluate their similarity in terms of technical characteristic with those of the old ones.

## 4.2 19<sup>th</sup> century tiles characterization

### 4.2.1 Ceramic body

Despite the fact that the production of glazed ceramic wall tiles in Portugal was initiated in the 16<sup>th</sup> century, then only accessible to the Church and nobility, only by the end of the 19<sup>th</sup> century with the introduction of new industrial processes was their use spread among people of middle/high classes, giving birth to the national trend of using tiles on building facades. Several cities of costal Portugal are very good examples of this cultural reality, displaying an immense collection of tile coated facades. Despite the very broad set of specimens dated from those early days, not much is known about the technical characteristics of Portuguese earthenware wall tiles (Cordeiro 1996).

In the Oporto production region, the so-called *calcitic pastes* were the most commonly used, since most of the existing tile ceramic plants were also faience tableware producers. For those production units, the most simple and practical thing to do was indeed, to use for wall tiles and for tableware products the same ceramic body and glaze as that which was used for tableware (Ferreira 2009). If on the one hand, the calcitic ceramic body was practical, on the other hand the glaze was expensive since its undesirable colour due to the presence of colouring elements like iron oxide, had to be hidden by an expensive opacified lead glaze. Tin oxide was the most common opacifier despite being a costly and imported product (Leão 1999). A different product was needed to avoid such an expensive glaze.

In the second half of the 18<sup>th</sup> century, Wedgwood, an English potter, formulated a new composition for the faience by mixing clay without coloured oxide with finely ground quartz sand and then firing this until the ceramic body presented no porosity creating the so called stoneware. In Portugal some production units used an adaptation of the English formula to low temperature so the fired ceramic body presented white colour but porosity far from the zero presented by the English stoneware. In this way, instead of simple clay (or mixture of clays) factories that introduced this technical novelty began to use a mixture of clays without iron with very fine ground quartz (called *pó de pedra*) (Leão 1999). *Pó de pedra* (stone dust) meaning kaolinized granitic rock or kaolin bearing quartz sand, both reduced to fine powders is characterized by a very white ceramic body coated with a transparent glaze. *Pó de pedra*,

being a ceramic mixture without lime or magnesium oxide, has less gas liberation during firing, resulting in a ceramic body with low volume of open pores but with larger pores, comparing with calcareous tiles (Cultrone, Sebastián et al. 2004). The final result was a white ceramic body, which dispenses the tin oxide glaze as a background for decoration purposes. The second firing stage or glaze firing was carried out at temperatures between 900 and 1200° C (Leão 1999). This amendment not only improved the mechanical qualities of the tile, but also decreased the manufacturing cost (Leão 1999, Ferreira 2009).

A statistic made with the present work (in item 4.2.2) and also based on another author' work (Ferreira 2009), reveals strong evidences that this kind of tile was not much used in the Northern part of Portugal.

The research carried out and presented in the present item focused on the old tile characterization, the probable raw materials used and on the probable manufacture technology of the ceramic body, encompassing both calcitic and *pó de pedra* tiles.

Twenty five samples of glazed ceramic wall tiles produced in the Oporto region, north of Portugal, from the late 19<sup>th</sup> century and early 20<sup>th</sup> century, were studied in an attempt to improve the knowledge on these materials and to create a basis for their replicas for restoration purposes. Sample references are the ones attributed originally by Ovar's restoration technicians that collected them in several Ovar house facades. Each reference corresponds to a different facade that was interventioned for conservation/restoration purposes. In this way, the samples are a random sampling of the dozens of Ovar tiles facades. Two types of ceramic bodies were found: calcitic and *pó de pedra*. All the tiles available for the present study were 15x15 cm. Not all had the production unit marked in the tile back, but most of the sampled tiles had the mark from the production units: J. Pereira Valente and A.A. Costa (Devesas). From all the samples obtained only 15% were *pó de pedra*. The number of specimens is rather small (only 4 samples) revealing the production tendencies of the time in question.

**Samples powder** was used to **determine their mineralogical and chemical composition, using XRD, FTIR, TGA and XRF techniques.**

Glazed tiles were tested to determine water absorption according to EN ISO 10545-3: Determination of water absorption of open porosity (Qualidade 2004), and the water absorption coefficient due to capillary action was tested according EN 1015-18, but using

different test times. As tiles are not thick enough (6 mm), 2, 3, 4, 5, 10 and 15 minutes test intervals have been practiced.

**Pore dimension** by mercury intrusion was performed in small **ceramic body pieces** as well as **SEM/EDS and optical microscope observations**.

Samples calcination was performed in small ceramic body pieces in three different tunnel industrial kilns: one with a 180 minutes cycle and 1180° C as set point (1150° C ring temperature), another with a 300 minutes cycle and 1100° C as set point (1100° C ring temperature) and a third with 360 minutes and 1380° C as set point (1363° C ring temperature). The ceramic pieces were weighed, and measured before and after calcination. XRD was performed before and after calcination.

#### **4.2.1.1 X- ray diffraction analysis**

During the ceramic process, chemical and particularly structural transformations take place to attain the system stability. Thus, some minerals collapse once their crystal structures reach their stability limit and simultaneously, others will form (Gomes 2002, Pardo and al 2011).

When analysing a XRD pattern of a fired composite, it cannot be forgotten that the technological properties of the materials present in the sample depend on their raw mineralogical composition, grain size distribution, processing and firing conditions (Konta 1995). During the firing process chemical and particularly structural transformations take place in the tile so that the system stability is continuously attained (Gomes 2002, Pardo and al 2011).

The 26 tiles under study where XRD analysed. Table 12 shows the typical high temperature crystalline phases being identified in the studied samples by XRD, using their specific diffraction patterns and maxima. The 9 crystalline phases present in Table 12 occur in simultaneous in some calcitic samples, revealing the complexity of the studied tiles. On the other hand, *pó de pedra* ceramic bodies present 4 crystalline phases, at the most.

It should be noted that **calcite was identified by XRD** in all calcitic samples and in one *pó de pedra* sample (P20). 53.8% of the samples present portlandite and 30.8% present

calcium sulphate, revealing that some of the calcium present in the ceramic body is not stable (the case of portlandite) or has already reacted with environmental pollution or ground water sulphates. In the course of the present work it will be demonstrated that the ceramic body has been originally fired at a temperature high enough to decompose all the calcite present as raw material (section 4.2.1.4 – Calcination tests) and the mentioned unexpected crystalline phases are secondary phases (section 4.2.1.5 – Microstructure).

Table 12– **Minerals and crystalline phases** present in the samples under study

	Calcitic ceramic bodies	<i>Pó de pedra</i> ceramic bodies
<b>quartz</b> (SiO <sub>2</sub> )	**	**
<b>Calcite</b> (CaCO <sub>3</sub> )	**	*
<b>gehlenite</b> (Ca <sub>2</sub> Al <sub>2</sub> SiO <sub>7</sub> )	**	--
<b>diopside</b> (CaMgSi <sub>2</sub> O <sub>6</sub> )	**	--
<b>hematite</b> (Fe <sub>2</sub> O <sub>3</sub> )	*	--
<b>mullite</b> (Al <sub>2</sub> O <sub>3</sub> SiO <sub>2</sub> )	**	**
<b>crystalite</b> (SiO <sub>2</sub> )	*	**
<b>anorthite</b> (CaAl <sub>2</sub> Si <sub>2</sub> O <sub>8</sub> )	**	--
<b>portlandite</b> Ca(OH) <sub>2</sub>	*	--
<b>calcium sulphate</b> (CaSO <sub>4</sub> )	*	--

Note (\*) – not present in all samples

(\*\*) – present in all samples

( -- ) – never present

Figure 46 shows the XRD pattern of a calcitic ceramic body presenting the six crystalline phases present in all calcitic ceramic bodies.

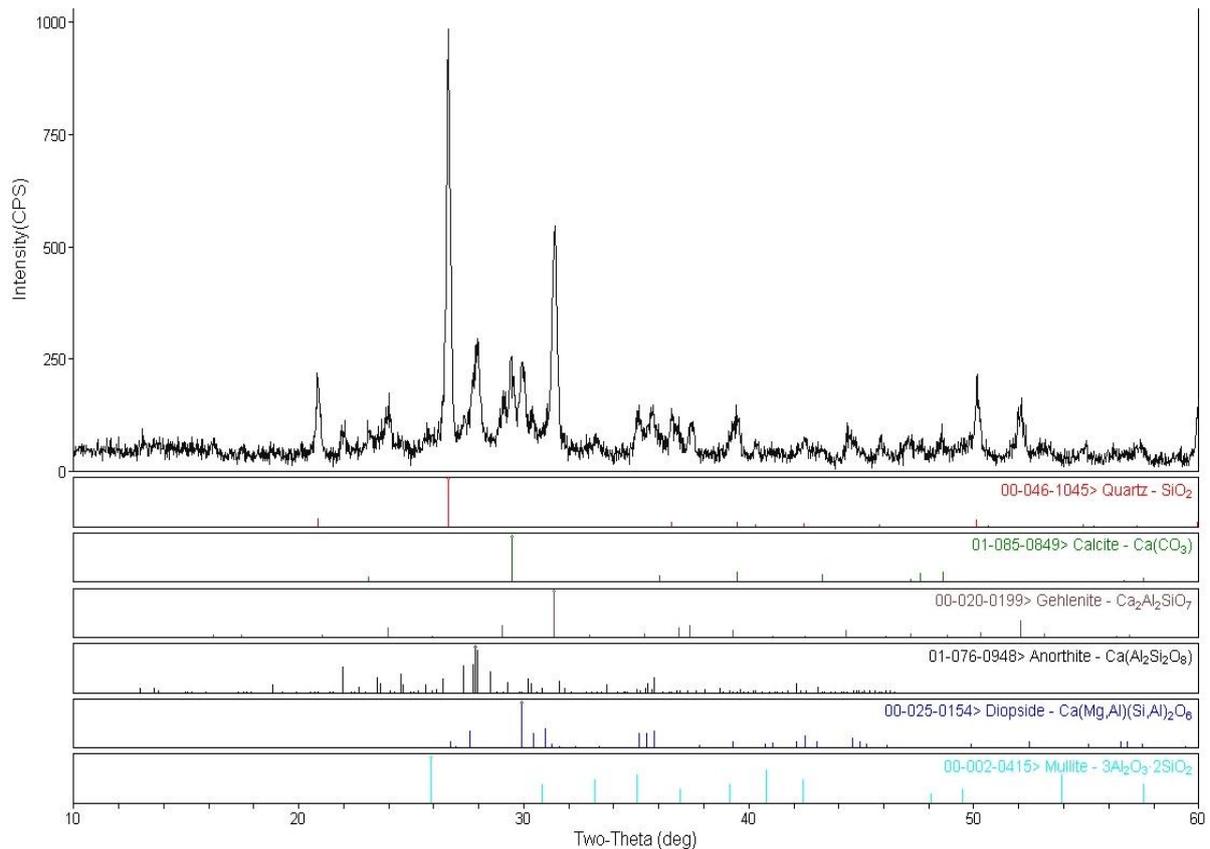


Figure 46 - X-ray diffraction maxima of a calcitic ceramic body

Figure 47 portrays a sample XRD pattern with a typical *pó de pedra* ceramic body. Comparing Figure 46 and 47, it can be easily seen that the ceramic bodies crystalline phases are quite different, revealing different raw materials used in the production of each kind of ceramic body. While calcitic ceramic bodies present 4 oxides, *pó de pedra* only exhibit 2.

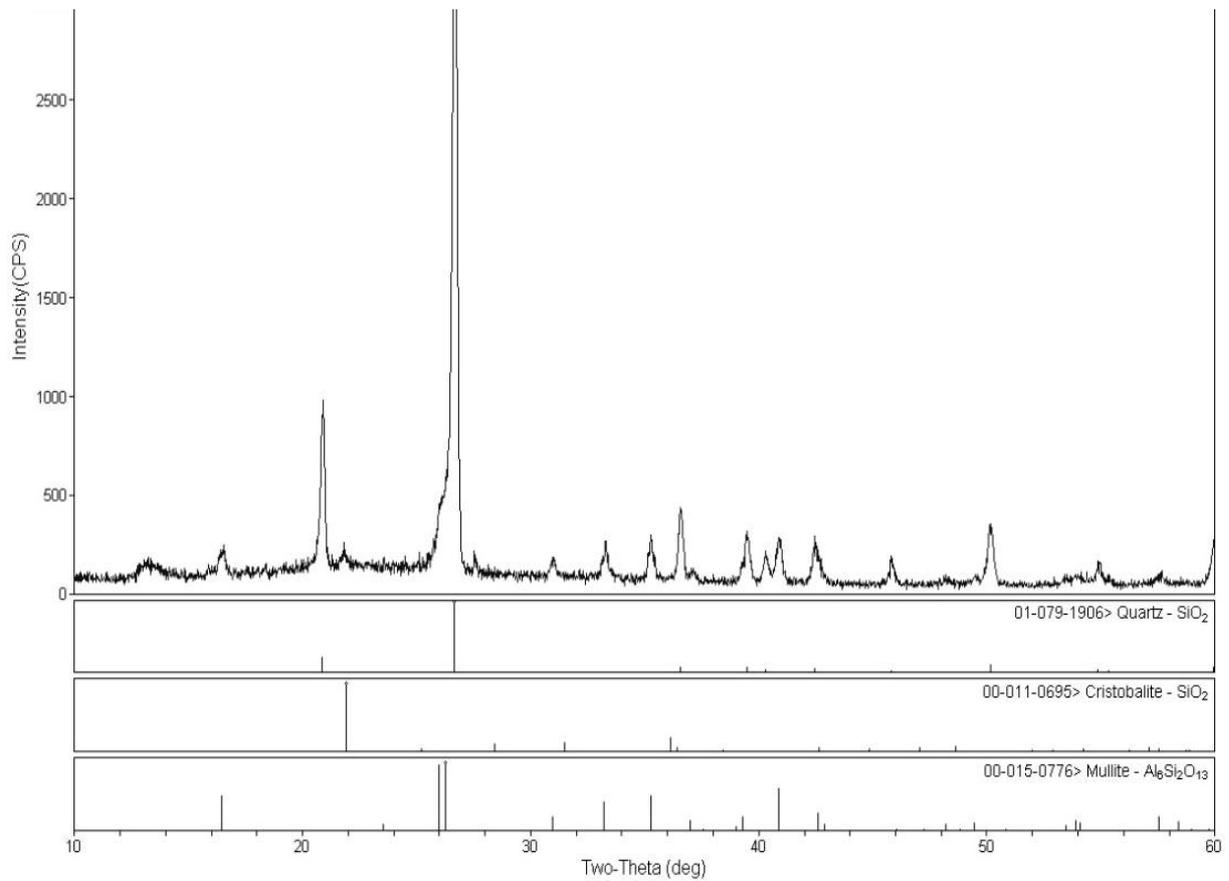


Figure 47 – X-ray diffraction maxima of a *pó de pedra* ceramic body

#### 4.2.1.2 X-ray fluorescence analysis

Table 13 shows the XRF results obtained for the 26 samples under study in which only the analytical data corresponding to the major elements is displayed.

Table 13 – **Chemical analysis** data of the studied samples, **obtained by XRF**

<b>Calcitic ceramic bodies</b>								
Oxide [%]	Na <sub>2</sub> O	MgO	Al <sub>2</sub> O <sub>3</sub>	SiO <sub>2</sub>	K <sub>2</sub> O	CaO	Fe <sub>2</sub> O <sub>3</sub>	L.O.I
Average value	0.4	3.9	17.6	43.8	1.8	23.6	3.3	4.5
Minimum value	0.3	2.0	16.2	40.2	0.9	20.0	2.9	2.7
Maximum value	0.9	6.7	22.3	46.1	2.5	28.3	3.9	6.6
<b>pó de pedra ceramic bodies</b>								
Oxides [%]	Na <sub>2</sub> O	MgO	Al <sub>2</sub> O <sub>3</sub>	SiO <sub>2</sub>	K <sub>2</sub> O	CaO	Fe <sub>2</sub> O <sub>3</sub>	L.O.I
Average value	0.3	0.2	23.7	71.5	1.5	1.1	0.6	0.6
Minimum value	0.2	0.1	22.5	70.2	1.4	0.7	0.5	0.2
Maximum value	0.4	0.2	26.1	73.4	1.7	1.8	0.7	1.1

It can be seen in Table 13 that *pó de pedra* samples have small quantity of Fe<sub>2</sub>O<sub>3</sub>, and the main constituents are Al<sub>2</sub>O<sub>3</sub> and SiO<sub>2</sub>, which explains the ceramic body white colour and the prevision of a considerable fire resistance. These ceramic bodies are not free from calcium, presenting as maximum value of 1.8% in P20, explaining the calcite crystalline phase seen in P20 XRD.

Calcitic tiles are characterized by high calcium content as well as an important quantity of iron oxide. The presence of magnesium in quantities that go from 2.0% until 6.7%, reveal a magnesium raw material supplier that should be or talk or dolomite. To better understand the high values of L.O.I. presented by calcitic samples thermal gravimetric analysis (TGA) and Fourier Transformed Infrared Spectroscopy (FTIR) were performed.

#### 4.2.1.3 Thermal Gravimetric Analysis and Fourier Transformed Infrared Spectroscopy

In order **to confirm XRD** and **XRF findings**, thermogravimetry (TGA) and **Fourier Transformed Infrared Spectroscopy (FTIR)** were performed.

In Figures 48 to 50, thermogravimetry of P89, P127 and P133 samples can be seen. Their thermogravimetric behaviour is quite similar, showing an exuberant peak of mass loss between 724°C and 766°C that corresponds to calcium carbonate decomposition.

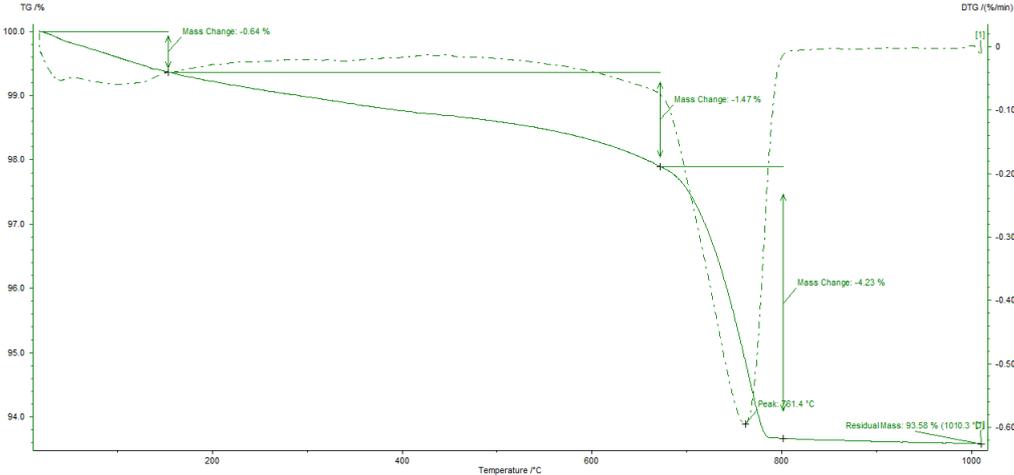


Figure 48 – TGA of P89 sample

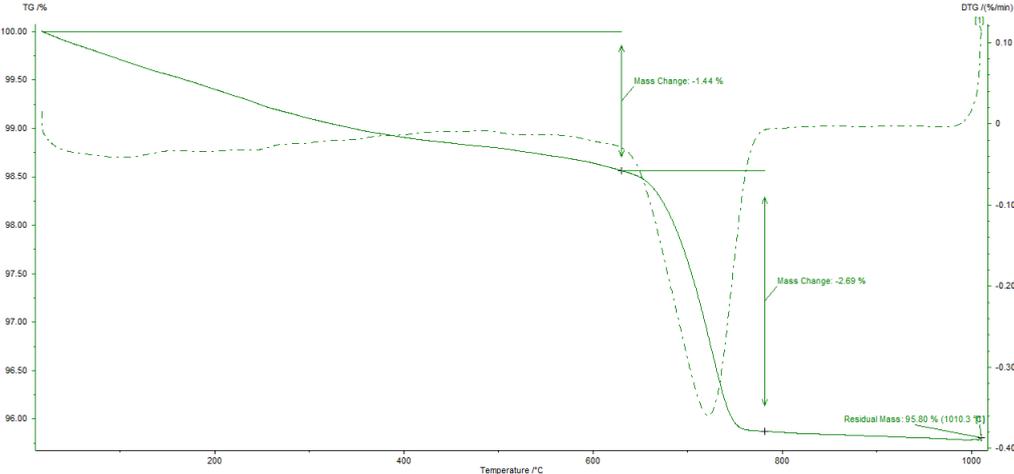


Figure 49 – TGA from P127 sample

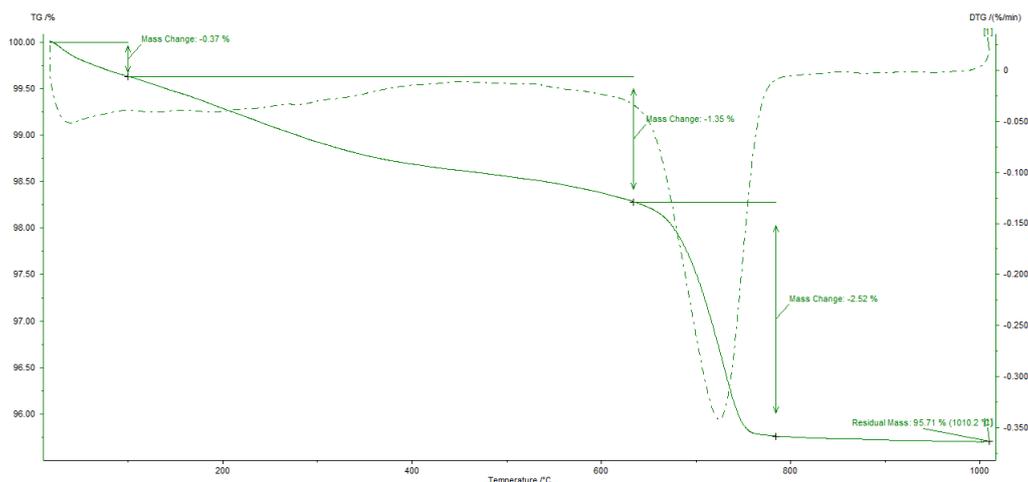


Figure 50 – TGA from P133 sample

In Table 14 it can be seen that the majority of weight lost corresponds to calcite decomposition. Comparing the total mass losses determined by termogravimetry and by L.O.I. (Table 13) it can be seen that the differences are quite acceptable.

Table 14 – P89, P127 and P133 weight losses analyses from TGA data

	Weight lost under 600°C [%]	Weight lost between 700° and 800°C [%]	Total weight lost [%]
P89	2.11	4.23	6.34
P127	1.44	2.69	4.13
P133	1.72	3.87	4.24

FTIR was performed in sample P24 which corresponds to a mixture composed of 9 crystalline phases, among which calcite and portlandite can be found. The existence of calcite is present as identified by the vibrations at 1430, 875 and 711  $\text{cm}^{-1}$ . Portlandite (vibration at 474  $\text{cm}^{-1}$ ) is present in a high amount (Figure 51).

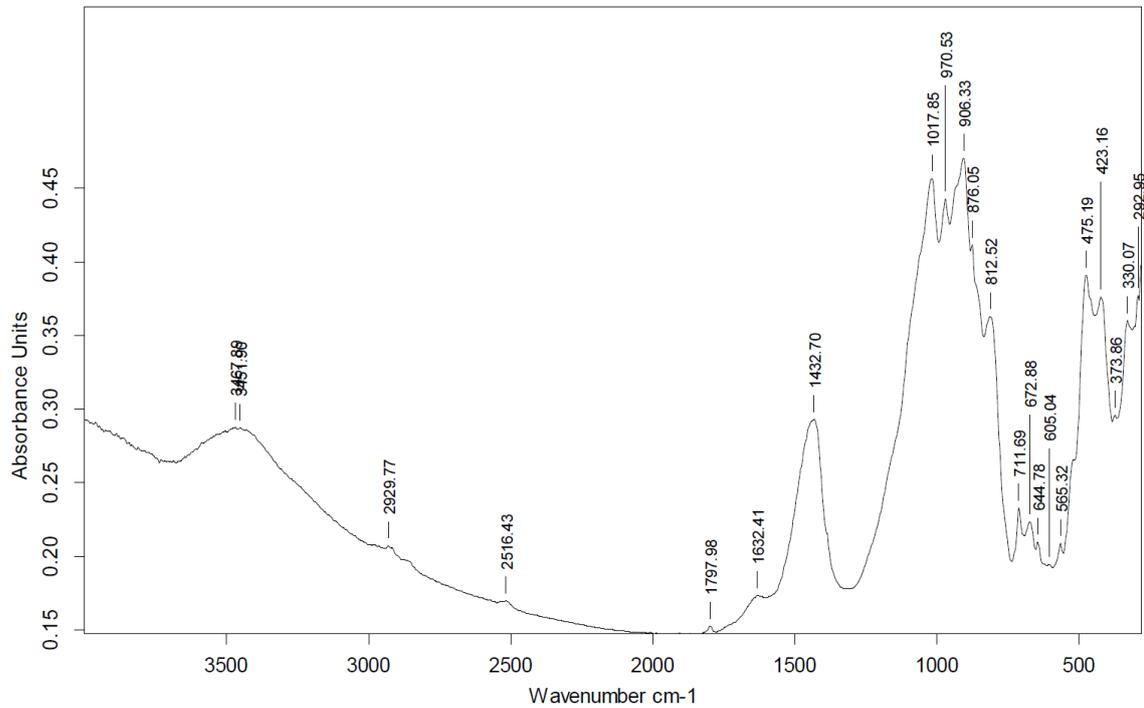


Figure 51 - Sample 24 FTIR spectrum

The 811  $\text{cm}^{-1}$  vibration is assigned to amorphous silica (Si-O, symmetric angular deformation). The deformation Si-O present at 1018, 970 and 906  $\text{cm}^{-1}$  corresponds to mullite, diopside and gehlenite.

Results of calcination of original tiles samples show that, at 1040° C none of the samples changed either dimensionally or in aspect but, however, they lost weight. Still in a rather rough approximation it may be said, that the ceramic body biscuit of the tiles in study were originally fired at least at 1040° C (ring temperature), temperature high enough to promote decomposition of the calcite present in the original ceramic body composition.

After calcinating the samples at 1040°C, new XRD were made and confirmed that calcite and portlandite peaks are no longer present. In Figure 52, P24 XRD before

calcination is shown, containing both calcite and portlandite. In Figure 53, the XRD from the same sample after calcination is shown. It can be seen that the calcite and portlandite crystalline phases, as expected (due to calcination temperature), are no longer present, indicating that calcite/portlandite was not used as raw material, as seen in Tschegg work (Tschegg, Ntaflos et al. 2009).

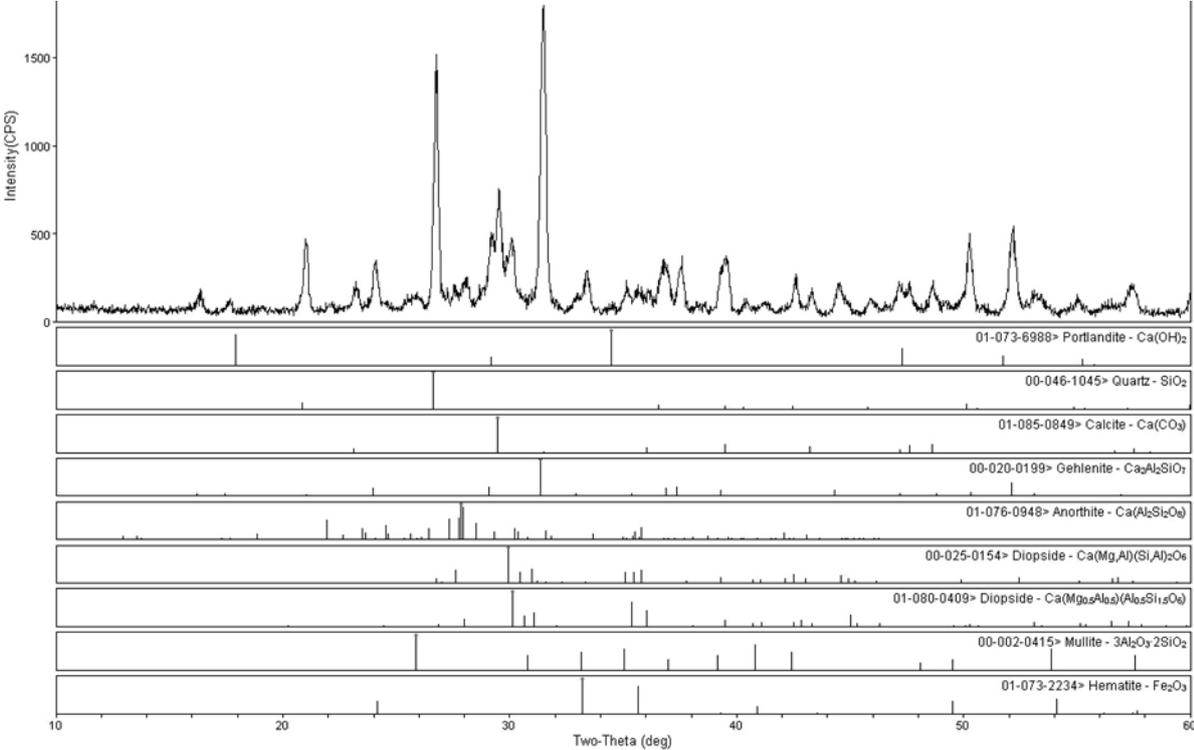


Figure 52 – P24 XRD maximum diffraction, presenting calcite and portlandite

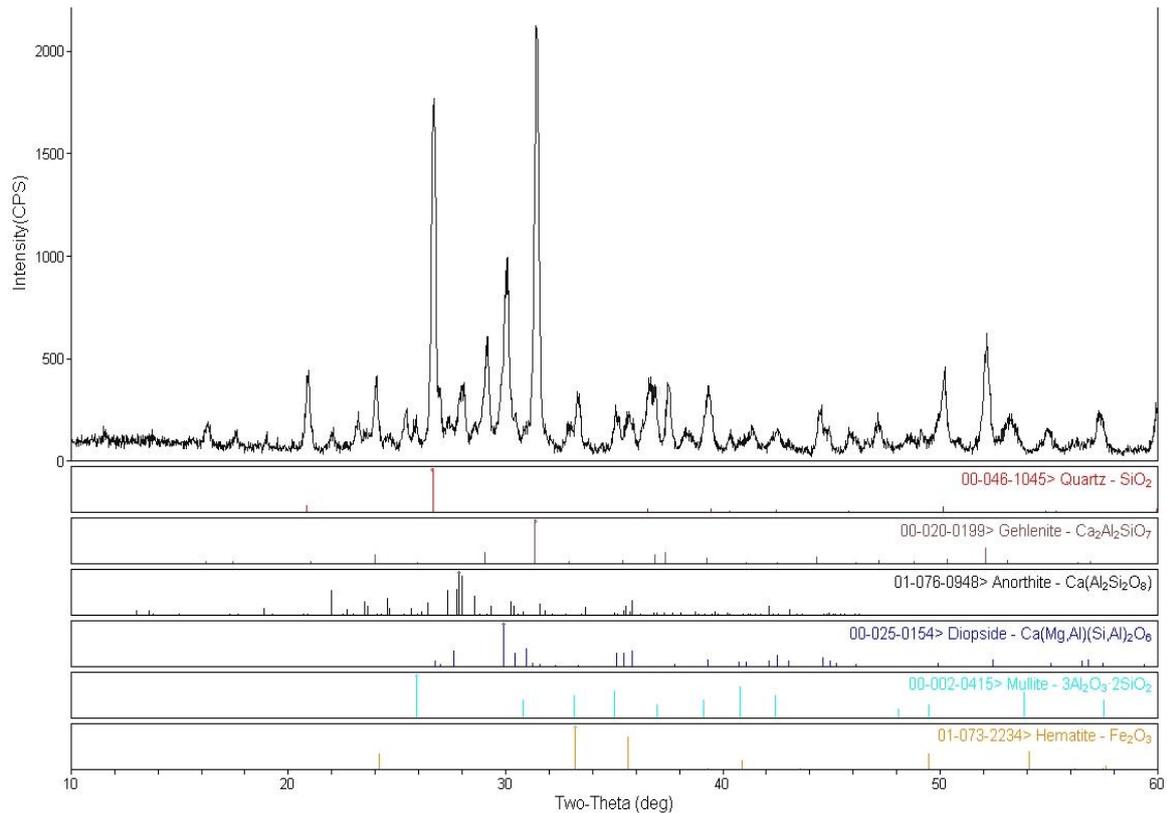


Figure 53 - XRD of P24 after calcination at 1040°C where calcite and portlandite main diffraction maximums are not found

#### 4.2.1.4 Calcination tests

After the calcination tests to determine the L.O.I. it became obvious that the next step would be point out, as accurately as possible, the original firing temperature of the sampled tiles ceramic bodies. The original firing temperature could give a clue for the origin of calcite in the ceramic bodies.

After calcination, no alterations were detected in the samples calcined at 1100°C. On the other hand, at 1150° all of the calcitic ceramic bodies presented an over-fired look with colour change, shrinkage, swelling and phase changes (shown in Table 15 and Figure 54), while the *pó de pedra* presented no changes.

Trying to get as close as possible to an industrial firing atmosphere, some small pieces of the samples suffered calcination tests in a ceramic factory where trials could be made: one with a 180 minutes cycle and 1180° C as set point (1150° C ring temperature) and another with a 300 minutes cycle and 1100° C as set point (1100° C ring temperature).

Table 15 – Calcination results of some calcitic samples

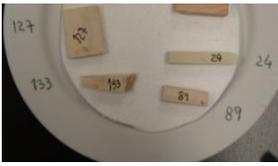
Samples	1100° Ring temperature	1150° Ring temperature
		
		
		
		



Figure 54 – Aspect of P104 over-fired sample at 1150°C

To evaluate the change of crystalline phases with temperature, one sample of P104 calcitic ceramic body, with XRD represented in Figure 55, was calcined at 1150°C (ring temperature). Figure 55 and Figure 56 show the diffraction maxima of the same ceramic body after original firing and after calcination, respectively. It can be seen that the intensity of anorthite diffraction maxima increased considerably as well as that of mullite, while calcite, gehlenite and hematite phases disappeared.

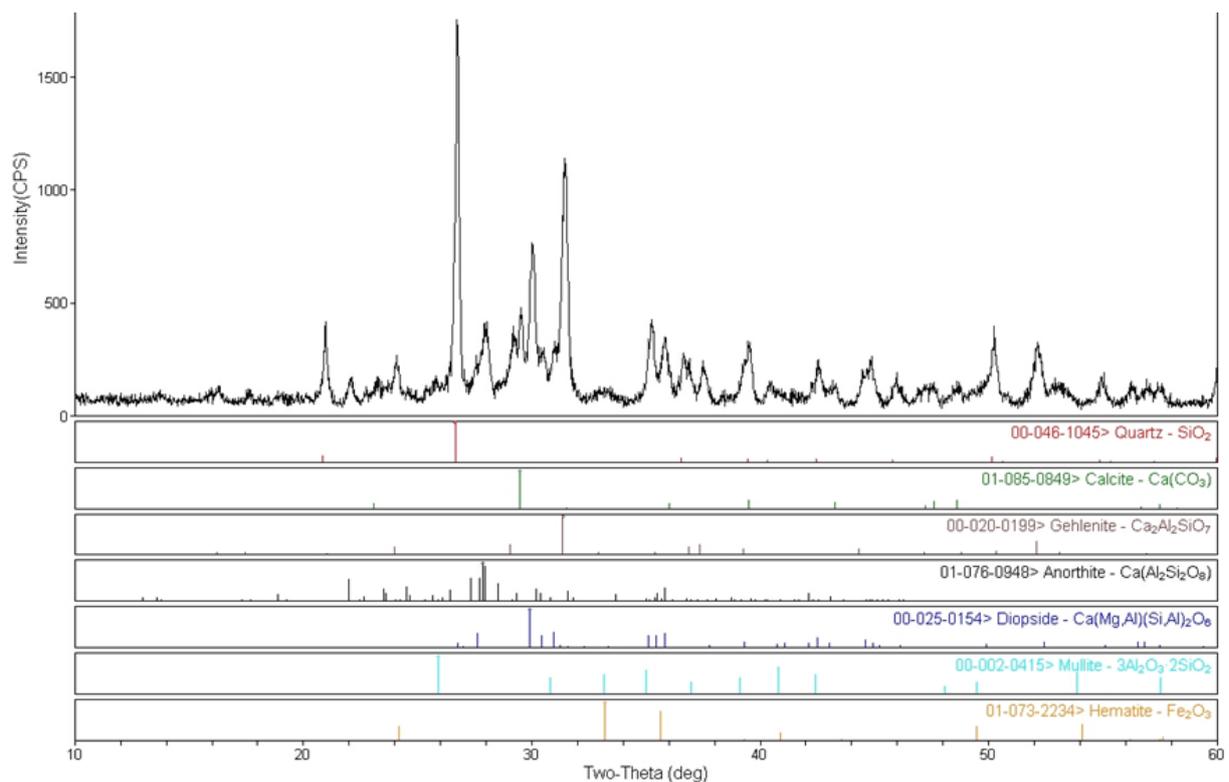


Figure 55 – X-ray diffraction maxima of P104 fired piece

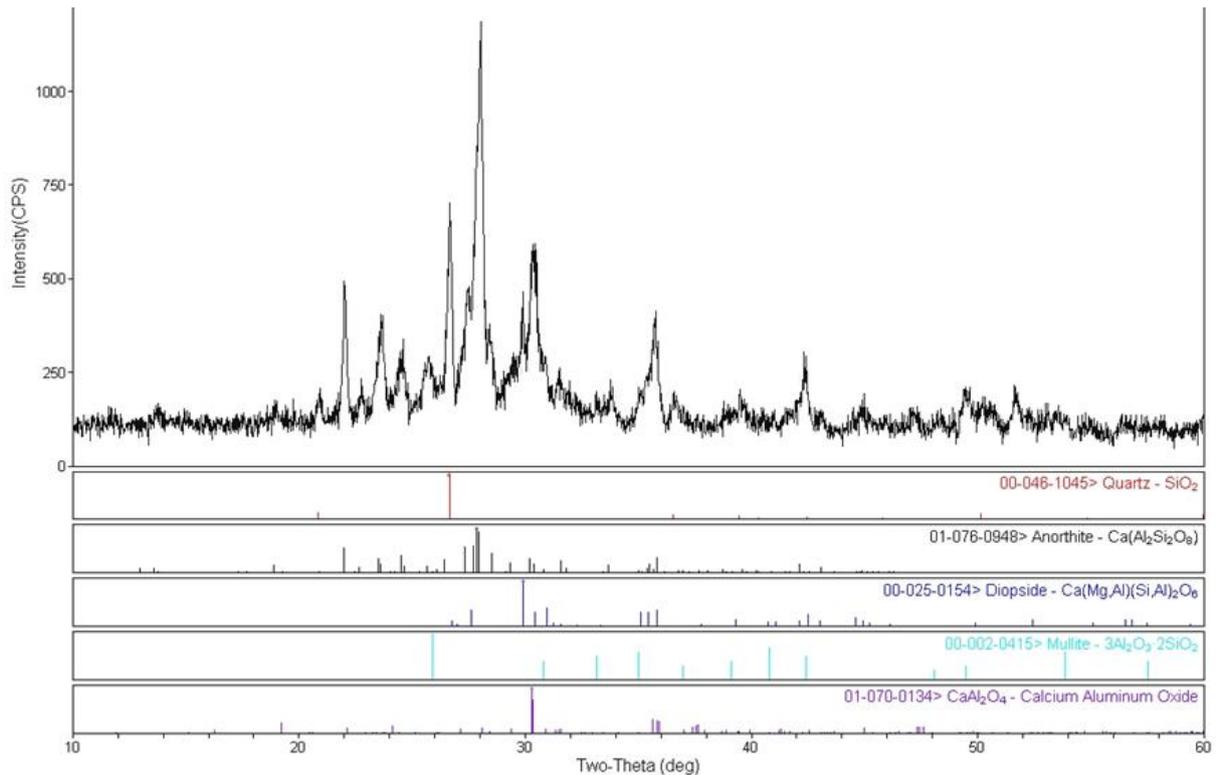


Figure 56 – X-ray diffraction pattern after P104 piece being calcined at 1150°C

As until 1150°C *pó de pedra* samples suffered no physical change, *pó de pedra* samples were calcined at 1360° C (the reason of using this temperature is explained in chapter 3) showing an average contraction of 10.6% revealing that these samples were originally fired at a temperature higher than 1150°C and lower than 1360°C.

#### 4.2.1.5 Microstructure

Old tiles microstructure shows a system with a large quantity of pores of different sizes, vacant spaces, salt crystals, and large particles of ungrounded raw materials as well as of other materials' particles. In Figure 57 and 58 it can be seen P10 and P89 ceramic bodies and glazes.

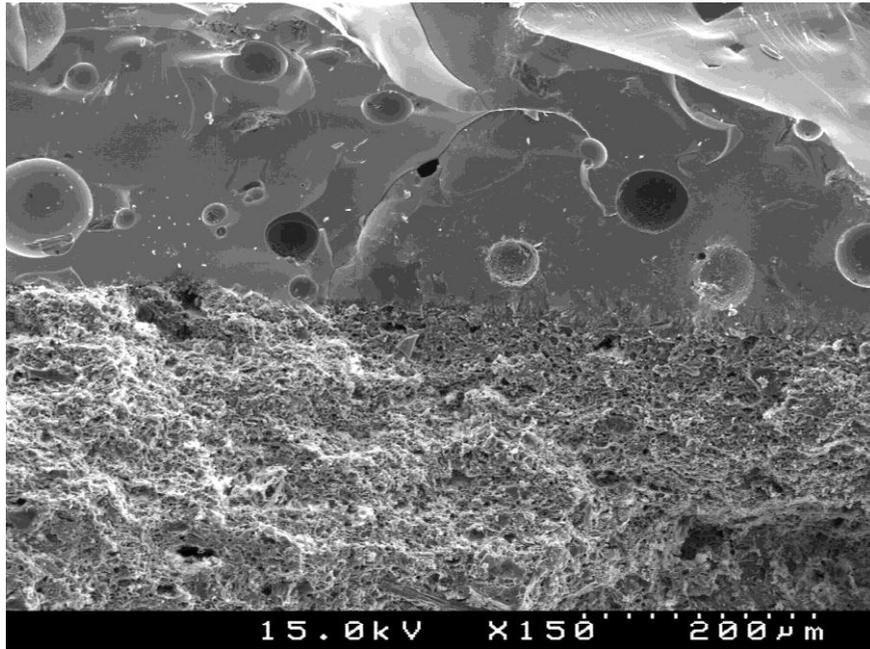


Figure 57 - P10 ceramic body and glaze

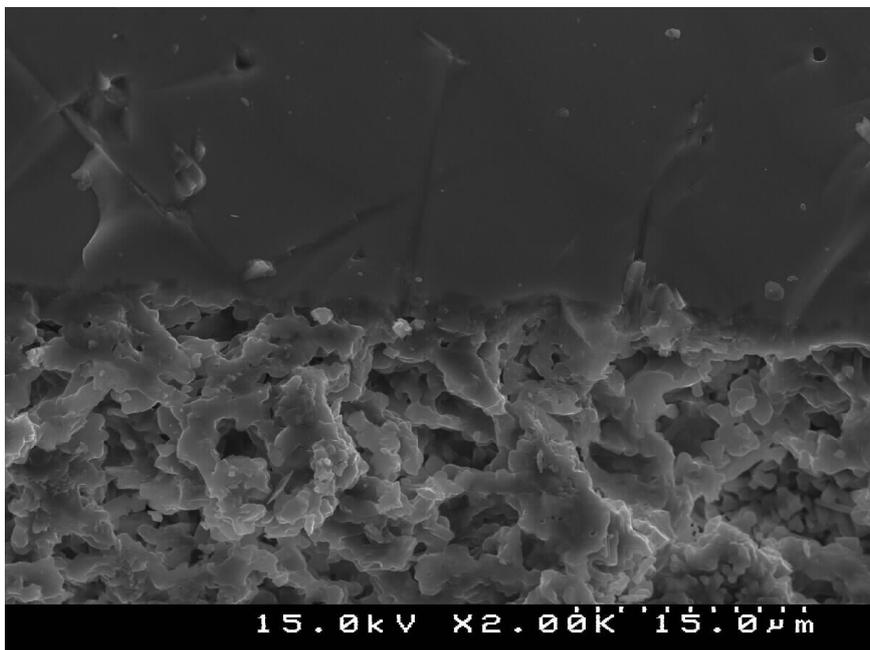


Figure 58 – P89 ceramic body and glaze, a closer look

In Figure 59 it can be seen P10 ceramic body' heterogeneities (vacant spaces, large raw material particles).

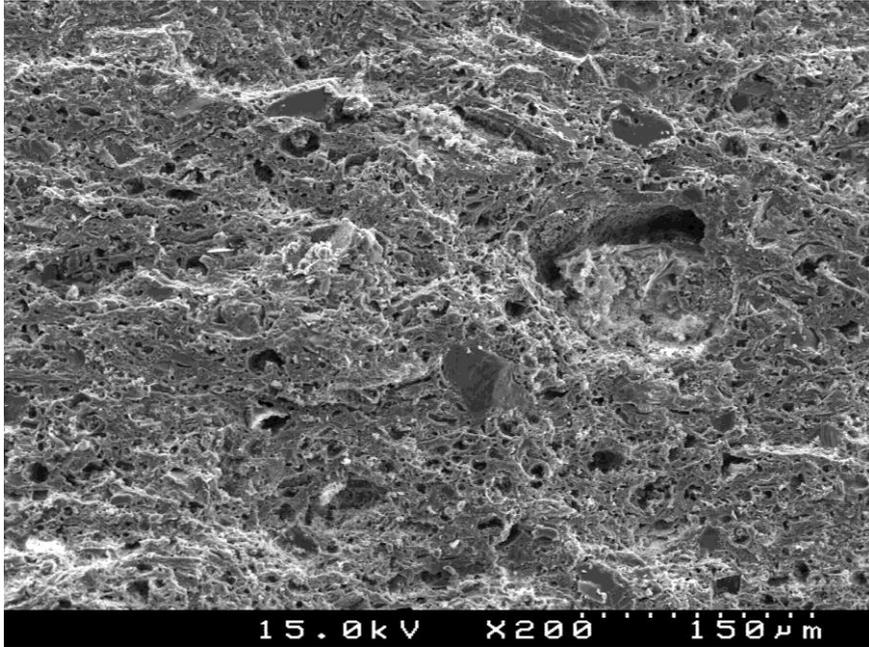


Figure 59 - P10 ceramic body heterogeneities

In Figure 60 and 61 it can be seen P89 and P133 ceramic body with salt crystals.

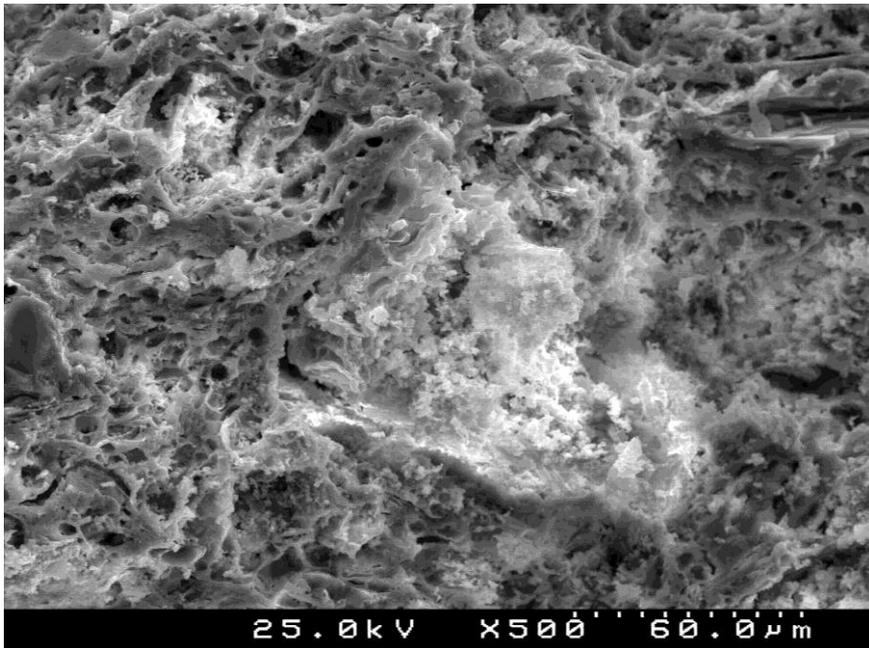


Figure 60 – P89 ceramic body with salt crystals

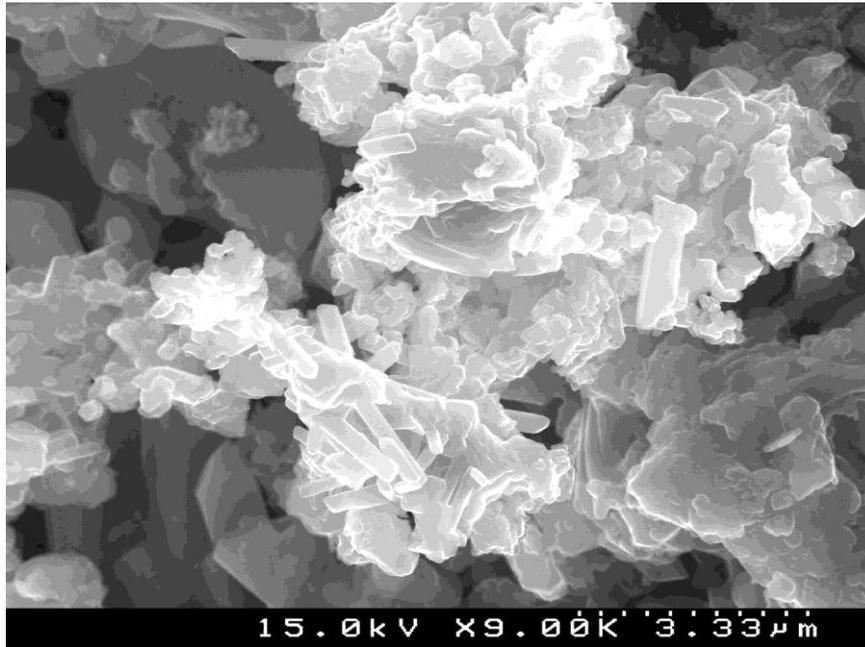


Figure 61 – P133 ceramic body with salt crystals

#### 4.2.1.6 Water absorption percentage

Open porosity is considered as the ratio of the total volume of the voids to total sample volume. The open porosity can be connected or not. Ancient tile ceramic bodies are very porous and there is a vast net of interconnected pores increasing the flow of weathering agents inside of the structure and, therefore, its deterioration. Determining open porosity is very important but it not enough as materials with the same open porosity may have different water behaviour (Santos, Vaz et al. 2012). That is why pore determination (open pore size, and volume) is important to characterize a building material such as tiles (Santos, Vaz et al. 2012). There are several pore characterization methods. In the present work it was considered the water absorption percentage, pore size distribution by mercury intrusion and water absorption due to capillary absorption.

Porous tiles placed in humid places on building façades might be victims of deterioration due to salt crystallization inside the pores. (Scherer 1999, Cultrone, Sebastián et

al. 2004, E.Molina, G.Cultrone et al. 2011, R.M.Pereira and Mimoso 2012). The fact that the pores might be partially occupied by salts interferes with original porosity and creates a distinct porous structure. The water absorption data determined on the 26 studied samples are pictured in Table 16, where average calcitic ceramic tiles average value seems normal for the typology of the studied tiles, as 18% is considered as the mean porosity value for contemporary calcitic ceramic bodies (Aiazzi 1988).

Table 16 - Water absorption percentage of the 26 studied samples

	Calcitic ceramic bodies	<i>Pó de pedra</i> ceramic bodies
Average [%]	20.4	13.5
Minimum [%]	17.7	12.1
Máximum [%]	22.8	14.0

#### 4.2.1.7 Water absorption coefficient due to capillary action and pore size determination

The water absorption coefficient is due to capillary action of the porous structure and influenced by pore size distribution and total ceramic body porosity. The water and the smaller lime particles of the mortar are introduced in the porous tile ceramic body network by capillary water due to capillary action. The carbonation of the binder forms the link (Botas, Veiga et al. 2012). The porosity of the tile's ceramic body is very important in this process (Santos, Vaz et al. 2012) because it is the size and amount of existing pores that enable absorption of the mortar paste, creating an interface.

Figure 62 portrays a mean calcitic and *pó de pedra* curve of pore size distribution resulting from mercury intrusion porosimetry test. The analysis of Figure 62 shows that *pó de pedra* has the majority of its pores larger than 1 $\mu\text{m}$  (the curve on the left side of the figure) in comparison to calcitic tiles (the right curve on the figure) where it can be seen that 50% of the pores are smaller than 0.5  $\mu\text{m}$ . The carbonates strongly influence porosity, promoting the formation of pores under 1 $\mu\text{m}$  in size (Cultrone, Sebastián et al. 2004). However, *pó de pedra* porous structure consists of large pores but not high open porosity, as seen by its water absorption percentage. These characteristics provides this material with less susceptibility to weathering (Flatt 2002, E.Molina, G.Cultrone et al. 2011).

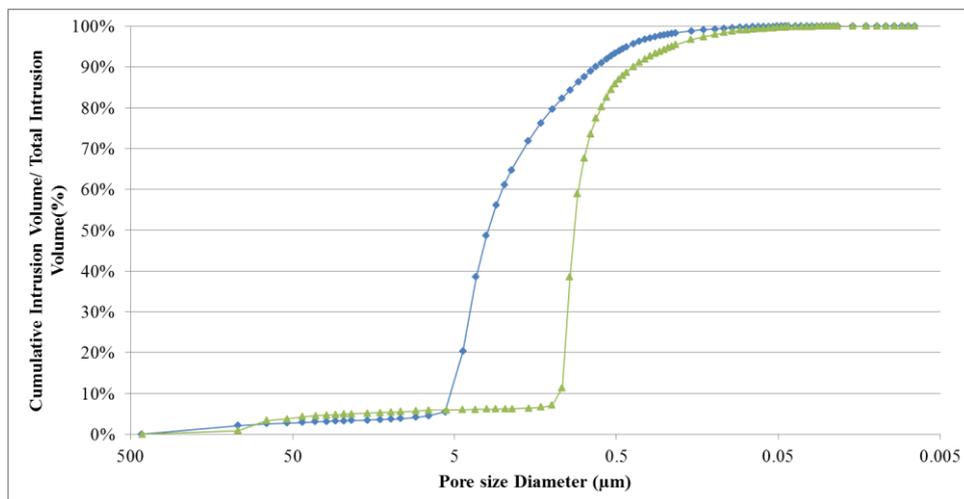


Figure 62- Typical pore size distribution assessed in the studied samples. *pó de pedra* the curve on the left and calcitic body on the right.

In Table 17 it can be seen the water absorption due to capillary action data of the 26 samples under study, where it is evident the higher values for calcitic ceramic bodies. In Figure 63 it can be seen an example of the water absorption due to capillary action curves of a *pó de pedra* (DA5) and a calcitic ceramic bodies (P116). In the first 2 minutes of the trial *pó de pedra* ceramic body shows a higher water absorption that fades with test time.

Table 17 - Values for water absorption coefficient due to capillary action

	Calcitic ceramic bodies	<i>Pó de pedra</i> ceramic bodies
Average [kg/m <sup>2</sup> h <sup>1/2</sup> ]	3.4	2.6
Minimum [kg/m <sup>2</sup> h <sup>1/2</sup> ]	3.1	2.2
Maximum [kg/m <sup>2</sup> h <sup>1/2</sup> ]	3.7	2.8

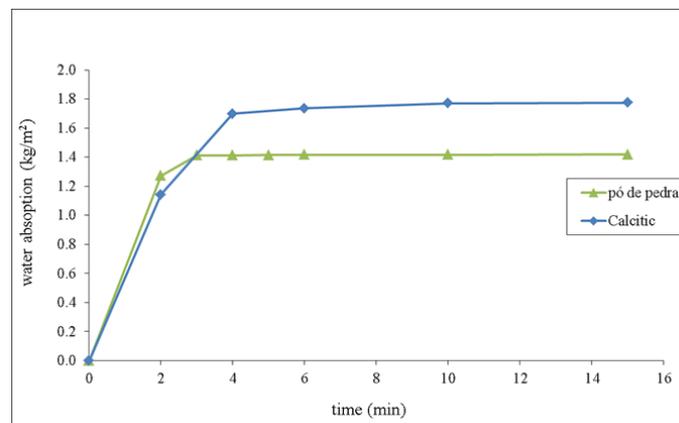


Figure 63 – An example of *pó de pedra* and calcitic ceramic bodies' water absorption due to capilar action curves

#### 4.2.1.8 The importance of the glaze/ceramic body interface in glaze detachment caused by salt crystallization

A very severe pathology suffered by early industrially produced tiles in Portugal is glaze detachment in wall tiles placed in the lower part of the façade. It is known that there are a wide number of probable causes for glaze detachment, such as mechanical stresses caused by the building, stresses caused by a poor joint design, poor joint elasticity, lack of

compatibility of thermal expansion coefficient between ceramic body and glaze, ceramic body moisture expansion and salt crystallization. From the 26 samples under study, 5 were chosen suffering from glaze detachment with visible salt attack placed in the lower part of the facade (some samples without showing crazing glaze) although the upper parts of the façades presented no glaze detachment.

The glazes of the tiles under study are lead-rich and were applied in a biscuit-fired body, previously fired at a higher temperature. During the glaze firing process, liquid phase is promoted due to fluxes and to the low lead melting point, penetrating into near-surface ceramic body pores and reacting with the ceramic body minerals forming a zone of chemical digestion that is a mix of both bodies which is called the interface zone, a layer that is composition, time and temperature dependent (Molera 1999, Molera, Pradell et al. 2001). The thickness of this layer is given by time/temperature binomial allowing, or not, the diffusion of elements between glaze and ceramic body (Kopar 2007). A study made to Italian majolica from XV to XVII century (M.S.Tite 2009) revealed that the interaction between the glaze and the ceramic body had about 20 to 30  $\mu\text{m}$ , to give an idea for comparison purposes although there are certainly regional variations of compositions and firing temperatures/cycles.

Studies made on the importance of the interface glaze/ceramic body reveal that the more effective the formation of the interaction layer between ceramic body and glaze, with an intermediate chemical composition due to diffusion of elements, the higher the glaze resistance to thermal shock and crazing (S.A.El-Defrawi, M.A.Serry et al. 1995, Kopar 2007). As glaze detachment caused by salt crystallization is a too frequent pathology in old wall ceramic tiles, placed in humid areas of the façade (normally closer to the ground), the question about the importance of the magnitude of glaze/ceramic body interface remained to be answered.

The aim of the present study is to understand how important this bonding layer can be, if it really dictates glaze durability in terms of glaze detachment caused by salt crystallization in the porous ceramic body structure. For that, SEM/EDS mapping and quantification techniques were used. Mapping allows tracing the relative quantity and localization of the existing elements in the samples.

In Table 18 are pictured the reference and looks of the 5 tiles studied, together with a contemporary tile (HC) used for comparing.

Table 18 – Tile pictures and references

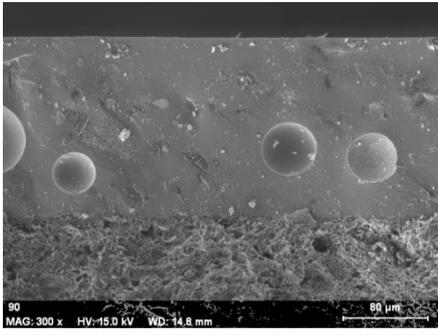
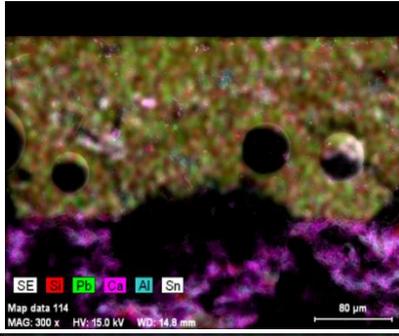
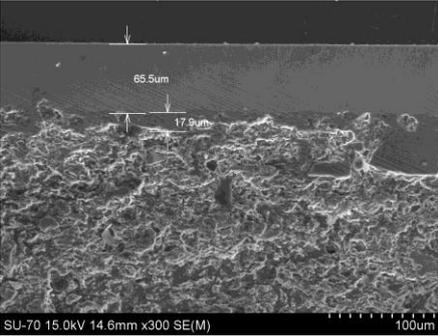
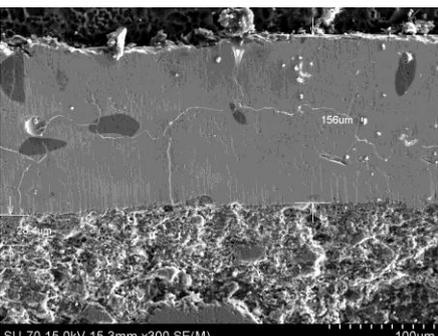
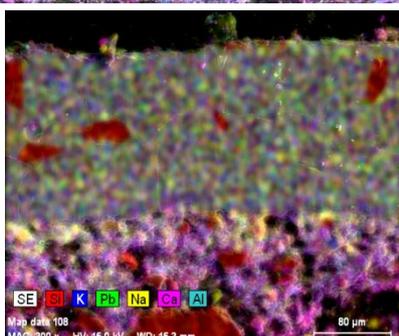
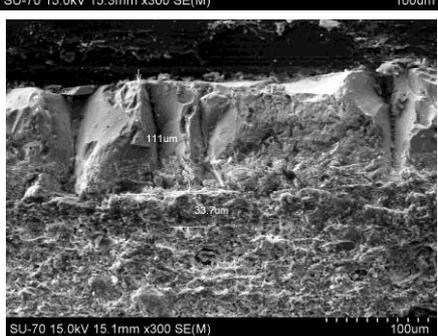
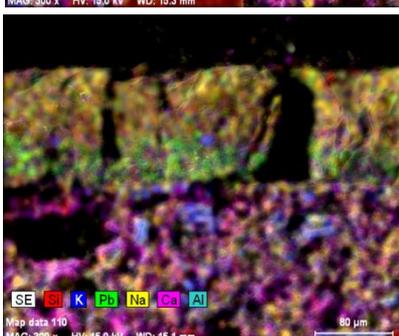
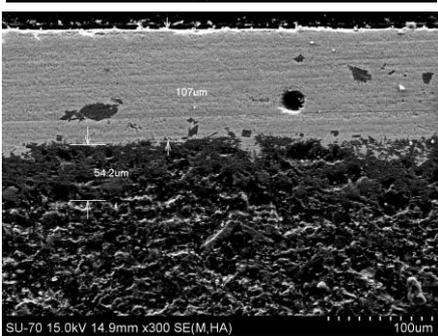
Ref.	P24	P89	P104	P127	P133	HC
Sampled tiles						
Glaze crazing	No	No	Yes	Yes	Yes	Not applicable

To enable the visualization of the glaze/ceramic body interface, vertical cuts with 1.5 cm long and 0.5 cm height were made in the tile with a sharp mechanical cutting machine, obtaining the simultaneous observation of the glaze, glaze/ceramic body interface and ceramic body. The samples were mounted in resin and polished until a smooth surface was obtained. Due to the samples ceramic bodies' easy pull off characteristic, in some samples it was not possible to reach an even surface.

SEM/EDS were used with an acceleration voltage of 15 kV for observation and measuring the interface and 30 kV for qualitative and quantitative element mapping. For EDS calculations purposes an 110 $\mu$ m x 25  $\mu$ m area was considered in the samples with measurable interface. In the samples where the average interface thickness is narrower than 25  $\mu$ m, the elemental values were obtained in the thicker parts of the interface.

Elemental mapping and quantification were performed for all the elements (comparisons between them can be made, as data was collected in the same conditions). SEM images and mapping can be seen in Table 19.

Table 19 – SEM images of the glaze, interface area and ceramic body of the studied samples

	Glaze/ceramic body	EDS Mapping
P24		
P89		
P104		
P127		
P133		

P127 has a severe visible crazing problem that is why the glaze presents cracks and sample has not an even look.

Table 20 shows the values of the major chemical elements present in the glazes, interface area and of the ceramic body near the interface region of the studied samples. The presented values were acquired by EDS and are the average of 3 measurings in different places of the sample.

Table 20 – EDS wt% values of the chemical elements present in the glaze, interface and ceramic body of the studied samples

GLAZE								
	Si	Pb	K	Al	Na	Ca	Sn	O and others
P24	20.7	19.7	5.2	1.0	0.2	--	4.1	49.1
P89	24.9	16.7	8.3	2.2	0.3	1.0	--	46.6
P104	26.4	12.1	8.6	2.9	0.4	0.5	--	49.1
P127	21.5	24.5	5.4	1.9	0.9	0.7	--	45.1
P133	20.6	26.5	6.7	2.5	0.5	1.6	--	41.3
INTERFACE								
	Si	Pb	K	Al	Na	Ca	Mg	O and others
P24	--	--	--	--	--	--	--	--
P89	18.8	--	10.7	10.8	1.2	9.6	0.2	48.7
P104	18.4	2.2	1.5	15.7	2.0	10.9	0.3	49.0
P127	20.6	2.5	4.0	9.0	2.2	9.0	0.4	52.3
P133	20.8	4.4	6.5	9.9	2.9	7.9	0.2	47.4
CERAMIC BODY								
	Si	Fe	K	Al	Na	Ca	Mg	O and others
P24	12.1	8.8	--	6.6	0.2	33.0	0.9	38.4
P89	16.2	3.4	0.9	6.8	0.6	16.0	1.9	54.2
P104	17.2	1.8	1.0	10.4	1.0	14.7	0.2	53.7
P127	18.2	1.5	2.5	12.6	2.7	9.7	0.1	52.7
P133	15.7	3.4	0.6	7.6	0.6	18.3	1.9	51.7

Analysing Table 19, it seems that when there is the development of an interface there are elements present like silicon, lead, potassium, aluminium, sodium and calcium. Those elements have contributions both from the glaze and the ceramic body. The presence of lead in the interface must depend on the glaze firing cycle, glaze melting point and open porosity of the ceramic body. From mapping it may be seen that the only element that diffuses beyond the interface area is potassium. The ceramic body has potassium in its constitution, but potassium concentration is larger near the interface. Sodium and aluminium are the elements that stand out in the interface composition (Table 20).

In Table 20 it can be seen that P24 presents tin while the other samples do not. That is because within the five samples, P24 is the only tin-lead glaze. P24 presents the absence of an interface and presented detachment of the glaze when the tile was cut for analysis. One of the possible explanations for this extraordinary behaviour can be low glaze firing temperature or excessive amount of tin. Lepierre study (Lepierre 1899) mentions that when tin percentage was raised in the industrial process, there was a detachment of the glaze from the ceramic body, characterized by a peel off.

In Table 21 the interface area elements of P133 can be seen (in the centre of the photos), showing a pronounced concentration of aluminium, sodium and potassium in that area, when compared with the glaze and ceramic body, revealing element migration both from the glaze and the ceramic body to the interface.

Table 21 – Elementary EDS photos of P133 (Al, Na, K)

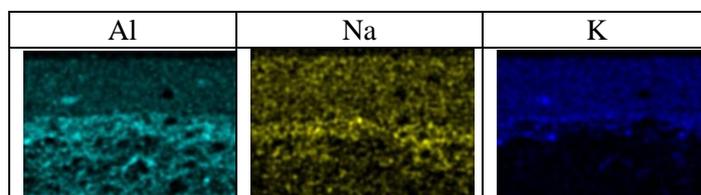


Table 22 shows the average of 5 different measurements made in the interface of each samples. It can be seen that samples present interfaces width variations, from an unmeasurable interface until an interface of about 54  $\mu\text{m}$ . When cutting P24, which has an interface that is not measurable, it became clear that glaze peeled off on the saw cutting path, revealing a deficient glaze/ceramic body interaction.

Table 22 – Average interface values observed in the analysed samples

Tile reference	Average interface observed [ $\mu\text{m}$ ]
P24	Not measurable
P89	17.9
P104	28.4
P127	33.7
P133	54.2

In order to have a comparison term concerning glaze/ceramic body interface, this feature was analysed in a contemporary tile used in restoration as a pictorial replica. As can be seen in Figure 64, the interface has a mean value of about 18  $\mu\text{m}$ . In Figure 65 an interface closer look can be seen, showing its uneven profile as well as the glassy aspect. As modern tile production is more controlled and stable than 100 years ago, it is considered that the interface value found in this contemporary tile is representative within its brand.

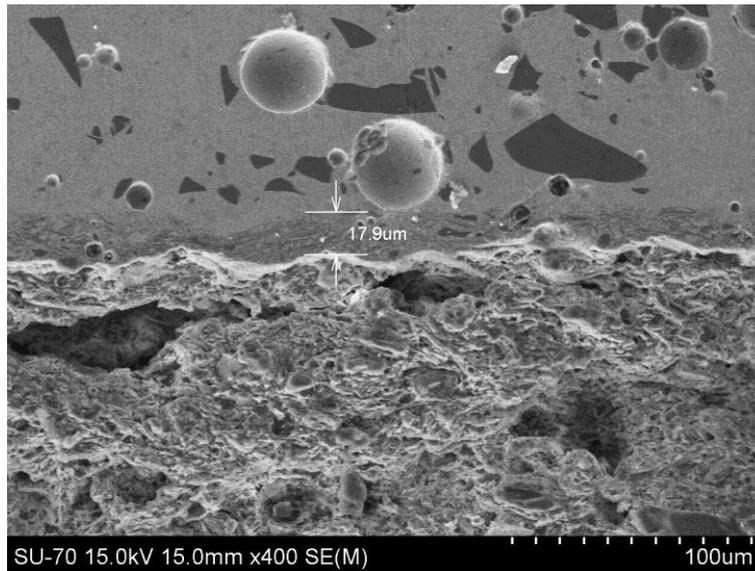


Figure 64 – SEM image of interface glaze/ceramic body of a contemporary tile (HC)

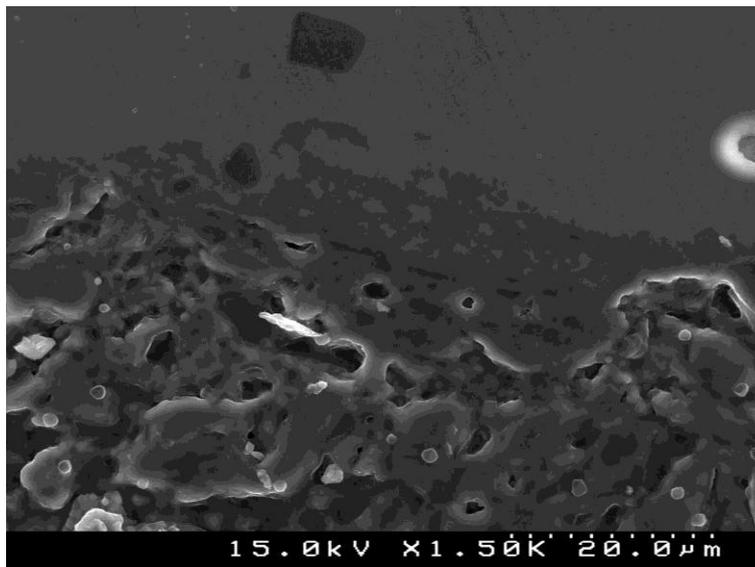


Figure 65 – HC interface glaze/ceramic body closer look

As all the samples suffered from glaze detachment caused by salt crystallisation, this suggests that these physical mechanisms are important enough to destroy what at first impression could seem a safe bond (54  $\mu\text{m}$  interface), comparing with the value found in the

modern tile. Far from humidity and salt attack tiles withstand the passing by of one hundred years without glaze detachment.

Hydration/dehydration of the supporting mortar, transports soluble salts to the tile ceramic body that crystallize in its pores, causing stresses high enough to cause the ceramic body breakdown (Scherer 1999, Cazalla, Rodriguez-Navarro et al. 2000, B.J.Smith, P.A.Warke et al. 2004, Scherer 2004). As in the interface between the ceramic body and the glaze, the porosity decreases abruptly (Coentro, Mimoso et al. 2010), it is expected that crypto-florescence will appear just beneath the interface. In the studied old ceramic bodies, high pore volume and considerable suction ability (promoted by the small pores), favour fluid circulation within its microstructure leading, inevitably, to deterioration (Scherer 1999, Cultrone, Sebastián et al. 2004, Dias 2007, E.Molina, G.Cultrone et al. 2011, R.M.Pereira and Mimoso 2012).

The evaluation of pore dimensions determined by mercury intrusion determination was performed in the 2 old tiles and in the contemporary one. The old tiles under study have calcitic ceramic bodies with high open porosity (Table 23) and most of the pores have less than 1  $\mu\text{m}$  size (Figure 66). In comparison, it can be seen that the modern tile (HC) has less open porosity and larger pores. The porosity features of the old tiles make them more prone to chemical and mechanical destruction by wetting/drying cycles promoted by weathering (Dias 2007).

Table 23 – Water absorption of the studied samples

	P24	P89	P104	P127	P133	HC
Water absorption [%]	21.6	20.8	18.1	22.0	22.6	14.7

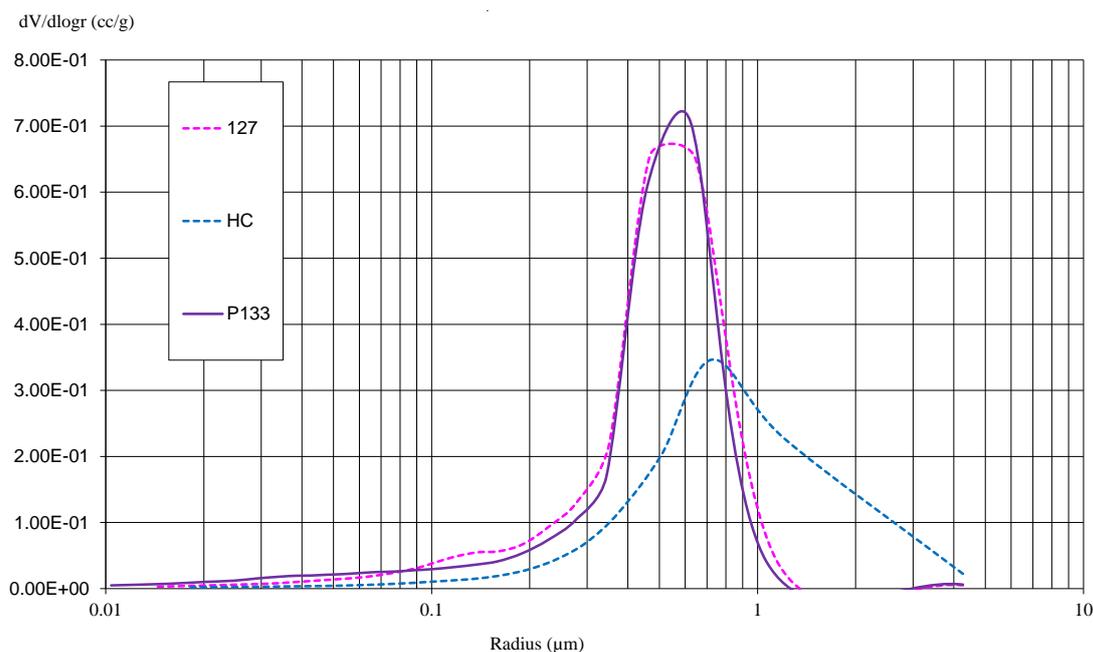


Figure 66 – Volume of mercury intrusion data in 3 samples (P127, HC and P133)

A P133 tile suffering from glaze detachment in some areas was cut and analysed by SEM, where glaze and the ceramic body are analysed in cross section. It was seen that the fracture that initiates the glaze detachment happens beneath the interface area, in the ceramic body (Figure 67), probably because porosity, which in this case is high, is the weakest part of the system. If the interface is defined as being the mix of ceramic body and glaze chemical elements and morphology, it seems that the interface is stronger than the ceramic body due to its lower porosity.

Analysing closely Figure 68, crystals (marked with a cross) can be seen occupying porosity underneath the glaze/ceramic body interface. In Figure 69, the crystals EDS can be seen. Analysing the EDS it cannot be forgotten that the signal from what is underneath the crystals is also captured by the EDS sensor.

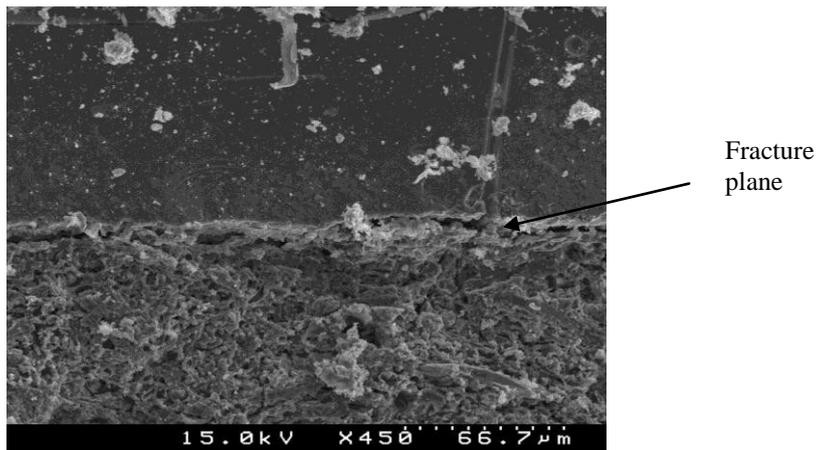


Figure 67 – A SEM cut view where can be seen a fracture beneath the glaze of P133



Figure 68 – Salts beneath the glaze of P133

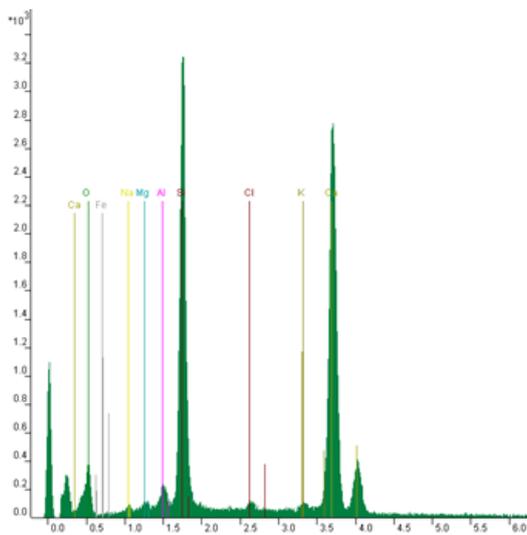


Figure 69 – EDS of the crystals marked in Figure 5

The studied samples, being already from the industrial era, have pressed ceramic bodies. Pressing gives the ceramic surface a flat and even surface, one of the characteristics that distinguish this production era from the previous ones. In Figure 70 a SEM view of the surface of the same tile used in Figure 67 (P133) is shown. It can be seen that the glaze detachment was made in depth, arriving at the ceramic body.

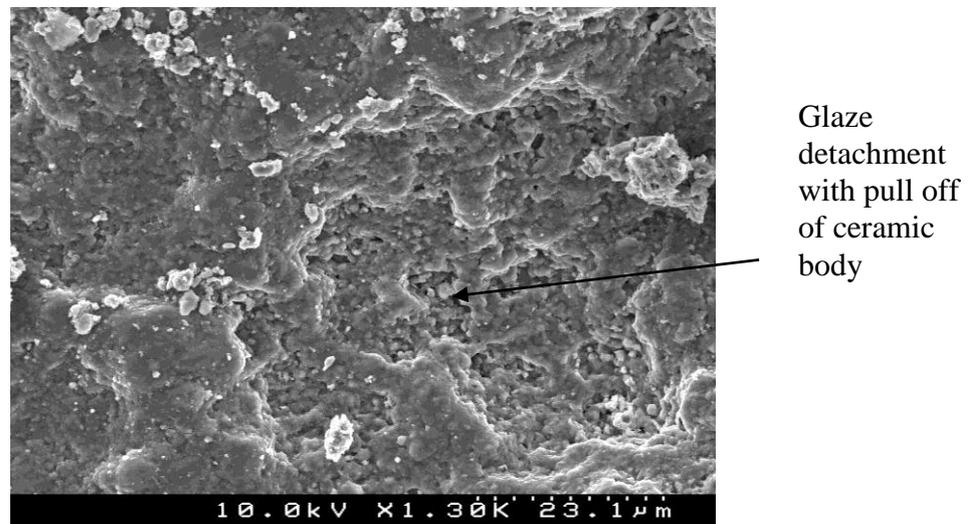


Figure 70 – A SEM view of the surface that suffered from glaze detachment

Comparing Figure 67 and Figure 70 it seems that the fracture propagation leading to glaze detachment due to salt attack is made under the interface of the glaze/ceramic body, probably meaning that interface thickness is not the most important characteristic to avoid the mentioned pathology. Therefore, probably, the ceramic body porous system is the most important feature.

From the present study some observations can already be made about the complex subject of glaze detachment in the studied tiles:

- When interface glaze/ceramic body is formed during firing, there is clear diffusion of potassium in most samples;

- The elements that seem more relevant in the interface composition are silicium, aluminium, sodium, lead and potassium;
- The presence of lead in the interface must be firing temperature dependant;
- Interface dimensions and composition are variable but it seems that even tiles with no measurable interface seem to withstand the passing of time if, even in the exterior of buildings when placed far from the ground and capillary water rise;
- Even tiles with expressive interface thickness do not resist to salt attack;
- In what concerns glaze detachment ability promoted by salt crystallization, volume and pore size of the ceramic body seems to be more determinant than glaze/ceramic body interface size.

#### 4.2.1.9 Ancient tiles raw materials proposal

Analysing all data that allowed proposing average **XRD and XRF** results, it can be said that in Oporto region, ceramic tiles producers under study used very **similar ceramic bodies' formulas** and very similar firing temperatures, revealing what might be called a regional trend of tile production. There are fluctuations of elements like Mg and Ca within the same producer, but it is not known if those variations represent different production era or are simply the reflex of the lack of the ceramic body correct raw material weighing (or volume measurement). What might differentiate the producers is not the **ceramic body composition**, but its production process. There are tiles with more technical flaws than others (like microestructural big heterogeneities and the presence of undesired materials), revealing less technical means or technical care. Nevertheless, in terms of final product, the tiles of late 19<sup>th</sup> century reveal high quality evolution when compared with previous production in Portugal.

From **XRD** data it is known that **calcitic ceramic bodies present** quartz, gehlenite, diopside, hematite, mulite, cristobalite and anorthite as primary crystalline phases **while pó de pedra present** quartz, mulite and cristobalite. As important quantities of alumina are present in all samples, kaolinitic clays were probably used. To have a magnitude idea, Pereira (R.M.Pereira and Mimoso 2012) characterized 17<sup>th</sup> to 18<sup>th</sup> century tiles that presented from 12.1% until 13.4% of alumina (the tiles under study presented from 22.5% until 26.1%).

Kaolin shows changes during firing, depending on the heating temperature and rate, and on the general chemical composition (Bulens, Leonard et al. 1978). The first mineralogical change is the transformation of kaolinite to metakaolinite (metakaolinite is amorphous or quasi-amorphous) (Lee, Kim et al. 1999). Kaolinite starts to decompose to metakaolinite at around 450° C and progresses until around 630° C. The decomposition process consists in the dehydroxylation of kaolinite (Lee, Kim et al. 1999).

It is known that the high temperature phases typically present after firing a kaolinitic clay+calcite mixture are gehlenite, wollastonite and anorthite, depending on the maximum firing temperature and the degree of decomposition of calcite (M.P.Riccardi, B.Messiga et al. 1999, Trindade and al 2008). Since the studied samples do not exhibit any diffraction maxima corresponding to wollastonite, one might conclude that calcite from the system would be completely decomposed at nucleation temperature of wollastonite that is, between 800 and 900° C, as follows:



Since at 800 - 900°C calcite probably was already decomposed in calcium oxide, above 900°C free calcium oxide reacts with free silica and alumina resulting from kaolinite decomposition, forming gehlenite, according to the reaction (Trindade and al 2008):



The diopside, present in all samples, is the result of the reaction between calcium oxide, magnesium oxide (from a magnesium provider mineral decomposition) and silica, at a temperature between 800° and 900° C (Trindade and al 2008). As the quantities of gehlenite and diopside phases existing in most samples are not negligible, it can be concluded that the system had a large quantity of free alumina, most probably provided by aluminium-rich clay, quite possibly kaolinitic clay (kaolin or ball-clay).

In all of the calcitic samples studied there is simultaneously gehlenite and anorthite, revealing a high concentration of calcium in the starting composition and that composition

had to be fired at high temperature (M.M.Jordán, Boix et al. 1999). Jordan (M.M.Jordán, Boix et al. 1999) states that anorthite can be found in calcitic ceramic bodies fired at temperatures over 1050°C.

As seen in Figure 56 (sample calcined at 1150°C), gehlenite diffraction maxima shown in the corresponding XRD pattern transformed into anorthite revealing that the original piece was originally fired at a lower temperature.

The presence of hematite in some calcitic samples (Table 12), relates to the amount of iron oxide contained in the raw materials. It is believed that the presence of iron in the system could be highly expected as we are dealing with non-beneficiated raw materials. The fired ceramic body that shows hematite has a light reddish colour. The iron needed for the formation of crystalline iron oxide could result from the iron contained in the structure or fixed at the surface of clay minerals that is liberated after their collapse (Baccour 2009). Hematite is formed by the double action of temperature and oxidizing firing conditions (Benedetto, R.Laviano et al. 2002). The samples in which iron oxide does not form hematite, show a pale yellow colour because instead of forming hematite, the iron oxide was incorporated into calcium iron silicates presenting a buff colour (M.S.Tite 2009).

The quartz present in the raw materials does not show any significant transformation during firing.

The intermediate stages of the transformation of kaolinite into mullite have been matter of much discussion. The mullite formed from metakaolinite varies in content depending on both kaolinite in clay and its thermal behaviour, as well as on the eventual occurrence of fluxes phases and impurities such as  $\text{Fe}_2\text{O}_3$ . Previous studies show that primary mullite can occur at temperature above 940° C (Lee, Kim et al. 1999, M.M.Jordán, Boix et al. 1999). As the temperature rises, the total removal of the residual hydroxyls of the short-range ordered structure of metakaolinite takes place at 940° C. The breakdown of metakaolinite promotes the formation of a poorly crystalline mullite and an important amount of amorphous silica. At this stage, the particle size of the microcrystalline mullite has less than 10 nm, persisting up to 1100° C and starting to increase at 1200° C. The early-formed mullite is an Al-rich structure (possibly a 2/1-mullite) that with temperature stabilizes in to a 3/2-mullite ( $3\text{Al}_2\text{O}_3 \cdot 2\text{SiO}_2$ ). At around 1200° C the crystallization of amorphous silica into cristobalite starts (Gomes 1986, Lee, Kim et al. 1999).

The high magnesium content existing in the calcitic tiles could be due to either to talc or dolomite, but dolomite is unreasonable due to high quantities needed.

Because of the crystalline phases present on the studied samples, it became evident that calcitic ceramic bodies were originally fired at least at 1050°C and *pó de pedra* at 1200°C. That was the thought present when choosing the industrial kilns and the maximum temperature achieved.

Calcination results point out that the calcitic samples under study were originally fired at a temperature between 1100°C and 1150°C (ring temperature). Although ternary diagrams of CaO-SiO<sub>2</sub>-Al<sub>2</sub>O<sub>3</sub> indicate 1400°C as the temperature at which mullite and cristobalite begin to be formed, in the ceramic bodies under study due to the fluxes they contain, the formation of those crystalline phases could be anticipated. In fact, mullite and, mullite and cristobalite, depending of the chemical and mineralogical composition of the body, can appear below 1200°C.

Analysing the crystalline phases present in Table 11, and the XRF data presented in Table 12, it can be concluded that the raw materials which were most probably used in the calcitic studied tiles could be: kaolinitic clay, quartz sand, calcite and talc and the raw materials most probably used in the studied *pó de pedra* tiles could be quartz sand and kaolin.

The calcination tests revealed that the samples under study were probably fired at temperatures between 1150° C and 1360° C. Considering that X-ray patterns show 3/2-mullite and cristobalite, a new minimum of temperature range can be re-established to 1200° C.

#### 4.2.2 Lead glazes of the studied samples

Since remote times, lead glazes have been used in tiles due to their brilliant finishing and a low melting temperature. The lead glaze is a mixture of mainly lead compounds and silica that after melting is a transparent shining surface. These two components suffered a melting process (frit), were ground down in to a fine powder and applied in a water suspension to the already fired ceramic body (at a higher temperature than the glaze firing).

Lead glazes were universally used by all the ancient tile producers (Molera 1999, Fernandes 2008, Senna 2008, Coentro 2011). In order to cover the colour of the ceramic body that usually was not white a small percentage of tin was added to the lead glaze in order to transform it into a white and opaque glaze. To the former glaze many cations could be added as colorants (Cu, Co, Mn, Fe, etc.), each of them promoting a different colour (Molera, Pradell et al. 2001).

All the tiles under study are lead-glazed. The advantages of using lead-glaze are known since remote times. It is known that around 2000 BC the first formulation of glazes with copper and lead was used (Fonseca 2000). Among the advantages of using lead glazes are the low melting point, high brilliancy, transparency and ability to be mixed with oxides that give colour and/or opacity. The lead glazes can be used in a wide range of temperatures, forming a more or less extensive interface, depending on the composition of glaze, ceramic body and thermal cycle. The final physical properties of glazed ceramic body-reactions depend on the glaze, and the chemical diffusion between glaze and ceramic body (Molera, Pradell et al. 2001, Kopar 2007).

One definition of glaze can be “an over cooled liquid, obtained by the fusion of inorganic oxides that is cooled until room temperature without facing crystallization” (Fernandes 2012) (Materials 1945, Renau 1994). The glaze can be transparent, opaque, colourless or coloured. Mechanically is hard but brittle and presents a micro conchoidal fracture (Fernandes 2012).

In the glaze composition there are compulsory elements: *glaze structural producers*, *net modifiers*, *net stabilisers* (Navarro 1991, Renau 1994, Alaimo, Bultrini et al. 2004). *Glaze structural producers* with the general chemical formula of  $RO_2$ ,  $RO_3$ ,  $R_2O_5$  (most common is  $SiO_2$ ) formed by structural units that don't repeat at regular distances from each other, forming an uneven net with random organization. *Net modifiers* are the elements that occupy the net holes, making the net bonds weaker, promoting the glaze fusion at lower temperatures. The most frequent net modifiers used are: Li, Na, K, Ca, Mg, Ba, Sr, Pb and Zn. The *net stabilizers* promote stability of the amorphous state of the glaze, avoiding its crystallization. The general chemical formula for net stabilizers is  $R_2O_3$ , being  $Al_2O_3$  the most important one (Renau 1994).

During glaze firing, liquid phase is formed due to the presence of fluxes and the low melting point of lead. This liquid penetrates the superficial pores of the ceramic body reacting

to a depth that is not only composition dependent but also of sintering time and temperature. The magnitude of this layer of great importance is given by the equation of time/temperature that allows, or not, the diffusion of elements between the glaze and the ceramic body (Aiazzi 1988). The greater the interaction between the glaze and the surface of the tile, the more its bonding strength.

The atmosphere and pressure of the kiln as well as a balanced thermal curve in such a way as to enable a smooth and effective degassing are the primary factors for the quality and appearance of the glaze. The melting point of the glaze is lower when its composition has higher amounts of Na<sub>2</sub>O and PbO, compared with glazes with higher K<sub>2</sub>O and CaO content (Guilherme, Coroado et al. 2011).

The wetting and coverage capacity of a glaze is determined by its surface tension, viscosity and opacity. This means that the wetting and coverage capacity depends on the chemical composition of the glaze (S.A.El-Defrawi, M.A.Serry et al. 1995).

*Pó de pedra* ceramic bodies are mainly composed by silica and alumina. As *pó de pedra* has a ceramic body with a white colour, there is no need to hide it with an opaque glaze. In this case, the glaze should have at least lead oxide, sand, and as defloculant, marine salt, perfect with its transparency and brilliant finishing (Leão 1999). Calcitic ceramic bodies, however, normally presents a pale yellow/reddish colour, making an opaque glaze necessary in order to hide it. In order to obtain a white opaque glaze, a few hundred nanometres particle size insoluble tin oxide (cassiterite; SnO<sub>2</sub>) used to be added up to 10%, together with 30% to 50% of quartz, 40% to 60% of lead and small quantities of sodium and potassium (Molera 1999, Molera and Vendrell-Saz 2001, Figueiredo, Veiga et al. 2005). This kind of lead-tin oxide opaque glazes were used until the beginning of the XX century, when the opacifier SnO<sub>2</sub> was replaced by other oxides, namely ZrSiO<sub>4</sub> (zircon), ZrO<sub>2</sub>, TiO<sub>2</sub> (S.A.El-Defrawi, M.A.Serry et al. 1995, Molera 1999).

As SnO<sub>2</sub> is a white opacifier, it should be expected that a whiter glaze should present a higher content of this oxide. Glazes with less than 5% of SnO<sub>2</sub> are not opaque enough, and contents over 10% are not necessary (Molera and Vendrell-Saz 2001). Nanometric sized tin oxide particles within the glaze scatter light in the blue region of the visible light spectrum (Molera 1999, M.S.Tite 2009). At the same time, the lead glaze itself absorbs in the blue region of the spectrum and that is why lead-alkali glazes appear whiter than the equivalent tin opacified alkali glazes. But there is a limit: tin opacified high content in lead glazes (up to

40%), tend to absorb too much in the blue region, appearing cream coloured (M.S.Tite 2009). It is known that its high price at the time justified the introduction of an engobe (*ingobbio*) visualized in the optical microscope as a white slip, covered by a glaze with small percentage of tin (or not at all) in order to decrease the amount of SnO<sub>2</sub> needed, not losing the desired white coloration too much (Alaimo, Bultrini et al. 2004) .

Considerations for the use of lead-alkali glazes, silica rich glazes, or/and the application of a transparent *coperta* layer over the decoration in Italian maiolica until the XVII century, were already pointed out by Piccolpasso in his work “The Three Books of the Potter’s Art” (M.S.Tite 2009). The *coperta* layer protected the painted decoration and helped to make an even and bright surface. All the technical choices made by our ancestors, were made in order to diminish costs without compromising the quality of the final product. One might think that for the same reasons, 19<sup>th</sup> century industrial tile producers began to use tin-lead glazes and with technical evolution, began to replace the tin opacified glaze with an engobe in which the decoration colours were applied with a final transparent glaze. To assure the engobe would completely cover the ceramic body colour, a mixture of a poor lead glaze rich in alumina was made (M.S.Tite 2009). In Portugal, importation from Britain, France and Holland would be almost exclusively reserved for glaze and decoration raw materials (Tin, sulphur, cobalt, sodium carbonate, potassium carbonate, prints and pigments) (Ferreira 2009).

As the ceramic body and the glaze are two very different entities, the simultaneous firing doesn’t guarantee a long lasting welding unless adequate linear thermal expansion compatibility between the glaze and the ceramic body in which it is applied is guaranteed (Navarro 1991). Linear thermal expansion is the dimensional variation of the tested specimen (glaze or ceramic body) with temperature rise and cooling. This dimensional variation has its cause in the thermal vibrations of the tested material (Renau 1994).

To experimentally determine the linear thermal expansion of the coupling ceramic body/glaze can be used a very rare instrument that measures simultaneously the linear thermal expansion of each body, with the temperature rising. When that kind of instrument cannot be used, one can cut the ceramic body into a dilatometer sample due to the ceramic body length and thickness, but not the glaze. Therefore, it was possible to experimentally determine the linear thermal expansion of the ceramic body of some of the studied samples, but it was impossible to get the same achievement with the glaze. For the glazes, theoretical calculations were made although the linear expansion coefficient of a glaze is maximum temperature and

cooling rate dependent (Froberg, Kronberg et al. 2007). In the same glaze, different cooling rates give different linear expansion coefficients (Renau 1994, Froberg, Kronberg et al. 2007).

During glaze firing, in the cooling process there are tensions generated by the coupling of two different materials with different thermal expansions. Glaze crazing appears when the glaze has a higher linear thermal expansion than the one shown by the ceramic body and is submitted to a tension force higher than its traction resistance. In the opposite situation, when the glaze linear thermal expansion is lower than that the ceramic body's, the glaze is subjected to a compression force (Navarro 1991, Renau 1994). If this compression force is higher than its compression resistance it will suffer from glaze peeling. Glaze resistance to traction is smaller (0,4 to 0,5 MPa) than the compression resistance (greater than 10 MPa), explaining why crazing appears much more often than peeling (Albero, Porcar et al. 1991).

In what concerns mechanical adjustment (thermal expansion of both bodies: ceramic body and glaze), most of the literature found only focuses on calcium-rich ceramic bodies, revealing that they adapt very well to lead glazes due to the fact that their expansion coefficient is very similar to that of the lead glazes (Lepierre 1899, Aiazzi 1988, Facincani 1993, Molera and Vendrell-Saz 2001, M.S.Tite 2009). The ideal enduring situation is that the linear thermal expansion ( $\alpha$ ) of the glaze is lower than that of the ceramic body (less than  $10 \times 10^{-7} \text{ }^\circ\text{C}^{-1}$ ) so the glaze is submitted to a moderate compression force studied as a satisfactory situation for crazing resistance (S.A.El-Defrawi, M.A.Serry et al. 1995). Crazing of glaze can also be promoted by ceramic body moisture expansion (Segadães, Carvalho et al. 2003, Mimoso 2011).

During the years of service of the **tiles in the façades**, the glaze coating **is exposed to extreme weathering**. Silica glazes are attacked by acid and the result is the leaching out by hydrogen ion of the alkaline and alkaline-earth cations present in the glaze network. Alkaline attack promotes the network dissolution with Si-O bonds rupture (Kopar 2007). On the other hand, lead glazes have a tendency towards leach ability under **acid conditions** (Belgaied 2003). Attending to the above considerations, it is expected that rain in contact with acid environmental pollution, causes, over the years **chemical attack to the glaze surface**.

Research data shown in this work will focus on increasing knowledge about the glaze layer as being a very important tile constituent as well as on the important **mechanical adjustment between the ceramic bodies and lead glazes**: the **thermal expansion coefficient**.

Twenty six glazed tiles were studied from which twelve are from the factory A.A.Costa, eight from J. Pereira Valente, one from a Lisbon factory Sacavém and five tiles with unknown production unit.

To enable the visualization of glaze/ceramic body assemblance in order to identify different typologies of glazing (the presence of engobe under the glaze coating, glaze degree of opacification), perpendicular fractures to the glaze surface were made and visualized in an optical microscope.

**SEM/EDS** was used with an acceleration voltage of 30 kV **for quantitative element determination** and acceleration voltage of 15 kV **for capturing images**, in fourteen samples.

Linear expansion coefficient was determined in six ceramic bodies.

All the samples were primarily visually inspected to evaluate the glaze integrity in what crazing concerns. Then, perpendicular fractures to the glaze were made, to enable the visualization of the glaze application type.

#### **4.2.2.1 – Optical microscope results of the glazed layer**

All the samples (26) were observed in the optical microscope and the conclusions about the glazing type used are summarized in Table 24, together with production units and glaze crazing percentage.

From the analysis of Table 24 it can be seen that all of the *pó de pedra* tile glazes are transparent and suffer from crazing. Furthermore, when engobe and transparent glaze was used in calcitic ceramic bodies, crazing was present in 80% of the studied samples. On the other hand, all the opaque glazes that were used in calcitic ceramic body present no crazing at all.

Table 24 – Summary of the observations made by optical microscope in the samples glazes

Sample description	Sample pictures	Factories	Sample references	crazing	% of crazing
Calcitic ceramic bodies with opaque glazes		A.A.Costa	P0, P58, P18, P21, P24 (5 samples)	0	0
		J.Pereira Valente			
		Unknown			
<i>Pó de pedra</i> ceramic bodies with transparent glazes		J.Pereira Valente	P20, P87, DA5, P137 (4 samples)	4	100
		J.Pereira and Sacavém			
Calcitic ceramic bodies with transparent glazes		J.Pereira Valente	P109, P14 (2 samples)	1	50
		Unknown			
Calcitic ceramic bodies with double glaze layer		A.A.Costa		12	80
					
					

			P9, P59, P66, P78, P98, P104, P115, P116, P124, P127, RJF229, P10, P19, P89, P133 (15 samples)		
		J.Pereira Valente			
		Unknown			

The transparent glazes applied in the *pó de pedra* range from 120  $\mu\text{m}$  up to 200  $\mu\text{m}$  and all of the samples observed suffered from severe crazing, as shown in the example in Figure 71.

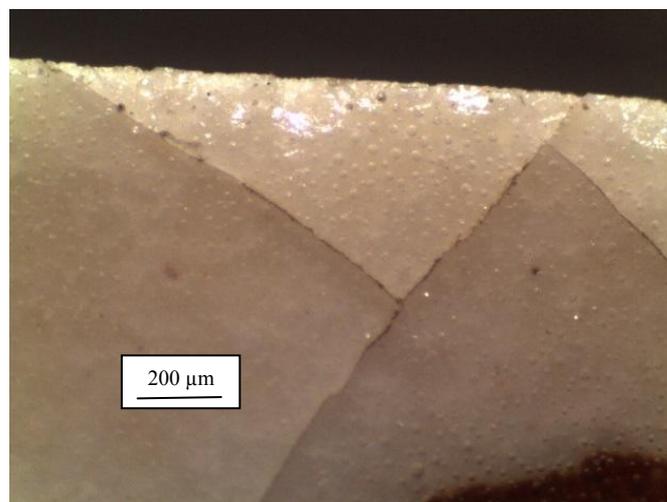


Figure 71 – Example of crazing suffered by all *pó de pedra* tiles' glazes

The opaque glazes thickness seen in the samples of calcitic ceramic bodies ranges from 200  $\mu\text{m}$  to 450  $\mu\text{m}$ . None of the analysed samples presented crazing evidences. In Figure 72 an example of opaque glaze can be seen in a perpendicular view.

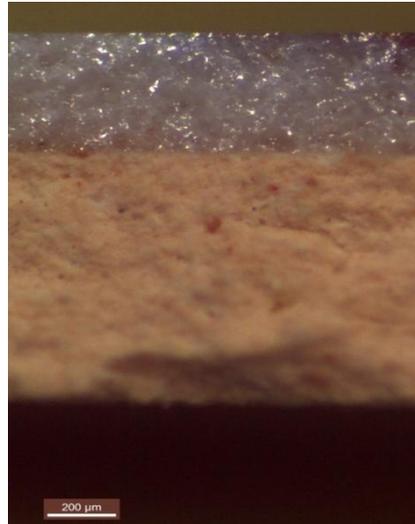


Figure 72 – Example of an opaque glaze in a perpendicular view

Fifteen of the twenty two calcitic tiles present a double glaze layer: one very white layer (engobe) just after the ceramic body and after that a transparent glaze. This trend, verified in 68% of the calcitic samples, helps to understand that the tiles in question are more recent than the rest of the studied samples, as tile glazing was executed in the same way as it is performed nowadays. In Figure 73, it can be seen a typical example of a calcitic tile with double glaze layer (engobbed ceramic) observed using optical microscope. The engobe layer found has a thickness ranging from 110 to 200  $\mu\text{m}$  and the transparent glaze beneath ranges from 200 until 300  $\mu\text{m}$ .

From the optical microscope observations, it is possible to summarise that the glazes of all the *pó de pedra* tiles suffer from severe crazing; the calcitic tiles with opaque glaze don't show any crazing. The remaining 17 samples of calcitic body, all but one tile of A.A Costa and one of J.Pereira Valente's, were produced with a double layer glaze. In the studied samples, double layer glazes are quite prone to crazing pathology (80%).

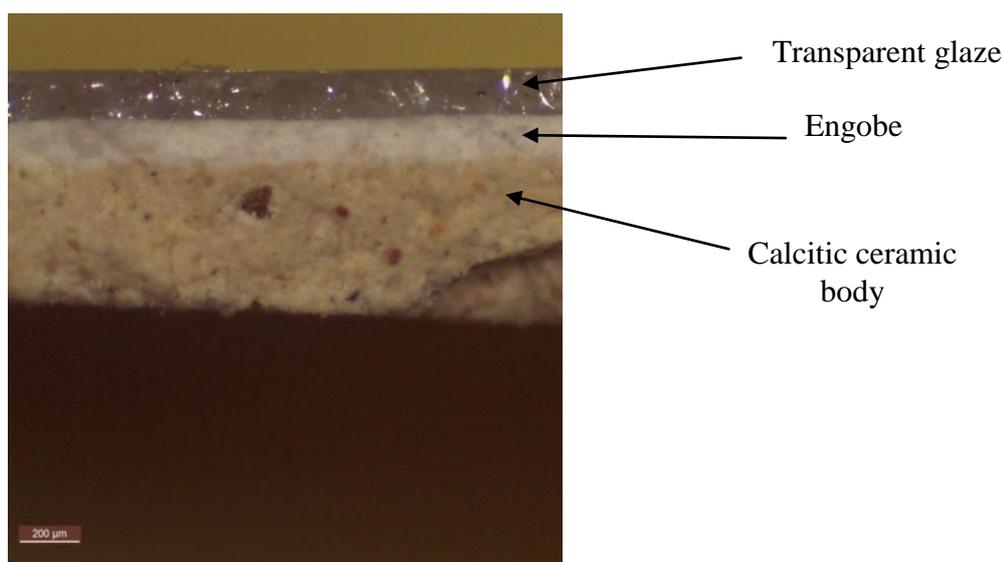


Figure 73 – Example of a calcitic tile with double glaze layer

#### 4.2.2.2 SEM/EDS values

From all the samples, fourteen were analysed using SEM/EDS. The elemental values obtained are displayed in Table 25 in which for all the glazes the analytical data was normalised to 100%. The uncertainty of the presented values varies between 0.1 and 2.8%, for the lowest and the highest values, respectively. For EDS calculations purposes a 10 µm long x 10 µm height area was considered and 2 to 4 measurements were performed on each glaze, in the non-decorated areas. The values presented are the medium values found. In Table 25 it can be seen that P137 glaze is quite different from the other *pó de pedra*'s because it is a Sacavém tile, a very different production approach.

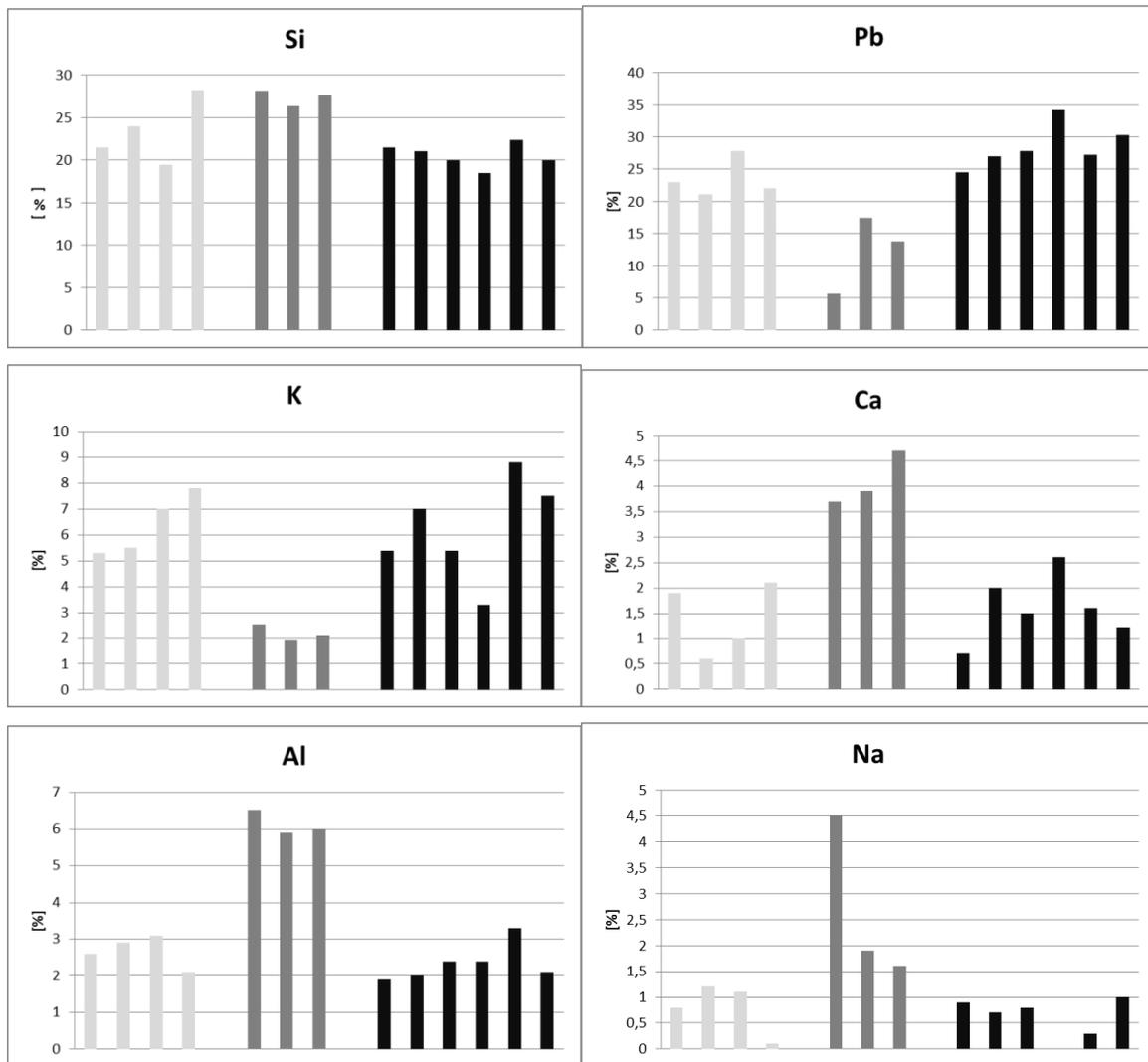
As previously seen, the lead-tin glazes were found only in samples without an engobe, as the tin oxide opacifies the glaze in a white colour, hiding the ceramic body. That is also the purpose of the engobe: hiding the ceramic body colour, transforming the visual aspect of the glaze to white.

Table 25 – EDS area analyses (wt %) obtained in 14 of the studied samples

Reference	Si	Pb	K	Ca	Al	Na	Mg	Sn	O	Observations
P0	21.5	23.0	5.3	1.9	2.6	0.8	0.2	7.0	37.2	Calcitic c. Body/Opaque glaze
P18	24	21.0	5.5	0.6	2.9	1.2	0.3	7.0	40.4	
P21	19.4	27.8	7.0	1.0	3.1	1.1	0.1	7.5	33.2	
P24	28.1	22.0	7.8	2.1	2.1	0.1	0	7.1	30.7	
P20	28.0	5.7	2.5	3.7	6.5	4.5	0.4	0	51.9	<i>Pó de pedra</i> /Transparent glaze
P87	26.3	17.4	1.9	3.9	5.9	1.9	0	0	43.0	
DA5	27.6	13.8	2.1	4.7	6.0	1,6	0.3	0	43.9	
P137	13.6	49.1	0.4	0.1	4.4	3.4	0	0	30.2	
P127	21.5	24.5	5.4	0.7	1.9	0.9	0	0	43.4	Calcitic c. Body/Engobe+trans
P133	21.0	27.0	7.0	2.0	2.0	0.7	0	0	41.0	
P78	20.0	27.8	5.4	1.5	2.4	0.8	0.2	3.7	38.0	
P10	18.5	34.2	3.3	2.6	2.4	0	0	0	31.0	
P14	22.4	27.2	8.8	1.6	3.3	0.3	0.1	0.9	35.5	
P9	20.0	30.3	7.5	1.2	2.1	1.0	0.3	0	37.5	

In the case of calcitic ceramic bodies with double layer glaze (with engobe), the presented values in Table 25 concern only the transparent layer. To assure that only the transparent glaze was analysed measurements were made in a perpendicular view, so the electron beam would not have the chemical interference of the engobe.

In Figure 74 it is graphically summarized the values of the elements Si, Pb, K, Ca, Al and Na of the studied samples. The curves on the left concern opaque glazes, the central curves concern *pó de pedra* transparent glazes and the curves on the right concern transparent glaze of the tiles with engobe.



opaque glazes; 
  transparent glazes in *pó de pedra* ceramic bodies; 
  transparent glazes in calcitic bodies

Figure 74 – Sum up of the value of Si, Pb, K, Ca, Al and Na in the studied glazes

Comparing elemental values of the opaque glazes with the transparent glazes from the *pó de pedra* samples in Table 25 and Figure 74, it can be seen that the latter didn't present any Sn, their content in Na, Ca and Al is higher, while the Pb and K contents are lower. Generally, the mentioned transparent glazes have less Pb and K but higher Ca, Al, Na and Si. PbO, Na<sub>2</sub>O, K<sub>2</sub>O and CaO are *net modifiers oxides* promoting net rupture points and weakening the

glazes. The more the quantity of net modifiers, the greater the expansion coefficient, lower melting point, lower mechanical strength, higher risk of crystallization, among other consequences (Renau 1994). To prevent crystallization and promote net stabilization, transparent glazes applied to *pó de pedra* ceramic bodies present higher content in  $\text{Al}_2\text{O}_3$ . Overall, thermal expansion coefficient of the mentioned transparent glazes isn't expected to be very different from the opaque ones.

Analysing Table 25 and Figure 74 it can be seen that chemically transparent layer and opaque glazes have similar values of Si, K, Ca, Al and Na. The differences between them are Sn and Pb content.

The transparent glaze of *pó de pedra* is rather different presenting less K and Pb but much higher Al, NA and Ca than the other glazes.

$\text{SnO}_2$  content in the glaze is reflected in the visual glaze homogeneity, colour and opacifying ability (Coentro, Mimoso et al. 2012). The samples under study in the present work present low tin content, when compared with other international studies on maiolica and Portuguese wall tiles till 17<sup>th</sup> century (Coentro, Mimoso et al. 2012).

#### 4.2.2.3 SEM - images of lead-tin glazes

SEM was performed in several glaze's samples in order to evaluate glaze weathering, glaze crazing and other particularities of interest.

P24 glaze is an opaque tin glaze and for that it was observed to try to find out the characteristics cassiterite ( $\text{SnO}_2$ ) insoluble nanometric crystals embedded in the glaze (Molera 1999, Padill, Schalm et al. 2005, Coentro, Mimoso et al. 2012).

Cassiterite crystals were observed and identified by EDS. These nanocrystals are disseminated in a non-homogeneous way in the entire glaze matrix (Figure 75).

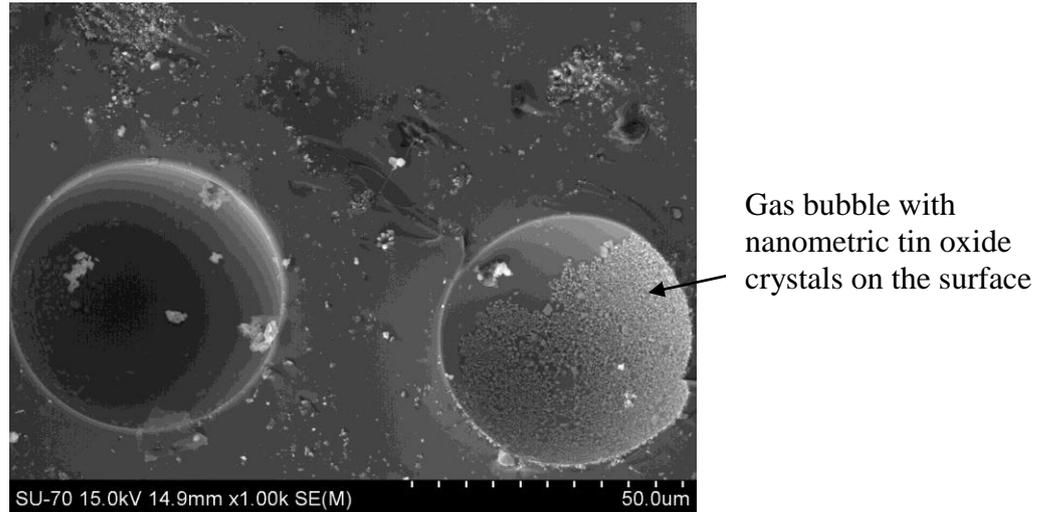


Figure 75 – Tin oxide cristalization in an opaque glaze (P24)

The glazed surface of the tile is in constant **contact with pollution elements** in the form of **gases** or as **rain**. These pollution elements have a **leaching action in the chemical elements** of the glaze causing **elements' release leading to their degradation**. Lead can be leached with **acid solution**, like **acid rain** or **humid sulphur oxide** (Belgaied 2003, Garcia-Heras, Carmona et al. 2005). Silica glazes are also attacked by acid solutions by leaching out alkaline and alkaline-earth cations from the glaze network. In these glazes, the alkaline attack leads to the rupture of sillicium-oxygen bonds leading to the network dissolution forming a superficial silica gel layer (Garcia-Heras, Carmona et al. 2005, Kopar 2007). Figure 76 shows a SEM image of P10 glaze surface **where chemical attack can be seen**.

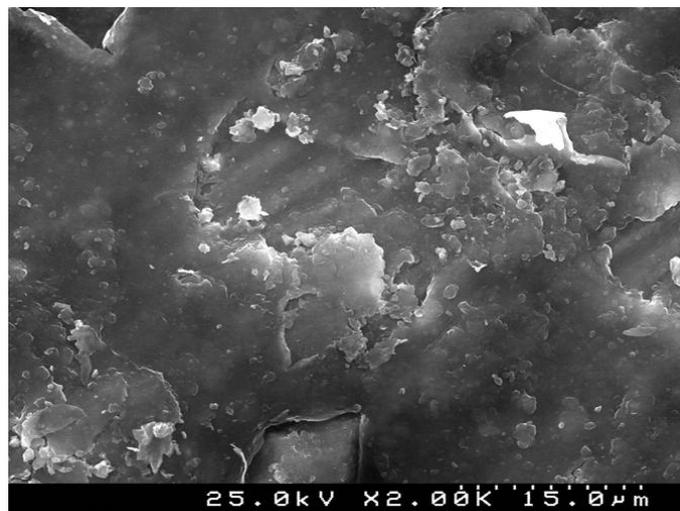


Figure 76 - P10 SEM glaze surface observation where chemical attack can be seen

Figure 77 is a SEM image of P133 tile suffering from glaze detachment. In this image a **surface salt crystallization** can be seen on the **tile surface** once the glaze is no longer a physical barrier.

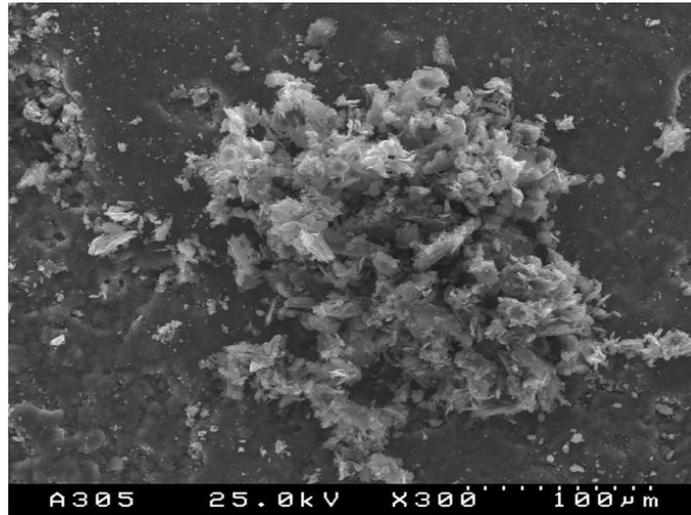


Figure 77 - SEM observation of the upper part of the P133 tile, were once the glaze was. Instead, salt crystals can be seen

#### 4.2.2.4 – Experimental determination of linear expansion coefficient ( $\alpha$ ) of the ceramic bodies

Each material has its characteristic volume thermal expansion. Cubic thermal expansion of a ceramic body can be defined as the unit volume increase by increasing its temperature by 1°C (Aiazzi 1988).

Six samples of ancient ceramic bodies were cut and analysed by dilatometry: three calcitic ceramic bodies and three *pó de pedra* bodies. The results obtained are displayed in Table 26. All linear expansion coefficient ( $\alpha$ ) data expressed in the present work was

considered between 20°C and 400°C because it is the temperature interval that is considered by the glaze and ceramic body enterprises, becoming the temperature interval better known.

Table 26 – Linear expansion coefficient of 6 samples of ancient ceramic bodies

	Calcitic ceramic bodies	<i>Pó de pedra</i> ceramic bodies
$\alpha$ [°C <sup>-1</sup> ]	7.2 x 10 <sup>-6</sup> to 8.4 x 10 <sup>-6</sup>	3.6 x 10 <sup>-6</sup> to 5.7 x 10 <sup>-6</sup>

By analysing Table 26 it can be seen that calcitic ceramic bodies have higher linear expansion coefficient than *pó de pedra*, making the former more suited to be used with lead glazes (Lepierre 1899, Albero, Porcar et al. 1991).

#### 4.2.2.5 - Theoretical discussion of the expansion coefficient ( $\alpha$ ) of the ancient glazes

As it is very difficult to find equipment able to experimentally determine thermal expansion coefficient of the glazes applied in the ancient tiles, a theoretical approach was undertaken, although this implied associated errors, as for instance, the lack of consideration of firing kinetics.

Theoretically the linear thermal expansion coefficient can be determined between 20° C and 400° C by using Formula 1 (Renau 1994):

$$\alpha = (1/100) \cdot \Sigma (m_i \cdot \alpha_i) \cdot 10^{-7} \text{ [}^{\circ}\text{C}^{-1}\text{]}$$

$m_i$  – molar percentage of each oxide present in the glaze

$\alpha_i$  – oxide factor (Appen serie)

In the case of the studied samples, the Appen oxide factor ( $\alpha_i$ ) can be determined by the use of the Table 27.

Table 27 – Appen oxide factors (Renau 1994)

Oxides	Appen oxide factor ( $\alpha_i$ ) (20-400°C)
SiO <sub>2</sub>	38
SnO <sub>2</sub>	-45
Al <sub>2</sub> O <sub>3</sub>	-30
MgO	60
CaO	130
PbO	130
NaO	395
K <sub>2</sub> O	465

Calculating each oxide molar content, and then using Formula 1, the theoretical linear expansion of the ancient glazes is shown in Table 28 together with ceramic bodies' experimental values.

Table 28 – Comparing theoretical glaze  $\alpha$  with experimental ceramic bodies'  $\alpha$

	Calcitic ceramic bodies with opaque glazes	Average values	<i>Pó de pedra</i> ceramic bodies with transparent glazes	Average values
$\alpha$ glaze ( <b>calculated</b> ) [°C <sup>-1</sup> ]	6.0 x 10 <sup>-6</sup> to 7.1 x 10 <sup>-6</sup>	6.6 x 10 <sup>-6</sup>	5.6 x 10 <sup>-6</sup> to 6.9 x 10 <sup>-6</sup>	6.3 x 10 <sup>-6</sup>
$\alpha$ ceramic body ( <b>experimental</b> ) [°C <sup>-1</sup> ]	7.2 x 10 <sup>-6</sup> to 8.4 x 10 <sup>-6</sup>	7.8 x 10 <sup>-6</sup>	3.6 x 10 <sup>-6</sup> to 5.7 x 10 <sup>-6</sup>	4.7 x 10 <sup>-6</sup>

Analysing Table 28, although it is a theoretical calculation, the opaque glazes and the transparent glazes in the *pó de pedra* tiles have similar  $\alpha$ , while the ceramic bodies show a large difference. As said before, the optimal thermal expansion situation for a durable glaze/ceramic body bonding is that the glaze has a thermal expansion coefficient lower than that of the ceramic body in  $10 \times 10^{-7} \text{ }^\circ\text{C}^{-1}$ , in order to be under compression. That situation exists in the calcitic ceramic body/opaque glaze samples, explaining the absence of crazing in these tiles. In the *pó de pedra*, however, the opposite can be seen: the glaze thermal expansion coefficient is much higher than the ceramic body's forcing the glaze to be highly tensioned. As the resistance of glazes to tension is very low (0.4 to 0.5 MPa) the glaze collapses in the form of crazing. This technical handicap probably is the responsible for the generalized glaze crazing present in all of the *pó de pedra* tiles.

Glaze crazing is a defect that, when seen closely, diminishes the beauty of the ancient tiles, as a decorative element and as cultural heritage legacy due to the possible introduction through the crazing fractures of microorganisms provoking stains, and salts efflorescence due to local wetting and drying preferential mechanism. Understanding it help us to increase the knowledge of the technical difficulties encompassed in the tile production despite great evolution of the industrial process. It is uncertain if crazing was considered as “technical flaw”, or just a peculiarity, in the second half of the 19<sup>th</sup> century and beginning of the 20<sup>th</sup> century.

During glaze firing, in the cooling process there are tensions generated by the coupling of the ceramic body and the glaze, materials with different thermal expansions that need to be adjusted to each other. In the present work it was found that all the SnO<sub>2</sub> opaque glazes are applied in calcitic ceramic bodies and present no crazing, probably due to the fact that glaze thermal expansion coefficient is smaller than that of the ceramic bodies around  $10 \times 10^{-6} \text{ }^\circ\text{C}^{-1}$  and all the transparent glazes applied in *pó de pedra* ceramic bodies suffer from severe crazing probably due to glaze thermal expansion coefficient being much higher than that of the ceramic bodies' due to the latter chemical/mineralogical composition. This situation promotes high stresses in the glaze that with time tend towards equilibrium, with crazing as consequence.

From the samples under analysis, results point out that in the factories A.A.Costa and J. P. Valente the evolution of the glazing technique went from PbO-SnO<sub>2</sub> opacified glazes to a more economical solution in early 20<sup>th</sup> century by using engobe plus a transparent glaze.

Within the samples under study there was one known Sacavém tile (P137) which is the only, as far as it is known, that is not from the Northern tile production centre. Through its characteristic technical data, it can be confirmed what was already known by the historical information: Sacavém had a completely different approach to raw materials utilization and tile composition. Through the present study, it can be seen that Sacavém transparent glaze used in a *pó de pedra* ceramic body had higher quantity of lead and less silica, calcium and potassium. These characteristics confer Sacavém glaze with the lowest thermal expansion coefficient among all samples.

In Figure 71 it can be seen that the crazing cracks of the *pó de pedra* tiles show abrasion and are filled with dust. That indicates that the cracks are very old, probably appearing not long after the tile production, revealing a production problem.

The present study helped to understand that the *pó de pedra* technique did not last long as a production solution, perhaps due to the difficulty of attaining a good technical match between the ceramic body and the glaze. The next logical direction was to use engobe, perhaps also with some technical difficulties in its first years of production.

### **4.3 Pathology and risk factors of the tile facades from late 19<sup>th</sup> early 20<sup>th</sup> century**

Because of its length and complexity, it is not intended to catalogue or suggest explanations for all kinds of pathology. The work will focus on the most applicants. The pathology encountered varies as to its extent and possible causes. This work will focus on the possible causes.

The pathology of tiles addressed in this work is solely those which, as far as is known, can promote pathology in the tile panel. The pathology associated with the production of tile at the beginning of industrialization is undoubtedly much less severe regarding visual appearance than that displayed by the tiles produced previously. This is obviously, a technological advancement that is reflected in more reproducible and harmonious aspect displayed by tile panels.

The tiles in question are already pressed, displaying in the back of the tile embossed marks with or without identification of the production unit. In general, the ceramic body no longer presents the more ancient tiles inhomogeneities, revealing more care in the ceramic body preparation. The application of glaze and decoration had new procedures that eliminated serious defects of the past, such as the crawling of the glaze that was caused by grease or powder deposited on the surface of the unglazed tile, common by the excessive waiting time that the ceramic body suffered before its decoration/glazing (Aiazzi 1988).

One of the examples of **manufacturing anomalies** observed in the studied tiles is **the pore**, which is characterized by being a depression in the glaze that goes down until the ceramic body, connecting it to the outer atmosphere.

On the left side of Figure 78 a tile with multiple pores can be observed in which with time and salt water attack, glaze detachment has occurred around the pore, as it is observed on the right hand side of the same figure.

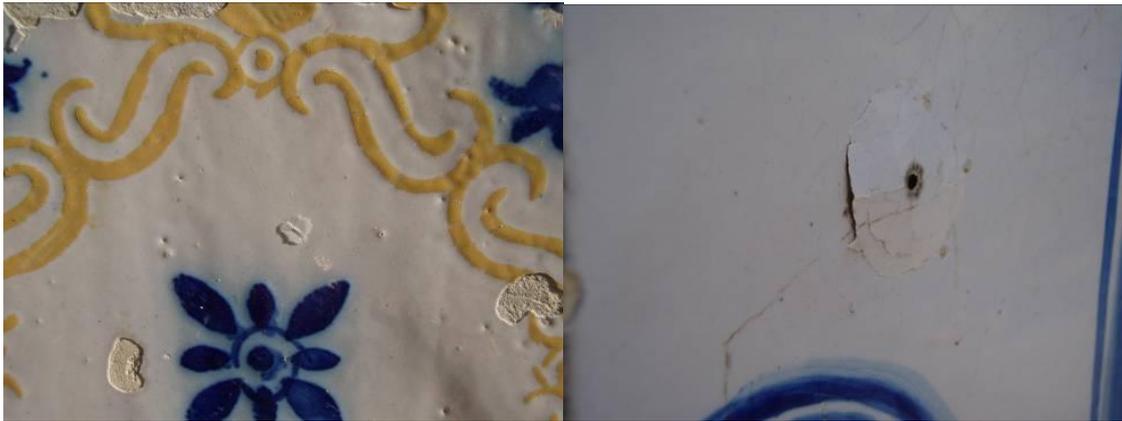


Figure 78 – Tiles with pores and associated pathology (author' photos)

Another frequent pathology in facades is glaze **crazing**. The glaze crazing consists of multiple interconnected fractures forming a network of polygons connected with each other (Mimoso 2011) as seen in Figure 79. However, it should be pointed out that the buildings facades of which display the complete array of tiles with profound visible glaze crazing pathology are not frequent in Ovar. Thus, the common feature is that the glaze crazing appears confined to areas of **frequent existence of humidity**, usually near the base of the panel. It is still difficult to unequivocally assign this pathology, as the phenomenon may be due to an inadequate agreement between ceramic body and glaze (which usually manifests itself a few months after production) or may be due to **ceramic body expansion** due to moisture, **exposing the glaze to excessive traction** and subsequently causing its rupture. However, it seems somewhat logical that when the façade presents all of its tiles (or most of them) with glaze crazing, they must suffer from **manufacturing problems concerning the ceramic body/glaze agreement**.

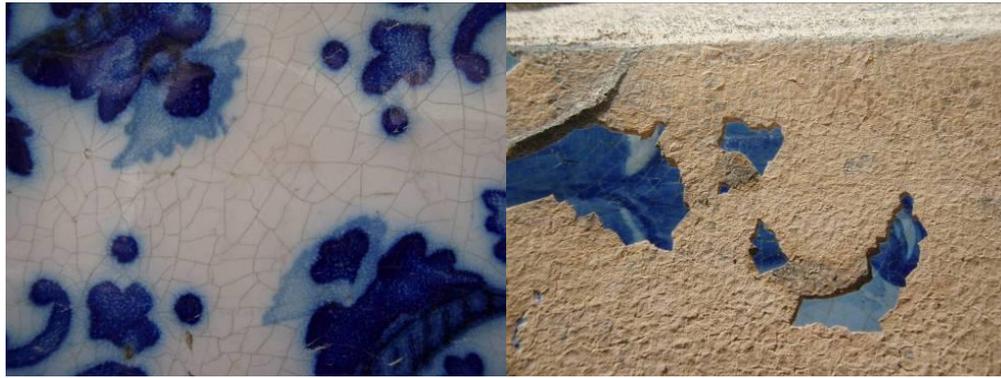


Figure 79 – Example of glaze crazing (on the left side) and glaze detachment by glaze crazing (on the right)

As an example of the previously spoken about the causes of the glaze crazing, Figure 80 exemplifies a tile in which only the part of its body exposed to frequent humidity presents glaze crazing (the right part of the figure), while the rest of the element has no apparent pathology.



Figure 80 – Example of glaze crazing provoked by persistent humidity (author's photos)

A very interesting tile defect is the colour detachment caused by differences between the colour and the glaze thermal expansion coefficient. This defect is easily detected as only one of the colours of the decoration misses in the drawing, as can be seen in Figure 81.



Figure 81 - Colour detachment due to a poor colour/glaze thermal expansion coefficient adjustment (author' photos)

Another of the recurrent pathology is the glaze detachment on the perimeter of the tile (Figure 82). Provoking this anomaly may be forces exerted by movements of the facade on the sides of the tile, causing detachment in their more fragile area (the glaze), deficient joints design, attack of salts crystallization since this is the area of tile where **wetting/drying** processes is easier or local moisture expansion of the ceramic body causing the glaze degradation by traction stresses (Monteiro 2012).



Figure 82– Examples of tile perimeter glaze detachment (author’ photos)

The lack of adhesion of the mortar to the ceramic material is one of the possible causes of tile detachment from building from the late 19<sup>th</sup> century beginning of 20<sup>th</sup> century. The tile detachment can lead to tile lacunae (Figure 83 on the left) or to the appearance of bulging (Figure 83 on the right).



Figure 83 – Examples of lack of mortar/tile adherence (author’ photos)

The pathology called bulging may also be due to moisture expansion of ceramic body of the tile where the mortar joint is not large enough or elastic enough to absorb this increase in size.

Another classic example consists of the glaze detachment caused by salty moisture (Figure 84). The degradation of the glaze is extensive and very often, there are visible cracks, suggesting a pressure exerted by salt crystallization greater than the bonding strength between the ceramic body and the glaze.



Figure 84 – Example of glaze detachment caused by salt crystallization (author's photos)

**Glaze detachment** is one of the most severe problems in old ceramic tiles in building facades, mainly appearing in the facade areas that are closer to the ground. Its appearance is undoubtedly connected to **rising ground water by capillarity** through the building structure and affects indistinctively all kinds of old tiles. Too frequently, restoration technicians face this problem without knowing its source that is why this pathology was carefully looked at.

In the present work tiles from the late 19<sup>th</sup> and early XX centuries from Ovar building facades, were studied in order to **evaluate the effect of capillary water absorption** by the building material throughout exposure time.

Due to the fact that mortar and tile act together as façade cladding, the influence of **mortar binder in tile pathology is determinant**. Due to this fact it will be discussed separately in 4.3.1.

#### 4.3.1 Glaze detachment in old ceramic wall tiles – The influence of mortar binder

Glaze detachment consists in the shedding of the glazed layer of the tile and consequent loss of the pictorial part together with the impermeable layer, leaving therefore the ceramic body unprotected (Figure 85).



Figure 85 – Example façade and tile suffering from glaze detachment

It is known that there are a wide number of probable causes for glaze detachment referred previously, such as mechanical stresses caused by the building, stresses caused by a poor joint design, **lack of compatibility of thermal expansion coefficient between ceramic body and glaze**, ceramic body moisture expansion and salt crystallization. In this study, with the use of bibliographical research and analytical techniques, a major cause for glaze detachment is encountered in the studied tiles.

Reviewing some possible glaze detachment causes, a study performed by Pereira (Pereira 2011) points as causes of early deterioration of the integrity of the glaze, linear thermal expansion and/or moisture expansion. It is known that when there are problems of linear thermal expansion agreement between the glaze and the ceramic body biscuit, visible cracks appears with time on the glaze as a way of alleviating stresses generated between the

two bodies. That can explain the glaze detachment in tiles suffering from production problems. However, it is observed that there are many tiles that suffer from glaze detachment without showing glaze crazing. Studies done by Molera (Molera and Vendrell-Saz 2001) show that the thermal expansion coefficient in ceramic rich in calcium is similar to the thermal coefficient of expansion of lead-glazed preventing cracks on cooling, reinforcing the idea that it would not be very usual to observe production crazing problems at the time. The same observation is made by Lepierre in his study of a significant number of Portuguese tiles from 1899 (Lepierre 1899).

Another study (Mimoso 2011) concludes that there could be a previous manufacturing defect in tiles as pinholes or cracks in order to initiate the deterioration process. That indeed explains some cases of glaze detachment, but it does not explain the specificity and extent of glaze detachment in tiles near the ground in almost all the old tile façades throughout the various city/town centres in Portugal.

On the other hand, the **phenomenon of ceramic body expansion by humidity** is one of the possible factors **causing tensions over** the years due to the **constant drying/wetting cycles** suffered by ceramic tiles in façades. **Studies on the expansion of the ceramic body due to humidity reveal** that the phenomenon is quite **dependent on the amount of amorphous phase** (Carvalho 2002, Segadães, Carvalho et al. 2003).

Looking at a great amount of façades, there are evidences that, as glaze detachment is so common and happens with all kinds of old exterior tiles, a more universal approach is necessary. **Porosity of studied samples** is a **major factor in the tile degradation process** as it is of major importance in the tile/mortar bond (Flatt 2002, Prikryl, Lokajíeek et al. 2003), (E.Molina, G.Cultrone et al. 2011, Botas, Veiga et al. 2012).

The total porosity of a material is constituted by the open and closed porosity, although the former is the one technically interesting because of its role in hydric issues. **The pores volume and distribution strongly affect material over time** (E.Molina, G.Cultrone et al. 2011). Porosity values of a fired ceramic body are highly dependent on the pressing conditions (pressure used, raw materials particle size, pressing moisture content), quantity of the gas liberated by the raw materials during firing decomposition, together with firing conditions (Aiazzi 1988). **The size and distribution of the open pores** constitutes the network of **porosity** that characterizes most **properties of ceramic materials such as mechanical strength, thermal**

conductivity, thermal shock resistance, water absorption and salt crystallization (Flatt 2002, Espinosa, Franke et al. 2008, Santos, Vaz et al. 2012).

The network of pores, besides being a very useful characteristic of the ceramic body to facilitate the penetration of mortar binder in the ceramic body and therefore improving adherence, is also a moisture input channel into the structure of the ceramic body. This pore network is susceptible to salt attack, when there is rising water brought by capillarity and posterior drying (Santos, Vaz et al. 2012). This phenomenon of wetting/drying cycle is more severe near the wall base, as usually, in 19<sup>th</sup> and early 20<sup>th</sup> century tile facade, the rising humidity doesn't exceed 2.5 meters from the ground (Ferreira 2009). In a wall in contact with ground water, water rise will dissolve all soluble salts in its path until it is saturated. When the evaporation begins on the wall surface and if it occurs at a slow rate or the quantity of saline solution at the surface is abundant, the concentration of crystallized salts takes place in the exterior of the wall, usually named as efflorescence (Figure 84) which can be defined as a “white substance with poor adherence, that present in tiles or in its joints, in places where the drying is possible” (Mimoso and Esteves 2011). If the rate of evaporation on the wall surface, where drying is possible, exceeds the rate of solution supplying at the surface of the material, the liquid/vapour interface retreats to the interior of the material. The concentration of salt occurs just below the surface, and the crystallization pressure is generated (Scherer 1999) or in the interior of the material. In these cases, crypto-florescence is present (Figure 86).

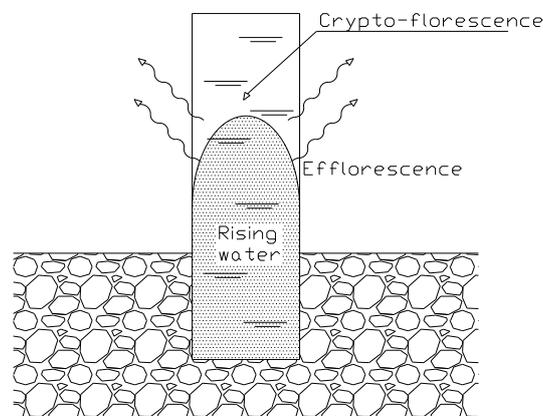


Figure 86 – Efflorescence and crypto-florescence example (Scherer 1999)

It is well known that the development of crystallization pressure requires supersaturation of the liquid film already involving crystallized salts (Scherer 1999, Scherer 2000, Flatt 2002, Espinosa, Franke et al. 2008). Most salts present in exterior porous building materials dissolve and precipitate in certain humidity and/or temperature conditions. The supersaturation develops upon the dissolution of a mineral of high solubility and precipitation driven by evaporation (Scherer 1999) and crystallization behaviour depends on salt type and porous structure (Scherer 1999, Scherer 2000, Flatt 2002, Scherer 2004, Linnow and Steiger 2007, Espinosa, Franke et al. 2008, Santos, Vaz et al. 2012). The supersaturation of the salt in solution, the pore size and repulsive force magnitude between salt and the confining pore surface, will determine if there will be salt crystallization and how much damage this crystallization will cause. Supersaturation of a solution in a pore depends on a variety of parameters such as salt nature, solution rate supply and water rate evaporation (Scherer 2004).

In Kirsten's study of salts in ancient tiles (Linnow, Halsberghe et al. 2006) it was found that the quantity of salts present in efflorescence was about 1% of the total salt quantity present in the studied tiles demonstrating that most of the salt crystallization is usually in the form of crypto-florescence. Although salt crystallization in a single pore doesn't cause any damage, crystal growth through a region of the porous structure may cause damage (Scherer 1999). The nature of the salt involved in the process, and the rates of solution supply versus evaporation in the ceramic body, highly influence the super saturation (López-Azevedo, Viedma et al. 1997, Scherer 2004). The capillary rise and evaporation (wetting and drying cycles) promoting supersaturation of the liquid in the pores, influence salt crystallization that can cause high crystallization pressure (La Iglesia, González et al. 1997, López-Azevedo, Viedma et al. 1997, Scherer 2004) . The intensity of salt formation and how much the generated stresses are able to cause damage, depend on factors like pore structure, the supersaturation of the solution and the energy of the interface pore wall/crystal (Scherer 1999, Scherer 2004, Espinosa, Franke et al. 2008). Studies reveal that salt damage is more severe in materials with high quantity of micrometric size pores than in materials with low pore quantity (La Iglesia, González et al. 1997, Viles and Goudie 2007). Salts that crystallize in the pores may be inherent to the material itself, to the mortar, to other building structure materials transported by ground water, or inherent to ground water itself (López-

Azevedo, Viedma et al. 1997, Scherer 2004). “Crystallization mechanism is substrate nature dependant (pore size and distribution) but also related to relative humidity/temperature and chemical composition of the penetrating solution” (López-Azevedo, Viedma et al. 1997).

All the degradation studies provoked by salt crystallization mentioned in the present work report to degradation of rocks because it is thought the wetting/drying mechanism can be applied to tiles. There is a vast quantity of these studies, while no scientific study on salt crystallization occurrence in tiles was found. Every kind of rock has different susceptibility to salt weathering depending on porosity and mechanical strength (mineralogy, micro hollows, micro cracks, etc) (Casal Moura, Carvalho et al. 2007, Viles and Goudie 2007). The use of sedimentary rocks in construction is well established as they are the most common of porous rocks (E.Molina, G.Cultrone et al. 2011). In his work, Molina studied sandstone, limestone, dolostone and travertine porosity. From this work (Figure 87) polarized optical microscope microphotographs can be seen showing pore morphologies of the mentioned rocks.

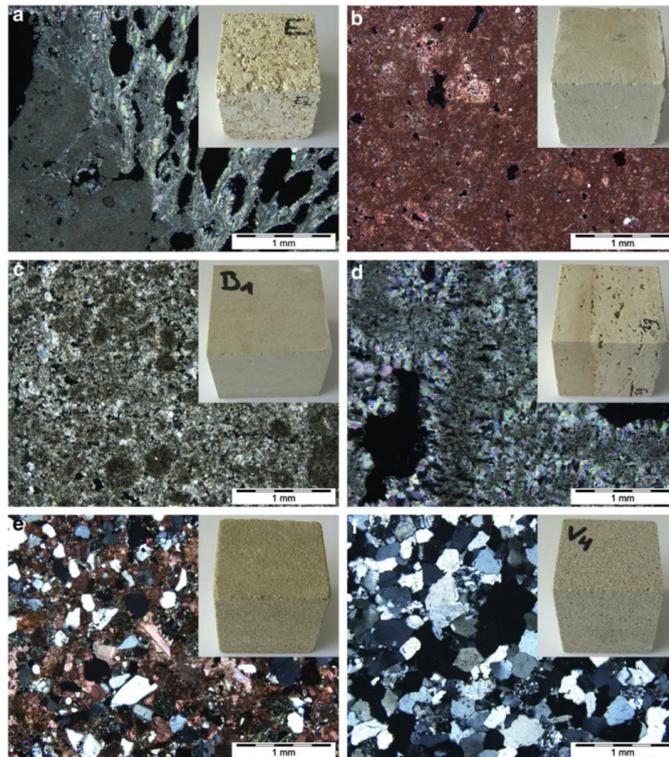


Figure 87 – Polarized optical microscope microphotographs of: a) Santa Pudia limestone (SP), b) Fraga limestone (CF), c) Bonar dolostone (DB), d) travertine from Albox (TA), e) Uncastillo sanstone (AU), f) Villaviciosa sanstone (AV) (E.Molina, G.Cultrone et al. 2011).

Porosity values obtained by mercury intrusion porosimetry for Molina samples are as shown in Figure 88. Water absorption values range from 7.8% until 33.4%. In the same study, Molina quotes Rodríguez Navarro saying that stones with a high percentage of small pores are more susceptible to salt decay than those with higher amounts of large pores (E.Molina, G.Cultrone et al. 2011).

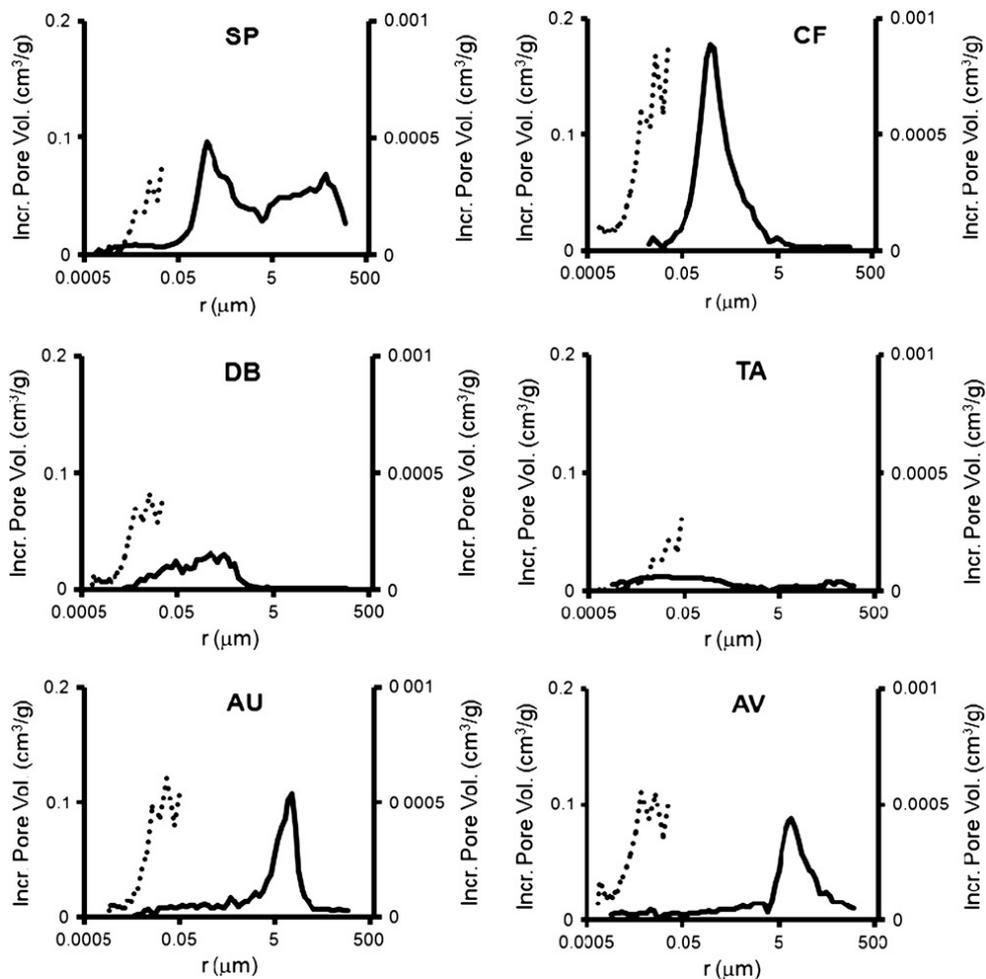


Figure 88 - Mercury intrusion porosimetry data (continuous line) of studied samples by Molina (E.Molina, G.Cultrone et al. 2011)

In Figure 89 mercury intrusion porosimetry data of calcitic tiles (P127, P133 and RJF230) and *pó de pedra* tiles (P20) of some of the old tiles under study in the present work is shown. It may be said that there is some similitude in terms of pore dimensions

distribution between calcitic paste bodies and CF. It is also clear that this type of porosity must be interconnected.

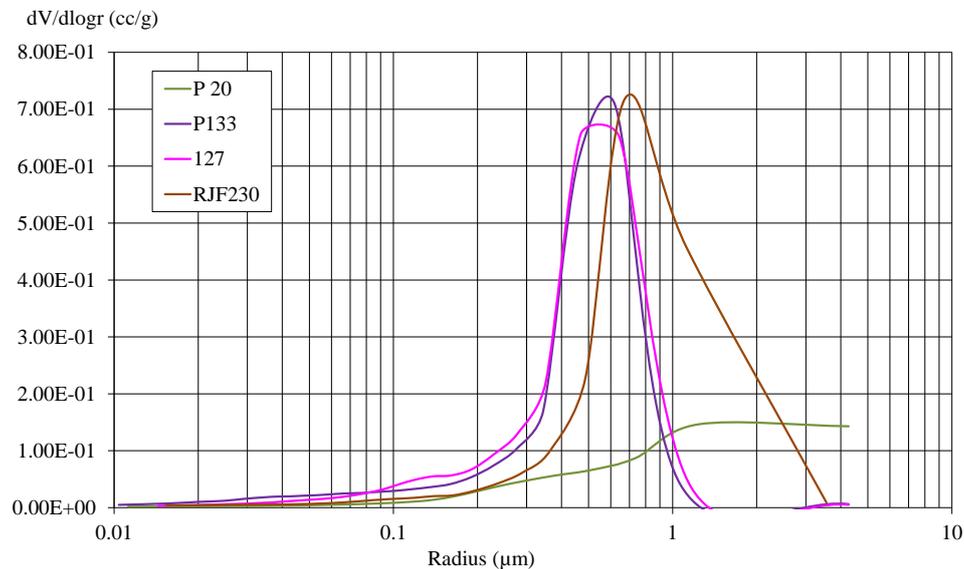


Figure 89 - Mercury intrusion porosimetry of some of the old tiles studied

Comparing Figure 88 and Figure 89 one can see that stone (CF) and old tile porous network have resemblances.

It is believed that studies performed on rock samples can be applied as guide lines to tiles as both have open interconnected porosity and the pathology of salt crystallization has similarities, although keeping in mind that tiles might have different susceptibility to salt weathering and higher porosity. In rocks applied to facades the entire rock surface is in contact with the environment, making the drying process easier. The ceramic tile has a water proof layer forcing the drying to be made by the tiles' borders. Although the drying in tiles is not made in the entire air exposed surface, the ceramic body porosity is usually higher than the stones'. For example, Portuguese limestone can have a water absorption up to 12% (Casal Moura, Carvalho et al. 2007) , demonstrating that it is more prone to salt degradation than rocks with less open porosity, like marble (0.1% of water absorption) or granite (0.4% of water absorption) (Viles and Goudie 2007), while the studied old tiles have open porosity from 13.5% up to 22.8%.

In the tile, the wetting can be made by the mortar joint or/and by the capillary rise of ground water, or by a pathology. Although the drying can only be made by the mortar joint and by the tile pathology (a slow drying) nevertheless, wetting and drying cycles are present in an environment full of soluble salts.

“Mortar porosity is defined as the space within the mortar which can be filled in by air” (Pereira 2008). These empty spaces result mostly from the evaporation of the water used during the components’ mixing, but also from the air that is trapped inside during the mixing process. The mixing water inside the mortar is a continuous film, and therefore, in the consequence of the drying of this water it originates porosity with a good degree of interconnection. In this way, the mortars become more permeable and drying will become easier, since the contact of the interior of the mortar with the exterior atmosphere is facilitated (Pereira 2008). The diffusion of water vapour is a process by which water vapour diffuses through a mortar. The process of diffusion of water vapour is due to the evaporation of water previously absorbed by the mortar. An increase in open porosity as well as the connectivity between pores increases the diffusion coefficient (Botas 2009). As air lime mortars have large interconnected porosity, it is characterized by having big diffusion coefficient of water vapour values (Pereira 2008). It is estimated that the joints in Ovar might have a 1:1 composition and many of them are dry joints (don’t have any joint mortar). In this way, drying through the mortar joints is made rapidly causing local preferential spots of salt crystallization development in the tile borders, which become a preferential place for glaze detachment (Figure 90).



Figure 90 - Glaze detachment in the tile borders caused by salt crystallization.

This phenomenon is well described by Isabel Ferreira (Ferreira 2009) in a book made out of her practical field work at ACRA (Ovar), when she states: “Most of Ovar’ tile facades efflorescence are from lime origin, commonly in the form of a whitish film on the tiles edges [...] Its origin and formation is usually pointed at masonry mortars and joints leaching out action [...] This phenomenon is more common in the South-facing facades of coastal areas, due to increased release of water vapor caused by sun exposure.

For the present study Oporto climate data were considered as Ovar is not far and is also a coastal town and there are no ancient values of weather following in Ovar. In Table 29 some of the weather characteristics (average data) since 1901 until 1990 can be seen.

Table 29 – Some average weather values in Oporto from 1901 to 1990 (Ferreira 2009)

	1901 to 1930	1931 to 1960	1961 to 1990
Number of days with temperatures below zero per year	4.1	--	5.0
Annual precipitation (mm)	1164.4	1152.2	1265.0
Annual relative air moisture content (%)	76.7	76.8	77.0
Annual wind speed (Km/h)	16.3	18.2	17.9
Sunny periods (h) per year	2591.1	--	2468.0

Note (--) missing data

As it can be understood by Table 29, building materials in Oporto as well as in Ovar don’t face frost problems but wetting/drying cycles succeed continually as there is much precipitation, much sunny days and wind. The frequency of wetting/drying cycles seem to

have an important role on degradation rates (Viles and Goudie 2007). The materials of the exterior of a building can experience a temperature 30°C above the environmental temperature (Ferreira 2009). Recent weather data show that 40°C is an easily attainable temperature in Summer in Ovar city centre (Monteiro 2012). In this way, facade materials can easily reach 70°C or more, creating a drying heat for the damped structures. In Ovar, as in Oporto, the dominant wind direction is North, carrying salty moisture bringing to the facade salts like sodium chloride (NaCl). Other salts that can be present in the façade materials are calcium sulphate (CaSO<sub>4</sub>), calcite (CaCO<sub>3</sub>), sodium nitrate (NaNO<sub>3</sub>), sodium sulphate (Na<sub>2</sub>SO<sub>4</sub>), among others coming from ground water, building materials placed before the tiles and atmospherical pollution (La Iglesia, González et al. 1997, López-Azevedo, Viedma et al. 1997, Ferreira 2009).

Recently, temperature and air moisture content in Ovar from 2007 until 2011 were collected from a private weather station located in Ovar city centre placed at 18 m high can see in Table 30.

Table 30 - Some Ovar's average weather data from 2007 to 2011(Monteiro 2012)

	2007 to 2011
Number of nights with temperatures below zero per year	2.5
Maximum temperature (°C)	35
Annual relative air moisture content (%)	79.5
Annual wind speed (Km/h)	8.4

Rain and sunny hours per year data is not available. Nevertheless, the presented data in Table 30 helps to validate some of Porto weather values used. Both weather informations allow to better understanding of the weather conditions at which the studied tiles might have been subjected throughout the tens of years placed in the facades. From recent data, it can be confirmed that frost is not one of the weather risk factors to the studied samples, but high air moisture, wind and high temperatures are the potential weather risk factors for crazing glaze in general (revealing thermal expansion coefficient deficient coupling, ceramic body moisture expansion and salt crystallization).

Although in mortar/tile interface there are two porous materials in contact with each other, there is a big difference between them: mortar, with calcium components, is chemically unstable and can be a supplier of soluble salts when water is present on a regular basis, while the porosity of the ceramic body is a good storage place. All the mortars used to fix the samples under study during more than 100 years on exterior walls are air lime mortars. Nowadays the preparation process and procedure that was used at the time for preparing these lime mortars is unknown. It is known that calcination temperature and retention time are important parameters that influence the ageing and the properties of lime putty and the carbonation process (Elert, Rodrigues-Navarro et al. 2002). The longer the slaked lime is left to mature (months or even years), the smaller the  $\text{Ca(OH)}_2$  crystals are and the bigger their solubility is (Elert, Rodrigues-Navarro et al. 2002).

Samples are from the same town, and from the same approximate period with some tens of years of difference, at the most. Studies made at the supporting mortars revealed that they are similar, with approximate compositions of 90% of clay sand ( $\pm 60\%$  of  $\text{SiO}_2$  + 30% of clay minerals) and 10% air lime (Ferreira 2009).

The “self-healing” capability of lime based mortars is well known. It consists of a process of dissolution, transport and re-precipitation of calcium compounds in the voids existing in the mortar. Water promotes the dissolution of calcium compounds in areas rich in binder and transports them to voids. The re-precipitated crystal habits are moisture content and carbonation degree dependent, among other factors. In some extent comparable to self-healing in lime mortars is the carbonate diagenesis basins; dissolution and re-precipitation of calcite (Lubelli, Nijland et al. 2010). Lime mortars used in the past, as the ones used today, had a great amount of  $\text{Ca(OH)}_2$  in their structure, that can take many years to carbonate (if ever).  $\text{Ca(OH)}_2$  solubility is about 100 times higher than that of  $\text{CaCO}_3$  polymorphs (Lubelli,

Nijland et al. 2010). For these reasons it is not difficult for water, arriving at the mortar by capillary rise from the building structure, to dissolve portlandite and transport it in solution mainly by capillary forces through the tile pore system. In a study of the process of self-healing in mortars it was found that self-healing of cracks by calcite can take place by re-crystallization of portlandite and posterior carbonation (Lubelli, Nijland et al. 2010) . The posterior carbonation of  $\text{Ca(OH)}_2$  salts in the porous structure of the ceramic material is a plausible possibility, which is under evaluation in this work.

In this study, eleven tiles with 14 x 14 cm were studied, nine with a calcitic ceramic body (P9, P24, P89, P109, P115, P116, P124, P127, P133) and two with *pó de pedra* ceramic body (P20 and DA5) as shown in Table 31. The samples suffering from severe glaze detachment were collected from the ground level of the facade up to a height of approximately 2.0 metres.

Table 31 – Samples pictures and references

Sample description	Sample pictures	Sample references
<i>Pó de pedra</i> ceramic body		DA5, P20
Calcitic ceramic bodies with double glaze layer		P109, P133, P24, P127, P89, P9, P124, P116, P115
		
		
		
		

The tiles ceramic bodies were ground and their powder was used to determine their mineralogical and chemical composition as well as their thermal behaviour (TGA) and Fourier Transformed Infrared Spectroscopy (FTIR). FTIR was used to ensure that the crystalline phases of calcite and portlandite were well indexed in the analysis of tiles XRD.

There were also tests made with the entire tile, as open porosity determination. A fracture of the ceramic body piece was used to analyse the presence of salts by SEM. To observe glaze/ceramic body/mortar interfaces, cut tile specimens were mounted in resin and polished.

In order to understand the origin of calcite as almost all samples are calcite ceramic pastes, and trying to define a temperature range of firing, small pieces of the ceramic body were cut and calcined in an industrial kiln at 1040° C ring temperature. XRD of samples after calcination was undertaken.

To understand how pores were affected by salt crystals, the water absorption method was used to evaluate porosity. Santos (Santos, Vaz et al. 2012) concluded that one can reach a good porosity estimation by using only water absorption procedure. The same samples used for the determination of water absorption were calcined at 1000° C and porosity was re-evaluated.

In order to compare the amount of mortar binder in the pore structure of tiles that underwent wetting/drying cycles in comparison with tiles that suffered no such cycles, an interior tile from 19<sup>th</sup> century was analysed by XRD, XRF and SEM/EDS.

In 10 of the 11 samples (all but DA5) XRD results show maximum diffraction peaks corresponding to calcite and in 5 samples, the existence of portlandite is evident. Figure 91 displays an example (P24) of an XRD with calcite and portlandite maximum diffraction peaks. The presence of calcite could raise doubt about its origin as most of the samples are calcite ceramic bodies. The presence of portlandite in many XRD might provide some clarifications indicating that there are calcium salts probably coming from the mortar due to solubilisation and water transport.

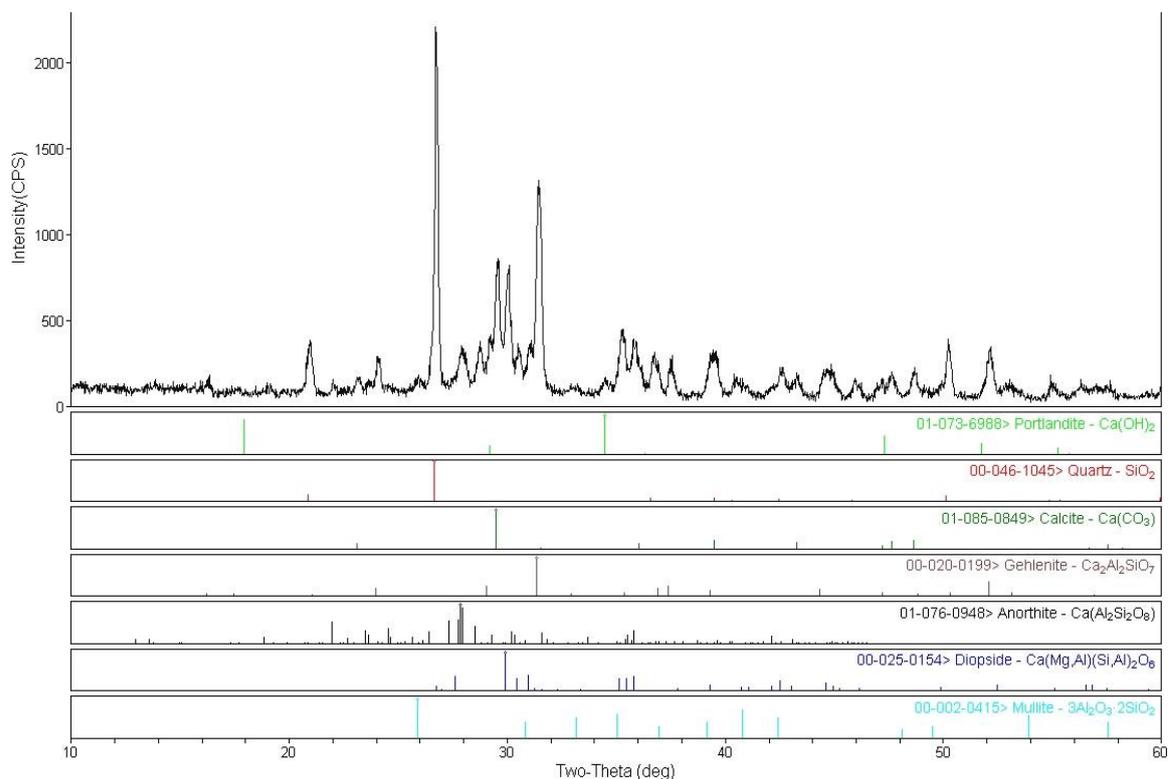


Figure 91 – P24 XRD, where calcite and portlandite main diffraction maximums can be seen

It was seen previously in section 4.2.1.9, *pó de pedra* samples were probably produced with kaolin and quartz. Nevertheless, DA5 and P20 have some CaO. P20 XRD analysis even shows a small diffraction maximum due to calcite. This might reveal that calcite might be brought to the system by an outside source.

The values shown in Table 32 infer the importance of the porous network, as calcitic tiles have a large amount of L.O.I while this is much lower in *pó de pedra* tiles. In Table 32 a calculation exercise is made considering that all L.O.I. is due to the decomposition of calcite, as suggested by the TGA already seen in section 4.2.1.3.

Table 32 – XRF of the main oxides of the studied samples

	SiO <sub>2</sub> [%]	Al <sub>2</sub> O <sub>3</sub> [%]	MgO [%]	CaO from the ceramic body [%]	LOI [%]	CaO from exterior source [%]
P9	44.6	17.6	6.5	15.0	3.9	5.0
P24	41.7	16.2	2.0	21.2	5.6	7.1
P89	40.4	16.5	4.0	16.2	6.6	8.4
P104	42.6	16.2	3.3	18.5	4.7	6.0
P109	42.0	17.6	2.7	23.3	3.5	4.5
P115	45.5	17.2	3.2	15.8	5.2	6.6
P116	44.8	18.1	5.1	17.1	3.4	4.3
P124	44.0	17.7	3.8	18.3	4.2	5.3
P127	41.1	17.0	5.7	18.2	4.3	5.5
P133	40.2	16.8	4.2	20.4	4.3	5.5
P20	70.7	22.5	0.2	0.0	1.1	0.4
DA5	73.4	22.5	0.2	0.0	0.9	0.3

As already mentioned, calcination trials showed that the ceramic body of the samples under study were fired at temperatures high enough for decomposition of the calcite present as raw material (at least 1040°C). In properly burnt clay products, efflorescence and cryptoflorescence can only be due to salt crystallization (Chatterji 2000), so the calcite that appears in the tiles is probably due to an external income.

Samples under study were calcined at 1000°C and open porosity determination was performed before and after calcination. Porosity results are shown in Table 30 where it may be seen that porosity increases from 4.2% up to 8.1% after calcinations, revealing that the loss of weight measured by ATG (Figure 48 to 50) was due to materials existing in the pores. The only samples in which porosity doesn't increase too much with calcination are the ones

that have the lower porosities (11 to 14%) identified as *pó de pedra* (P20 and DA5), demonstrating in a clear way, once again, the importance of the pore structure in the ability for salt crystallization.

Table 33 – Water absorption of tile samples before and after calcinations at 1000° C

Ref <sup>a</sup>	P9	P24	P89	P109	P115	P116	P124	P127	P133	DA5	P20
Removed from the wall and cleaned (%)	22.7	21.6	20.8	17.7	19.8	22.3	19.7	22.0	22.6	10.8	13.6
After calcination (%)	29.1	27.4	28.9	22.6	24.0	28.6	24.6	26.7	28.0	12.1	14.1

In Table 33, most tiles under study show water absorption higher than 18%, although what is being measured is a long term result of degradation and salts accumulation. As most of the ceramic bodies under study are calcite pastes it was expected a high porosity due to carbonates decomposition during firing process.

Visualizing P89 in fracture at SEM, crystallized salts can be seen all over the ceramic body (Figure 92). EDS was performed in some salt agglomerates and all the crystals analysed were similar, following the standard analysis shown in Figure 93, with well-defined calcium peaks (as well as silica and alumina from the ceramic body beneath).

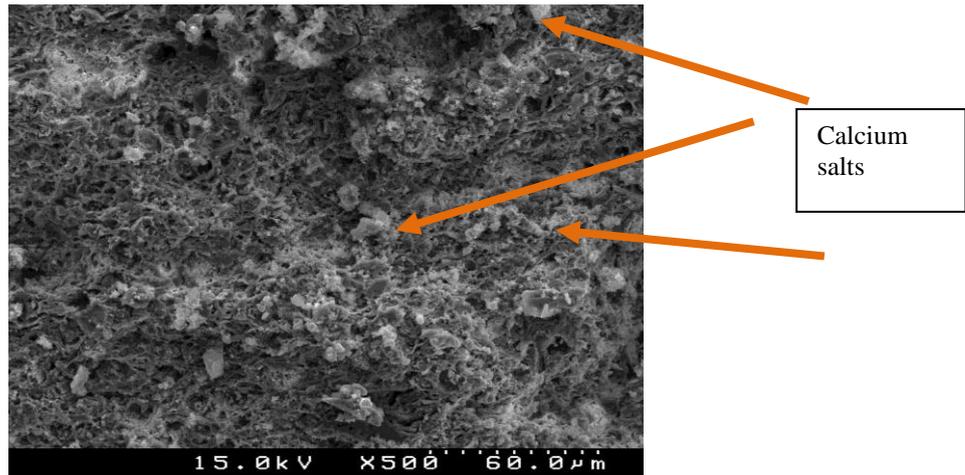


Figure 92 – P89 ceramic body with numerous calcium crystallizations

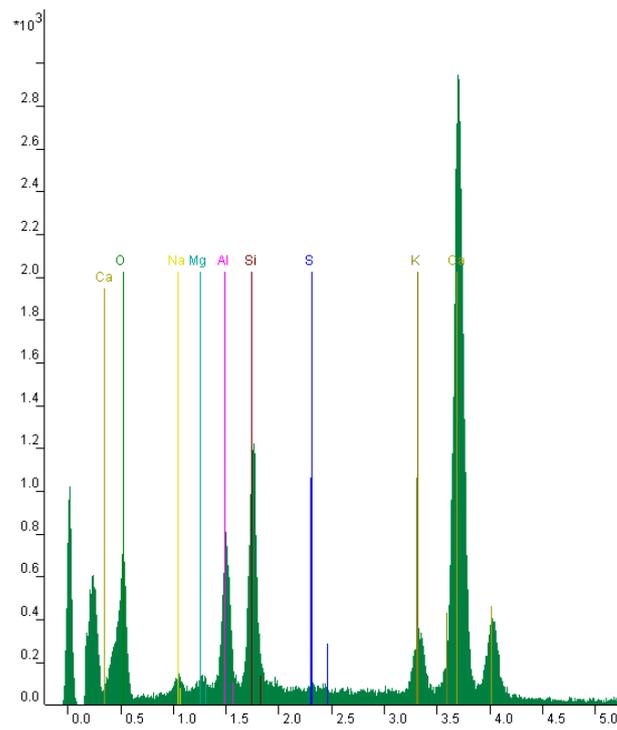


Figure 93 – EDS of the crystals

If crystallized salts can frequently be found in the porous ceramic body, it is possible that this may be more severe in the glaze/ceramic body interface where porosity ends in an abrupt way due to the existence of an impermeable area. Analysing glaze/ceramic body region from P89 using SEM, stacked salt crystals between the ceramic body and the glaze can

be seen, promoting distortion in these structures, leading sometimes to rupture. EDS analysis show that the salts in question are from calcium, like in the porous region (Figure 93). It is known that carbonation of  $\text{Ca}(\text{OH})_2$  leads to an increase in weight of 35% and in volume 11.8% (Elert, Rodrigues-Navarro et al. 2002), so as  $\text{Ca}(\text{OH})_2$  arrives to the ceramic structure, it carbonates and creates pressure in pore structure wall. The degree of carbonation increases with relative humidity and periodic wetting (Elert, Rodrigues-Navarro et al. 2002, Houst and Wittmann 2002) which is a phenomenon that may occur frequently in this interface.

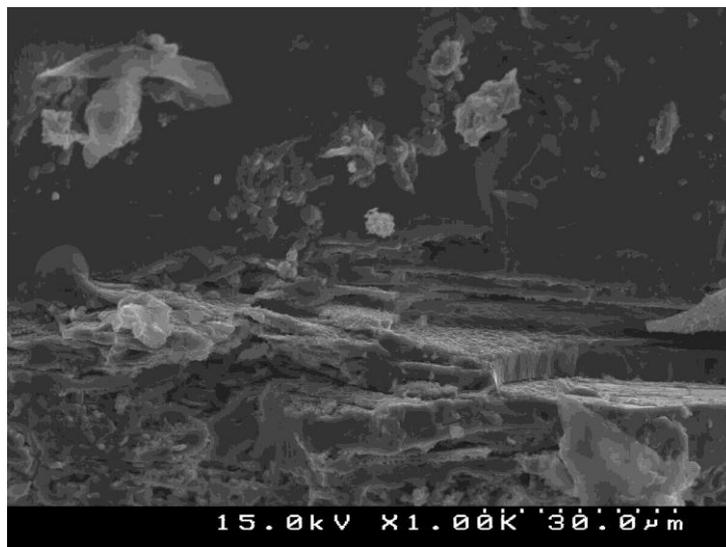


Figure 94 – Crystallized salts in the ceramic body/glaze interface, provoking structural rupture

The plate-like habit of the crystals in Figure 94 can be due to the presence of  $\text{Ca}(\text{OH})_2$ . As it was reported in Hedin's work (Chatterji 2005) a low degree of supersaturation in  $\text{Ca}(\text{OH})_2$  of the arriving solution promotes the growth crystallization direction of  $\text{Ca}(\text{OH})_2$  crystals parallel to the basal plane and crystals have plate-like habits.

Analysing Figure 92 it seems that portlandite salts ascend from the mortar up to the biscuit/glaze interface, developing crystallization in the pores and throughout the area underneath the glaze, destroying the links of those two structures (Figure 94), playing a primary role in the rupture of the glaze and subsequent detachment promoted by the pressure caused by the growth of cristal salts in the porous structures and thus causing permanent

damage (Linnow, Halsberghe et al. 2006). When there are pores in the glaze (pinholes), there is preferential ascension of salts up to the surface producing destruction in their path and thereby weakening the whole surrounding area (R.M.Pereira and Mimoso 2012), as may be seen in Figure 95.

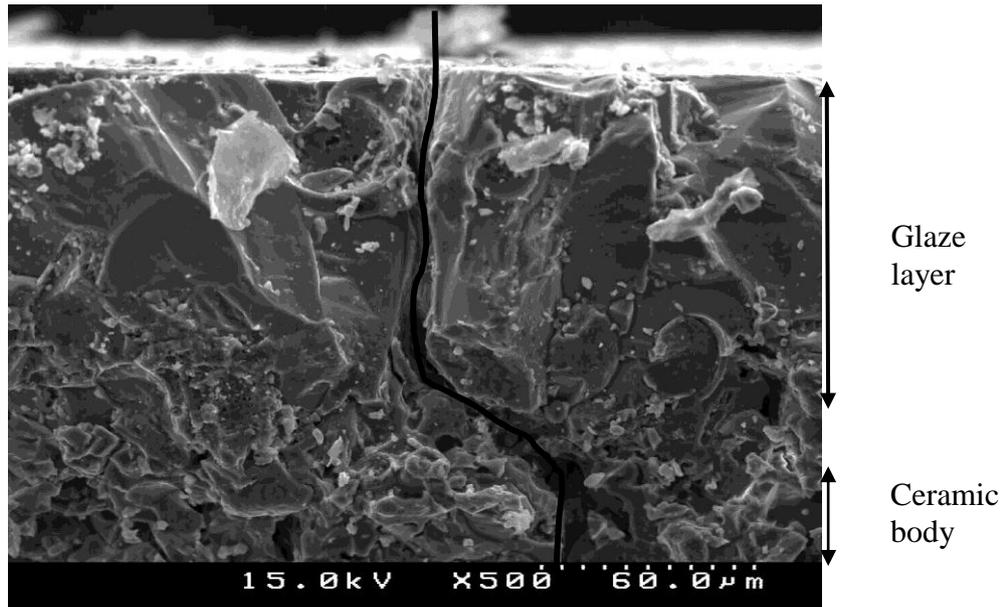


Figure 95 – Path of destruction made by salt ascension

It appears that the amount of portlandite crystallized under the glaze can be significant (Figure 94) which certainly generates enormous pressure under the glaze destroying glaze and ceramic body biscuit bonding. This helps to explain why the glaze/ceramic body interface magnitude might not be determinant in glaze detachment due to salt crystallization, but the material porosity network, as seen in section 4.2.1.8.

Results of analysis of an unfinished tile (ceramic body before glaze application) found in industrial archaeology excavations in a 19<sup>th</sup> century factory that was not subject to wetting/drying cycles support this theory as no calcium crystals were found in its pores (Figure 96).

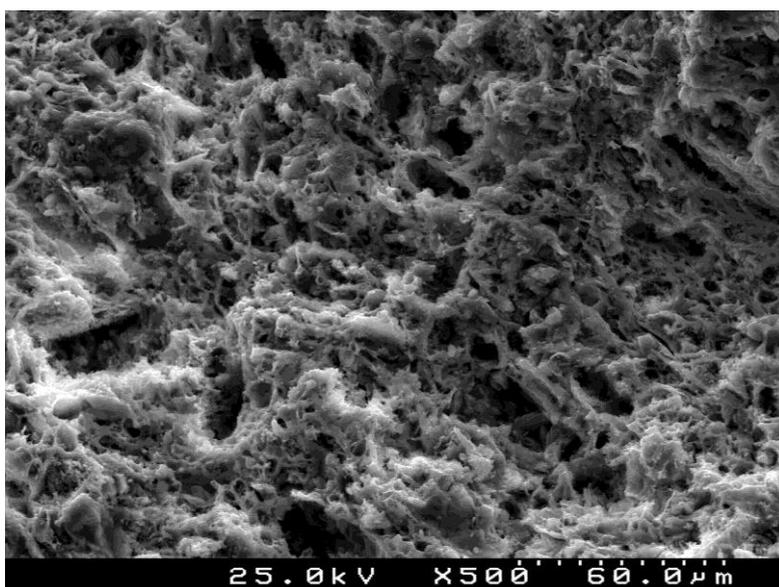


Figure 96 – Microstructure of a tile never used

Figure 92 allows the understanding of the binding process between tiles and lime mortars that is, indeed, made by binder absorption by the porous system of the tile. This transference is continually made if there is a water supply to the system, together with drying periods.

Lepierre (Lepierre 1899) analysed chemically all the Portuguese ceramics existent at the time and states in his work that that ceramic tiles after firing had non-existence of free carbonates, characteristic indicated by the author as sufficient to distinguish this modern faience (1899) from the oldest. On the other hand Magalhães (Magalhães 2002) states that the dissolution and crystallization of lime in supporting materials (mortars) frequently causes efflorescence. In his work, Faria (Faria 2004) reveals that in the mortar applied on the walls it is often difficult to achieve satisfactory carbonation, and the conversion of the calcium hydroxide (portlandite) into calcium carbonate (calcite) is very slowly and may take centuries. Significant amounts of chemically free calcium hydroxide stay available in several of the construction elements.

To provide a greater understanding about the possible destructive mechanism of moisture and salts, a sample designated as P24 with no measurable interface found demonstrates that it is possible that tiles without visible interface resist to the passing of one

hundred years, as long as they are placed far from areas subject to capillary water rise, as seen in section 4.2.1.8.

When tiles are removed from the facades for conservation, it is important that in salt removal treatments, effectively all the potentially destructive salts are removed before re-application to determine critical conditions have to be avoided to prevent more damages promoted by crystal growth.

It is thought that the calcite that appears in the ceramic body pores of the studied samples in the form of crystals are the result of the dissolution of calcium hydroxide from the mortar (since this is about 100 times more soluble than calcite) and that is transported by humidity to the ceramic body that, by evaporation it turns the water solution so concentrated that the salt crystallizes. It is thought that the salts alone are able, over time, to destroy porous construction materials causing their collapse, especially in old buildings (Dias 2007). With this work it is demonstrated that portlandite is within the list of the destructive salts.

The use of air lime mortars is not in itself deleterious, but the constant action of water must be avoided in order to minimize dissolution/crystallization processes.

## **4.4. Replicas preparation and analysis**

In the scope of the present work, technical replicas of the tile ceramic bodies are understood as nowadays ceramic body produced with the same chemical, mineralogical and micro-structural characteristics as those of the original tiles. The chemical and mineralogical characteristics ensure as much as possible, thermal and moisture expansion behaviour closer to the old tiles. Micro-structural features are linked with the ceramic body water behaviour compatibility. A good match of the mentioned technical characteristics from the replica with the originals old tiles gives a uniformity of behaviour with the rest of the façade. For the present work it is more important, in terms of restoration methodology, to ensure the unity in terms of water behaviour to prevent faster degradation of the old tiles, than a more resistant element which might contribute to faster panel degradation in what concerns weathering issues.

Before starting replicas development, contemporary tiles usually used for restoration purposes were studied to evaluate their compatibility with the old tiles.

### **4.4.1 Contemporary tiles used in restoration**

Restoration nowadays is made with contemporary ceramic bodies, marked as special tiles for being used in ancient facades. In reality these tiles are technically similar to the ones used in everyday tile utilization. Two different kind of ceramic bodies were analysed in order to compare their technical characteristics with those of the original tiles. Modern samples will be numbered 1 and 2, in order to protect industrial sources.

In the present chapter glazed replicas using contemporary ceramic body tiles, decorated and glazed in a restoration atelier (decoration replicas), were also analysed. Many of these tiles presented glaze crazing some months after production (even without wall application). These glazed samples were numbered 3 as reference.

All the analysed tiles are calcitic and were never used in a wall, or were in contact with mortar.

#### 4.4.1.1 Sample 1 characterization

Sample 1 is from a traditional factory in the market that has been produced ceramics for more than 150 years. This unit's policy was to maintain production of ceramic bodies similar throughout the years, making almost no changes to their characteristics although; production technology was up-to-dated. The ceramic body diffraction maxima (Figure 97) have the same crystalline phases as those of ancient tiles but with low intensity. This sample has a high content of quartz. Sample 1 presents a much higher silica content (54% versus 44% of average value for ancient tiles), lower calcium content (13% against 23% for ancient tiles). Overall it can be said that XRD maxima are not very intense, perhaps due to a fast firing technique.

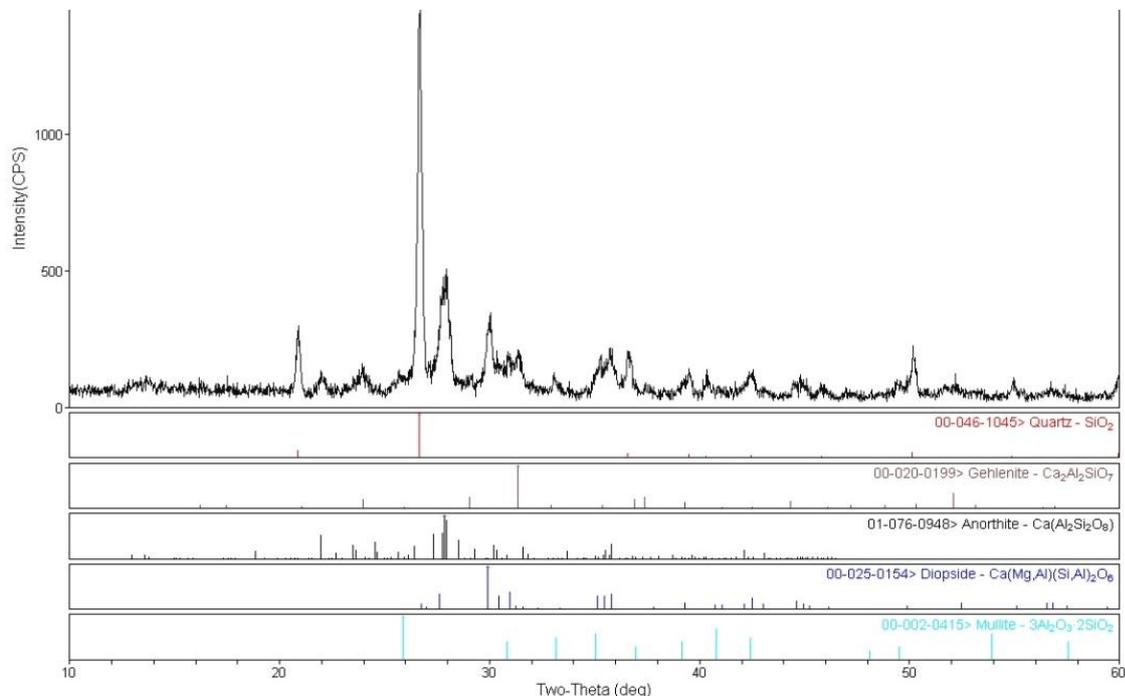


Figure 97 – Sample 1 XRD

Table 34 - Sample 1 XRF values

	LOI	SiO <sub>2</sub>	Al <sub>2</sub> O <sub>3</sub>	CaO	MgO	K <sub>2</sub> O	Fe <sub>2</sub> O <sub>3</sub>	TiO <sub>2</sub>	Na <sub>2</sub> O
(%)	0.3	54.4	20.3	13.0	5.4	1.9	3.2	0.6	0.2

In Table 34 it can be seen that although water absorption percentage presented by Sample 1 is rather low compared with ancient tiles (ancient tiles present an average water absorption percentage of 20.4%), water absorption due to capillary action is quite acceptable (ancient tiles have an average value of 3.4 kg/(m<sup>2</sup>h<sup>1/2</sup>)).

Table 35 – Sample 1, water absorption due to capillary action and percentage

	Water absorption [%]	Water absorption due to capillary action [kg/(m <sup>2</sup> h <sup>1/2</sup> )]
Sample 1	15.4	3.3

In Figure 98 Sample 1 microstructure may be observed. A glassy phase can be seen in the microstructure revealing a liquid phase sintering probably due to the high temperature attained during firing. Fast firing is characterized for having higher temperature than “traditional” firing, in order to balance time/temperature enthalpy.

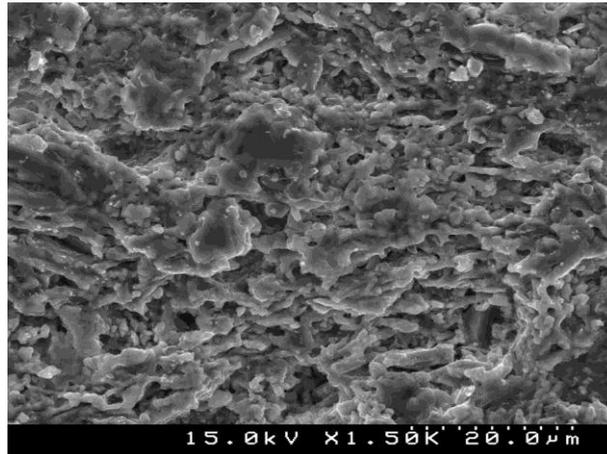


Figure 98 – Sample 1 microstructure

Figure 99 shows a fracture of Sample 1 where glaze with a thickness of circa 500µm and containing a large amount of air bubbles can be seen. Comparing sample 1 SEM glaze aspect with an old tile (Figure 100) is evident that the old tile glaze has a lower amount of air bubbles but these displays a larger size. This reveals that the contemporary tile, in the moment of the glaze firing, had little time to degasify, corroborating the conclusion that sample 1 tile probably suffered a fast firing process.

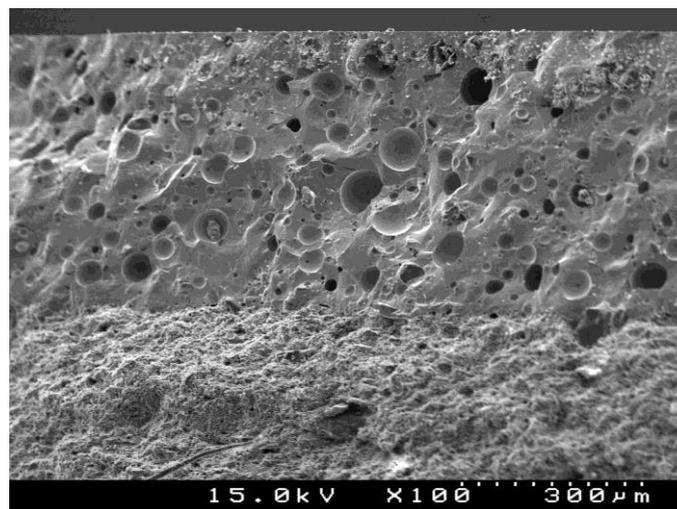


Figure 99 – Sample 1 glaze and ceramic body SEM observation. Sample in fracture

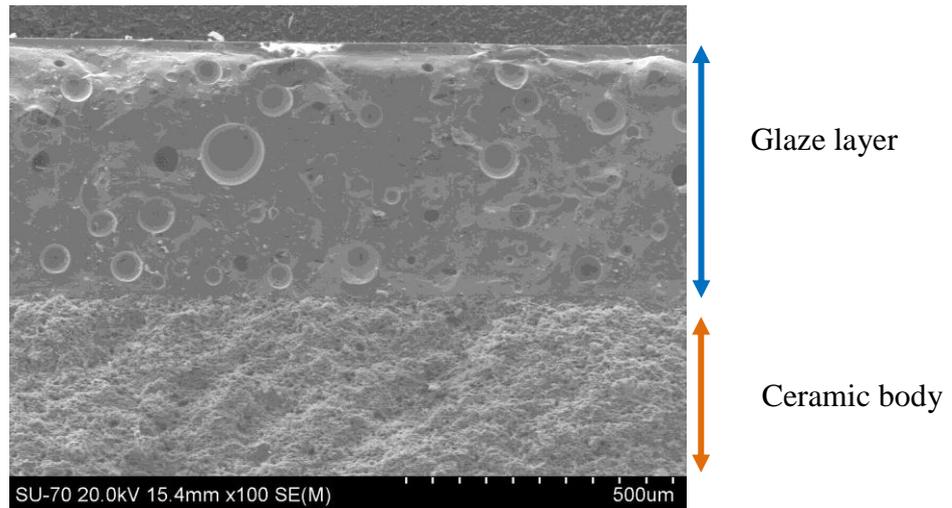


Figure 100 – Old tile glaze and ceramic body SEM observation. Sample in fracture

#### 4.4.1.2 Sample 2 characterization

Sample 2 is also from a contemporary tile factory but quite different from the previous tile analysed, as a modern production concept is established. As it can be seen by Figure 101, this sample has neither gehlenite nor diopside and the quartz diffraction maximum has an extraordinary intensity with presence of anorthite. The possible reason for this fact can be found in XRF data shown in Table 36, as the tile under study presents no significant quantity of magnesia, a very low calcium content but a high silica quantity, compared with the old tiles.

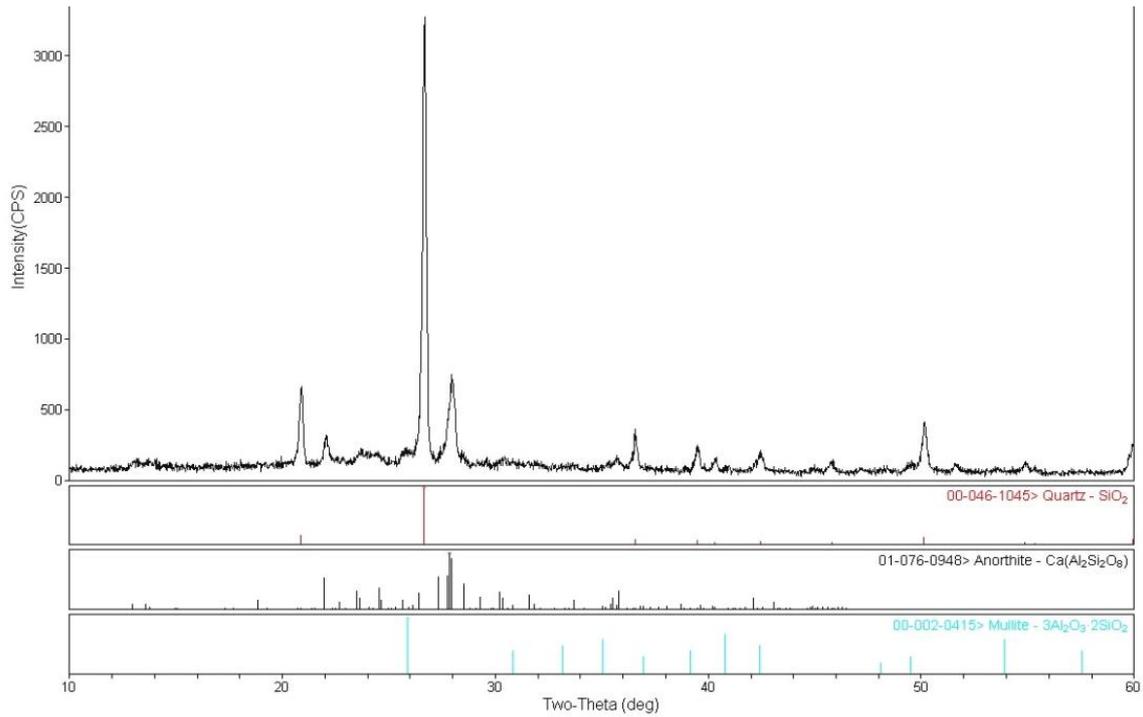


Figure 101 – Sample 2, XRD

Table 36 – Sample 2 XRF values

	LOI	SiO <sub>2</sub>	Al <sub>2</sub> O <sub>3</sub>	CaO	MgO	K <sub>2</sub> O	Fe <sub>2</sub> O <sub>3</sub>	TiO <sub>2</sub>	Na <sub>2</sub> O
(%)	0.2	69.2	19.4	7.0	0.3	1.4	1.0	0.3	0.8

As it can be seen, Sample 2 tile ceramic body is quite different from the old samples under study. The water absorption percentage and water absorption due to capillary action values found in Sample 2 are far from the ideal as shown in Table 37 (the old samples water absorption percentage are higher than 18% and water absorption due to capillary action circa 3.4 kg/(m<sup>2</sup>h<sup>1/2</sup>)).

Table 37 - Sample 2, water absorption due to capillary action and percentage

	Water absorption [%]	Water absorption due to capillary action [kg/(m <sup>2</sup> h <sup>1/2</sup> )]
Sample 2	11.7	2.0

In Figure 102 a fracture of Sample 2 can be seen in which the microstructure is evident, showing less glassy phase than Sample 1 because although also fired in fast firing, its chemical composition presents much less fluxes (CaO, MgO, Fe<sub>2</sub>O<sub>3</sub>) and a considerably higher SiO<sub>2</sub> content.

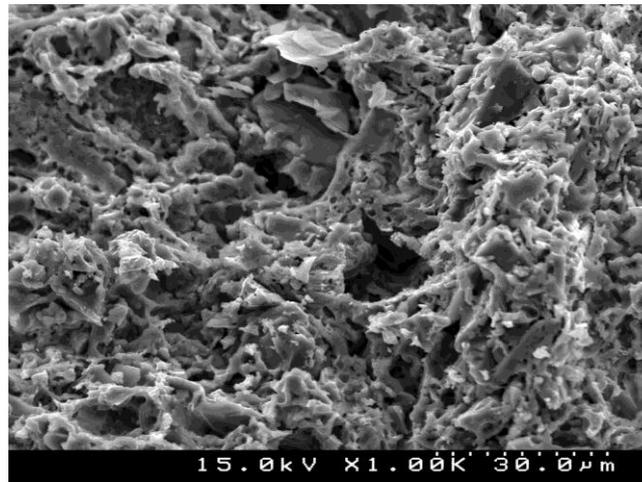


Figure 102 – Samples 2 microstructure

As already considered in the present work, the most important technical characteristics to attain in technical replicas are the thermal expansion of the ceramic body, the crystalline content and the water behaviour. Having this in mind, neither Sample 1 nor sample 2 have the correct data. Sample 1 shows a low water absorption and high amorphous content (glassy

phase) predicting a larger moisture expansion than the old tiles. Besides not having the correct water behaviour, Sample 2 chemical composition leads to ceramic body' thermal expansion coefficient quite different from old tiles'. In both Samples, compatibility would not be assured.

#### 4.4.2 Ceramic body replicas suggestion

After having the old ceramic bodies characterized, the probable raw materials identified and the contemporary raw materials chosen, the raw materials relative quantity was tested until the chemical values of the old tiles were reached. After this procedure, the firing curve was tested until reaching all the diffraction maxima requested. The final parameters, but the most difficult to reach, where the combination between raw materials grinding level and composite pressing pressure in order to obtain all the water compatibility parameters desired. The final aim was to reproduce the technical characteristic of both types of ceramic bodies (calcitic and *pó de pedra*), suggesting raw materials to be used, their grinding level, pressing pressure and small scale firing curve. Overall, for the calcitic ceramic bodies' replicas the following trials were performed: 5 raw materials grinding level tests, 14 raw materials composition trials, 7 different pressing pressures and 5 firing curves evaluated. For *pó de pedra* ceramic body replicas were performed: 2 different raw materials grinding level, 6 raw materials composition, 5 different pressing pressure and 3 firing curves. Besides the mentioned tests, in the beginning of this research the homogeneity of the composite mixture evaluation was performed by preparing the ceramic composite in dry and humid via. The conclusion taken was that the raw materials mixture has to be made in wet conditions to ensure a perfect compound homogeneity. Much has been learned in all of these trials. The importance of a slow temperature rise for phase formation, the importance of grinding level and pressing pressure for water absorption due to capillary rise ability and the importance of pressing pressure for total water uptake. The higher the pressing pressure and grinding level, the lower the water absorption percentage and the faster water absorption due to capillary rise. The present work also revealed how small pieces missing on a tile can be reproduced without

suffering contraction by drawing in the ceramic mixture the exact size of the missing piece without the need of contraction calculations because the ceramic body firing doesn't contract. Trials made revealed that mixtures with 30-35% of CaCO<sub>3</sub> contract very little to nothing at all. Several replicas formulas tested contracted from 0.3% until 0%. All the replicas samples were tested in a 4 cm pressed discs with 3mm high.

The raw-materials used for the replicas production are Portuguese, commonly used in the ceramic industry, with the technical characteristics as shown in chapter 3 and chemical composition as shown in Table 38.

Table 38 – Chemical analysis data of the raw materials used in the replicas preparation

	<b>Ball Clay</b>	<b>Kaolin</b>	<b>Quartz sand</b>	<b>Lime</b>	<b>Talc</b>
<b>L.O.I</b>	11.4	12.7	0.2	38.4	7.0
<b>SiO<sub>2</sub></b>	55.1	49.2	99.3	0.3	55.0
<b>Al<sub>2</sub>O<sub>3</sub></b>	28.5	35.7	0.3	0.1	4.4
<b>CaO</b>	0.1	0.0	0.0	60.9	1.2
<b>MgO</b>	0.5	0.1	0.1	0.3	23.3
<b>K<sub>2</sub>O</b>	1.5	1.2	0.0	0.0	0.0
<b>Na<sub>2</sub>O</b>	0.1	0.0	0.0	0.0	0.0
<b>Fe<sub>2</sub>O<sub>3</sub></b>	1.6	0.9	0.0	0.0	6.6

#### 4.4.2.1 Calcitic ceramic body

With the support of pondered calculations based on MgO, due to the consideration that diopside is the only crystalline phase with magnesium; it was possible to formulate ceramic bodies' compositions with the estimated talc percentage. After that, empirical balances with the rest of the possible raw materials were made in order to obtain the final chemical

composition desired. After making some adjustments in the raw materials percentage, final characteristics were evaluated arriving to a ceramic composite with unfired composition of 33% of ball clay, 11% of kaolin, 10% of quartz sand, 35% of lime and 11% of talc. All the raw materials were ground in an agate fast mill, until the final mixture had an average particle size distribution with a median diameter of 4  $\mu\text{m}$ . The raw composite was pressed at 546 bar, and fired in a 19:30 hours heating curve until 1080°C as maximum temperature (Figure 103). All the soaks lasted 3 hours each, and measured ring temperature was 1120° C ring. The cooling took place inside the furnace, once the furnace was turned off.

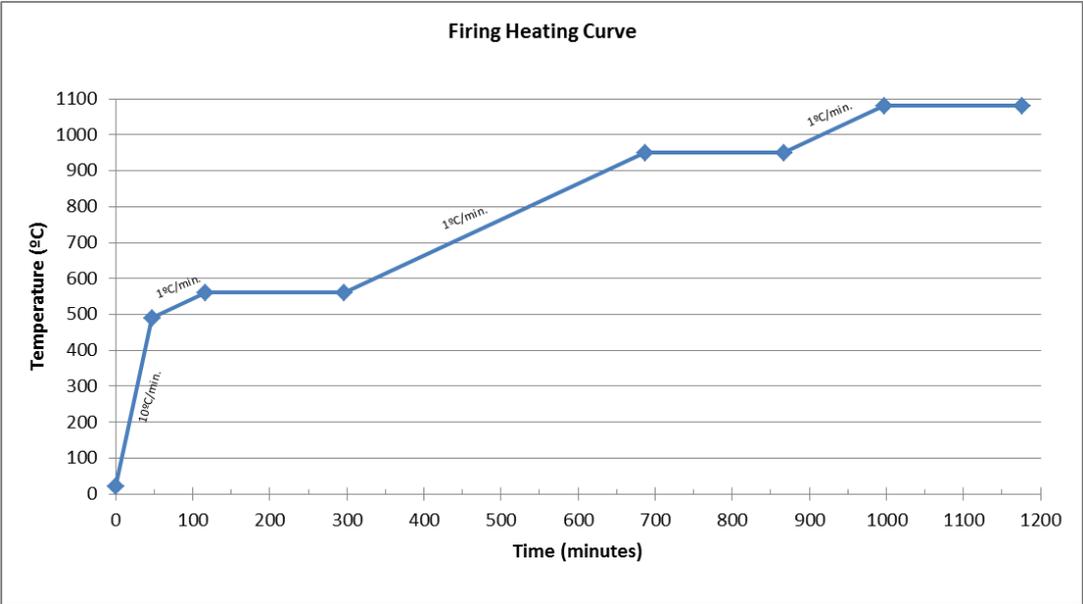
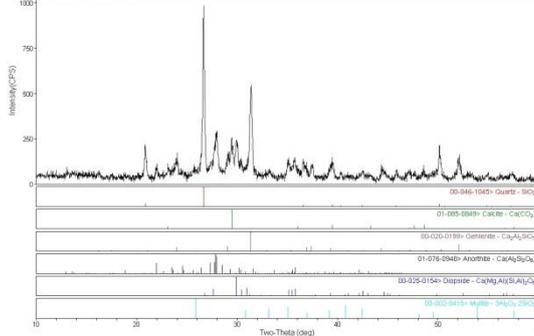
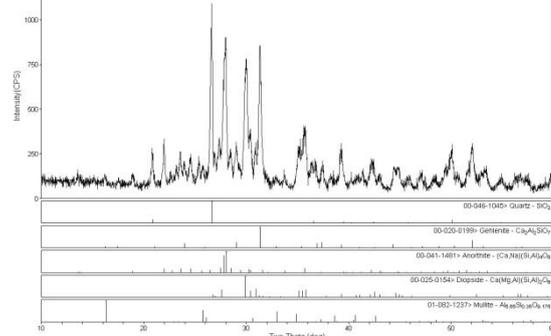


Figure 103 – Calcitic replicas firing curve

The results of the ceramic composite after firing are shown in Table 39. Replicas must have similar porous characteristics to the old tiles so that the mortars replicas have an adherence mechanism similar to original one and in order to ensure similar behaviour in terms of water intake. The mentioned characteristics were evaluated in the replicas by the determination of water absorption percentage and water coefficient due to capillary action (following texting procedures described in 3.2.3.4 and 3.2.3.5). For the replica data evaluation 2 specimens were used.

Table 39 – Results of the studied samples and replicas after firing

	Results of the studied samples	Results of the replicas after firing
XRD		
XRF [%]	<p>Na<sub>2</sub>O – 0.3 to 0.9 (average=0.4)</p> <p>MgO – 2.9 to 6.7 (average=3.9)</p> <p>Al<sub>2</sub>O<sub>3</sub> – 16.2 to 22.3 (average=17.6)</p> <p>SiO<sub>2</sub> – 40.2 to 46.1 (average=43.8)</p> <p>K<sub>2</sub>O – 0.9 to 2.5 (average=1.8)</p> <p>CaO – 20 to 28.3 (average=23.6)</p> <p>Fe<sub>2</sub>O<sub>3</sub> – 2.9 to 3.9 (average=3.3)</p>	<p>Na<sub>2</sub>O – 0.2</p> <p>MgO – 4.0</p> <p>Al<sub>2</sub>O<sub>3</sub> – 19.7</p> <p>SiO<sub>2</sub> – 49.0</p> <p>K<sub>2</sub>O – 1.0</p> <p>CaO – 22.2</p> <p>Fe<sub>2</sub>O<sub>3</sub> – 1.8</p> <p>L.O.I – 22.1 %</p> <p>Contraction – 0.3 %</p>
Water absorption [%]	17.7 to 22.8 (average=20.4)	20.7
Water absorption coefficient due to capillary action [kg/(m <sup>2</sup> h <sup>1/2</sup> )]	3.1 to 3.7 (average=3.4)	3.5
Linear thermal expansion coefficient [°C <sup>-1</sup> ]	7.2E <sup>-6</sup> to 8.4E <sup>-6</sup> (average=7.8E <sup>-6</sup> )	7.8E <sup>-6</sup>

Comparing the crystalline phases present, chemical analysis and water behaviour of the values of the replicas with the results of the ancient tiles it can be seen that all of the crystalline phases of the ancient tiles are present in the replica, although more developed in

the latter. The chemical analysis is within the range of value although the replica has more SiO<sub>2</sub>, which has no negative influence in the water characteristics. The iron content is smaller in the replicas because they were produced with beneficiated raw materials. Very important characteristic to be achieved is water behaviour and replicas are within the expected values. Replicas chemical and crystalline phase data are within the old tiles' results ensuring, as far as it is possible, a similar thermal and moisture expansion as the old tiles. Experimental linear thermal expansion coefficient of both old tiles and proposed replicas are alike. By all this, it can be said, that the replicas achieved can be considered as “technical replicas”, as they will have a similar physical and chemical behaviour to the old tiles when used side by side in a restored façade, contributing to its homogeneity and integrity.

#### **4.4.2.2 *pó de pedra* ceramic body**

Although *pó de pedra* tiles are less common, they often suffer from a severe pathology expressed by the detachment of the glaze layer, making their replacement with replicated tiles necessary.

In the analysed samples the single phase present containing alumina is mullite, so the amount of kaolinite present could be calculated, with the help of XRF data. Making the rational analysis of the raw materials, choosing one of the chemical composition values it was possible to calculate the percentage of kaolinite needed to have similar results as the ancient tiles, the silica percentage introduced by kaolinite and the quartz percentage introduced by quartz sand.

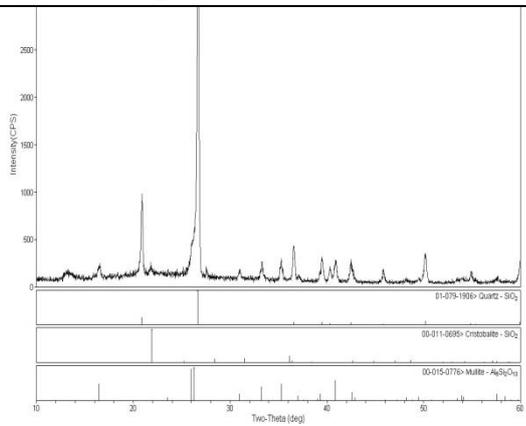
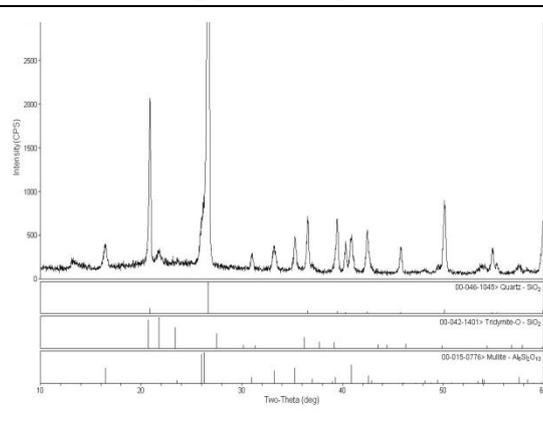
Only by analysing XRD and XRF data the composition of the replica ceramic body could be estimated: 42.2% of quartz sand plus around 57% of kaolin. After some chemical adjustments needed because of the kaolin used as raw material, replicas composition was obtained: 41.5% of quartz sand + 58.5% of kaolin.

In order to obtain porosity and capillarity absorption adequate characteristics, the two raw materials were ground in an agate fast mill until a modal diameter of 6 µm being obtained (the modal diameter is the diameter at the peak of the differential distribution) and then pressed at 780 bars. The trial specimens were fired up to 1210° C at a heating rate of 1°C/min,

with a soaking time of 2 hours at the maximum temperature. The ring temperature obtained was 1235° C.

Table 40 shows the results obtained for the *pó de pedra* replicas after firing at 1235° C (2 samples), with comparison with ancient tiles results. Good data matches are found.

Table 40 – Analytical results of the stoneware replicas after firing at 1235°C

	Properties of ancient tiles	Properties of replicas
XRD		
XRF [%]	<p>Na<sub>2</sub>O – 0.1 to 0.4 (average=0.3)</p> <p>Al<sub>2</sub>O<sub>3</sub> – 22.5 to 26.0 (average=23.7)</p> <p>SiO<sub>2</sub> – 70.2 to 73.4 (average=71.5)</p> <p>K<sub>2</sub>O – 1.4 to 1.6 (average=1.5)</p> <p>Fe<sub>2</sub>O<sub>3</sub> – 0.5 to 0.7 (average=0.6)</p>	<p>Na<sub>2</sub>O – 0.1</p> <p>Al<sub>2</sub>O<sub>3</sub> – 25.6</p> <p>SiO<sub>2</sub> – 72.0</p> <p>K<sub>2</sub>O – 0.8</p> <p>Fe<sub>2</sub>O<sub>3</sub> – 0.5</p> <p>L.O.I – 9%</p> <p>Contraction – 4.3%</p>
Water absorption percentage [%]	12.1 to 14.0 (average=13.5)	13.9
Water absorption coefficient due to capillary action [kg/(m <sup>2</sup> h <sup>1/2</sup> )]	2.2 to 2.8 (average=2.6)	2.9
Linear thermal expansion coefficient [°C <sup>-1</sup> ]	3.6E <sup>-6</sup> to 5.7 <sup>-6</sup>	5.3E <sup>-6</sup>

In the XRD of the replicas it can be seen that the intensity of quartz diffraction maxima is stronger than from the old tiles. This is probably due to the fact that ancient production units used kaolin rich in quartz sand and in the replicas made it was used sieved kaolin and quartz sand. This probably inputs to the ceramic body higher crystalline quartz content.

#### 4.4.3 Glazing of new tiles – procedure for adequate performance

Another distinction between old and new tiles is linked to glaze. Both Sample 1 and 2 (new tiles) the glaze had a non-elastic behaviour to cutting, presenting glaze conchoidal fracture. In ancient glaze cutting this was not observed in any sample, meaning that lead glaze is quite elastic. The glaze conchoidal fractures due to cutting can be seen in Figure 104.

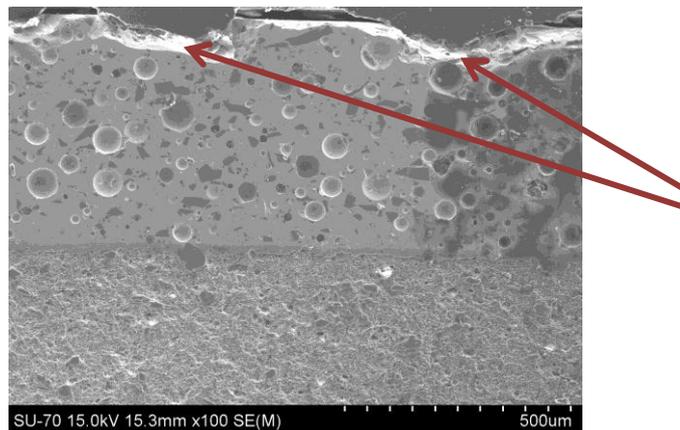


Figure 104 – Sample 2 glaze fracture due to cutting

Samples 3 (restoration tile) presented a spread crazing glaze phenomenon in almost all the replicas that were produced, regardless of the decoration motif. This widespread

pathology, present even in tiles that remained unused in facades (stayed indoors without use), immediately suggested that the cause had to be due to glaze/ceramic body coupling.

As mentioned in Section 4.2.2 (Lead glazes of the studied samples), the technically stable coupling of the ceramic body and the glaze is evaluated by the similitude of thermal expansion coefficients  $\alpha$ , that must be within strict conditions. For a suitable coupling that is, no crazing effect, the thermal expansion of the glaze must be lower in less than  $1.0 \times 10^{-6} \text{ }^\circ\text{C}^{-1}$  than that of the ceramic body's or engobe. The ideal difference is  $0.5$  to  $0.6 \times 10^{-6} \text{ }^\circ\text{C}^{-1}$ .

As the glazes and engobe used were available in dust form and the ceramic body used was also available it was possible to perform the thermal expansion coefficient of these entities. Two kinds of glaze were thermal expansion coefficient tested, as they were both used to produce decoration replicas, depending on the type of decoration to be reproduced and the values found are displayed in Table 41. All  $\alpha$  data expressed was calculated between  $20^\circ\text{C}$  and  $400^\circ\text{C}$  and the values presented are of linear thermal expansion coefficient.

Table 41 – Sample 3 ceramic body and glaze results

	Sample 3 Ceramic body	Engobe	Transparent glaze	Opaque glaze
$\alpha$ [ $^\circ\text{C}^{-1}$ ]	$5.856 \times 10^{-6}$	$6.33 \times 10^{-6}$	$5.046 \times 10^{-6}$	$4.924 \times 10^{-6}$

From table 41 it can be seen that the linear thermal expansion coefficients of the engobe and glazes are completely inadequate and out of the limit of acceptance for a good thermal coupling because they do not fulfil the safety values interval. The engobe is the ceramic body's next element and instead of having a lower thermal expansion than the ceramic body, it presents a higher value causing strain on the interface. In this way, the engobe is on traction in contact with the ceramic body and in contraction in contact with the glaze. This highly stressed situation causes the engobe and glaze collapse. Before buying an engobe or glazes for replicas, all the technical parameters must be known to make a good technical choice and only than the colour or aesthetical aspect must be considered.

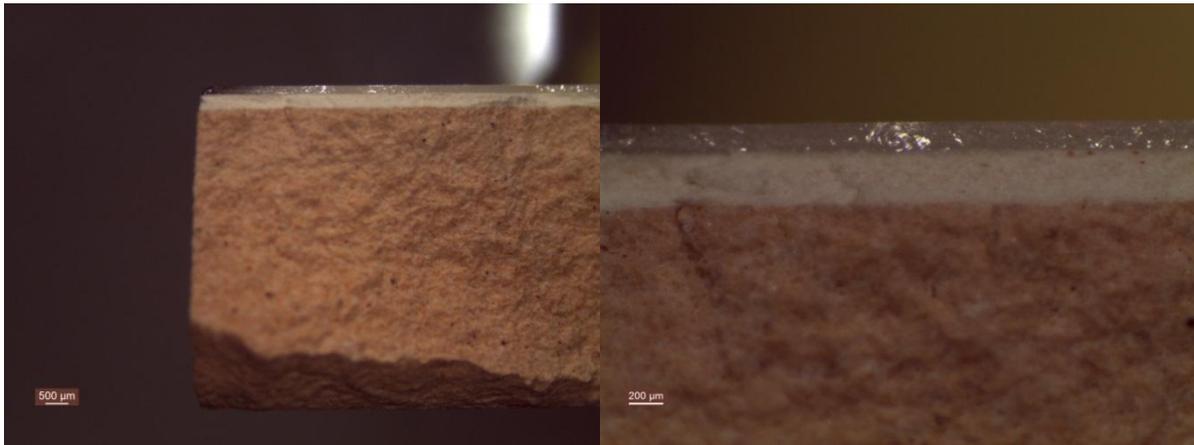


Figure 105 – Engobe and glaze thickness seen by optical microscope

In Figure 105 it can be clearly seen that in Sample 3 there is a larger amount of engobe than glaze, contributing to the development of stresses. When producing replicas in a restoration workshop where there is no optical microscope available, there is one very practical way, as an example, to see if the engobe and glaze quantities are in the correct proportion. The engobe and glaze slips must be prepared and two fired ceramic bodies must be used; one with a layer of engobe, and the other with a layer of glaze. The porosity of the ceramic body rapidly absorbs all the water of the mentioned slips allowing its manipulation. With a metallic flat instrument all the engobe and glaze attached to the fired ceramic body must be removed out and weighed. The weight of the engobe must be half of the glaze weight. For a practical example: a 30 x 30 tile must have 10 g of engobe and 20/22 g of glaze. When the relationship between engobe and glaze quantities are not correct, adjustments must be made in the glazing technique or in the slips' densities.

Modern solutions for ceramic body restoration tiles have to be carefully analysed as compatibility might not be assured only by a commercial label. Even the most traditional factories products have some technical important differences from the old tiles.

After an adequate ceramic body evaluation, the glazing technique and the glazes (including engobe when used) must be carefully chosen, attending to their thermal expansion coefficient and quantity to be applied. A good replica is not only a compatible and lookalike ceramic piece, but is also a piece without technical problems.

In the case of glazes for ceramic body replicas, their  $\alpha$  should be circa  $7.2E^{-6} \text{ } ^\circ\text{C}^{-1}$  for calcitic ceramic bodies and circa  $4.7E^{-6} \text{ } ^\circ\text{C}^{-1}$  considering the replicas ceramic bodies'  $\alpha$  found.

In the present work the search for a technical replica for the glaze was not done because it would take more time than the possible to conclude the present thesis. It is thought that finding glaze replica for the ceramic body replica would be a very interesting work for the future, as well as studying the found couple to all sorts of weathering. Perhaps precious learning would come out for a better interpretation of the ancient tiles pathology.

## References

Aiazzi, F. e. G. (1988). Tecnologia Ceramica. La Stoviglieria. Editora Faenza. Italia.

Alaimo, R., G. Bultrini and G. Montana (2004). "Microchemical and microstructural characterization of medieval and post-medieval ceramic glaze coating." Applied Physics A 79: 263-272.

Albero, J. L. A., V. B. Porcar, A. B. Fuentes and J. E. E. Navarro (1991). Defectos de Fabricación de Pavimentos y Revestimientos Cerámicos. Instituto Cerâmico de Valencia. Espanha

Aleluia, Fábrica (1955). História da Fábrica Aleluia - 1905 – 1955. Fábrica Aleluia. Aveiro

Amadori, M. L. and L. Ruffinelli (2009). Azulejos: historical-technical notes and conservation problems. International seminar "conservation of glazed ceramic tiles. Research and practice". Laboratório Nacional de Engenharia Civil. Lisboa.

Aveiro, Museu da Cidade (2008). "15x15" Aveiro - a essência colorida do azulejo. Câmara Municipal de Aveiro.

Azulejo, Museu do. (2012). "<http://mnazulejo.imc-ip.pt/Data/Documents/Cronologia%20do%20Azulejo%20em%20Portugal.pdf>." Retrieved Novembro 2012.

B.J.Smith, P.A.Warke, J.P.McGreevy and H.L.Kane (2004). "Salt-weathering simulation under hot desert conditions: agents of enlightenment or perpetrators of preconceptions?" Geomorphology 67: 211-227.

Baccour, H. a. a. (2009). "Influence of firing temperature on ceramic properties of Triassic clays from Tunisia." Journal of Materials Processing Technology: 2812-2817.

Belgaied, J. E. (2003). "Release of heavy metals from Tunisian traditional earthenware." Food and Chemical Toxicology 41: 95 - 98.

Benedetto, G. E. D., R.Laviano, L.Sabbatini and P.G.Zambonin (2002). "Infrared spectroscopy in the mineralogical characterization of ancient pottery." Journal of Cultural Heritage 3: 177-186.

Botas, S., R. Veiga and A. Velosa (2012) "Mecanismos de aderência na interface azulejo/argamassa." [www.apfac.pt/congresso2012/comunicacoes/Paper%2018\\_2012](http://www.apfac.pt/congresso2012/comunicacoes/Paper%2018_2012).

Botas, S. M. d. S. (2009). Avaliação do Comportamento de Argamassas em Climats Frios. Master. Universidade Nova de Lisboa.

Botas, S. M. S., M. R. S. Veiga and A. L. Velosa (2012). "Reapplication mortars for old tiles: characteristics of tiles and mortars and selection criteria." International Journal of Architectural Heritage. Accepted author version.

Bulens, M., A. Leonard and B. Delmon (1978). "Spectroscopic Investigations of the kaolinite-mulite reaction sequence." Journal of American Ceramic Society 61: 81-84.

Carvalho, Maria Arlete (2002). Expansão por humidade de materiais cerâmicos de construção. Master. Universidade de Aveiro.

Casal Moura, A., C. Carvalho and I. A. Almeida (2007). Mármore e Calcários ornamentais de Portugal. LNEG. Lisboa

Cavaquinho, Fábrica (1999). "[http://www.portoxxi.com/cultura/ver\\_folha.php?id=19](http://www.portoxxi.com/cultura/ver_folha.php?id=19)." Retrieved Fevereiro 2011.

Cazalla, O., C. Rodriguez-Navarro and G. Cultrone (2000). "Aging of lime putty: Effects on traditional lime mortar carbonation." Journal of American Ceramic Society 83: 1070-1076.

Charnoz, I. m. P. (2010). "<http://vents dumorvan.org/pdfs/pdfs/vdm-0773.pdf>." Retrieved Janeiro 2011.

Chatterji, S. (2000). "A discussion of the paper "Crystallization in pores" by G.W. Scherer." Cement and concrete research 30: 669-671.

Chatterji, S. (2005). "Aspects of generation of destructive crystal growth pressure." Journal of crystal growth 277: 566-577.

- Coelho, A. M. S. (2006). Depósitos de caulino associados a faixas de fracturação: Geologia, morfotectónica e georecurso. Master. Universidade de Aveiro.
- Coentro, S., J. Mimoso and V. S. F. Muralha (2012). "Multy-analytical identification of pigments and pigments mixtures used in 17th century Portuguese azulejos." Journal of the European Ceramic Society 32: 37 - 48.
- Coentro, S. X. (2011). Estudo da camada pictórica na azulejaria portuguesa do século XVII. Mestrado. Laboratório Nacional de Engenharia Civil. Lisboa
- Coentro, S. X., J. M. Mimoso and A. S. Silva (2010). Investigação da morfologia da interface vidro/chacota em azulejos históricos. Laboratório Nacional de Engenharia Civil. Lisboa
- Cordeiro, J. M. L. (1996). As fábricas portuenses e a produção de azulejos de fachada (Sécs.XIX-XX), Divisão de Património Cultural.
- Cultrone, G., E. Sebastián and C. Rodriguez-Navarro (2004). "Influence of Mineralogy and Firing Temperature on the Porosity of Bricks." Journal of European Ceramic Society 24: 547-564.
- Dias, Teresa Claudio Diaz Gonçalves Enes (2007). Salt crystallization in plastered or rendered walls. Master. Instituto Superior Técnico de Lisboa
- Domingues, Ana Portela (2003). António Almeida da Costa e a Fábrica de Cerâmica das Devesas. Master. Universidade do Porto.
- E.Molina, G.Cultrone, E.Sebastián and F.J.Alonso (2011). "The Pore System of Sedimentary Rocks as a Key Factor in the Durability of Building Materials." Engineering Geology 118: 110-121.
- Elert, K., C. Rodrigues-Navarro, E. S. Pardo, E. Hansen and O. Cazalla (2002). "Lime mortars for the conservation of historic buildings." Studies in conservation 47: 62-75.
- Espinosa, R. M., L. Franke and G. Deckelmann (2008). "Model for mechanical stress due to the salt crystallization in porous materials." Construction and Building Materials 22: 1350-1367.
- Facincani, E. (1993). Tecnologia Ceramica. Los ladrillos. Faenza Editrice Iberica S.L. Italia.

Faria, Maria Paulina (2004). Argamassas de revestimento para alvenarias antigas. Contribuição para o estudo da influência do ligante. Doutoramento. Universidade Nova de Lisboa.

Fernandes, H. A. G. (2012). Development of lithium disilicates based glass-ceramics. Doutoramento. Universidade de Aveiro.

Fernandes, Isabel M. (2008). A Fábrica de Louça de Miragaia. Instituto dos Museus e da Conservação. Lisboa.

Ferreira, L. M. (2009). O azulejo na arquitectura da cidade do Porto [1850 - 1920]. Caracterização e intervenção. Doutoramento. Universidade do País Vasco.

Ferreira, Maria Isabel. (2009). Azulejos tradicionais de fachada em Ovar contributos para metodologia de conservação e restauro. Camara Municipal de Ovar.

Figueiredo, M. O., J. P. Veiga, T. P. Silva, J. P. Mirao and S. Pascarelli (2005). "Chemistry versus phase constitution of yellow ancient tile glazes: A non-destructive insight through XAS." Nuclear Instruments & Methods in Physics Research Section B-Beam Interactions with Materials and Atoms 238(1-4): 134-137.

Flatt, R. J. (2002). "Salt damage in porous materials: how high supersaturation are generated". Journal of crystal growth 242: 435-454.

Fonseca, António Tomás (2000). Tecnologia do processamento cerâmico. Universidade Aberta. Lisboa.

Froberg, L., T. Kronberg, L. Hupa and M. Hupa (2007). "Influence of firing parameters on phase composition of raw glazes." Journal of the European Ceramic Society 27: 1671-1675.

Fábricas, C. <http://paginas.fe.up.pt/porto-ol/mlr/index.html> - Consultado em Novembro 2011.

Garcia-Heras, M., N. Carmona, A. Ruiz-Conde, P. Sanchez-Soto and J. J. Benitez (2005). "Application of atomic force microscopy to the study of glass decay." Materials Characterization 55(4-5): 272-280.

GmbH, Netzsch-Geratebau (2005). "Improving zircónia ceramics through thermoanalytical characterization." <http://www.netzsch-thermal->

[analysis.com/en/searchresults.html?tx\\_solr%5Bq%5D=improving+zirconia+ceramics](http://analysis.com/en/searchresults.html?tx_solr%5Bq%5D=improving+zirconia+ceramics)

Retrieved May 2013.

Gomes, C. (1986). Argilas o que são e para que servem. Fundação Calouste Gulbenkian. Lisboa

Gomes, C. (2002). Argilas - aplicação na indústria. Dinterna. Lisboa

Gomes, C. F. (1979). Raios X no estudo de materiais. Universidade de Aveiro.

Gomes, Jim Robert Puga (2011). Exemplos da Azulejaria dos Séculos XVI e XVII em Coimbra. Master, Universidade de Coimbra.

Guilherme, A., J. Coroado and M. L. Carvalho (2011). "X-ray fluorescence (conventional and 3D) and scanning electron microscopy for the investigation of Portuguese polychrome glazed ceramics:Advances in the knowledge of the manufacturing techniques." Spectrochimica Acta Part B. 66(5): 297-307.

Harvey, W. (2010). "A Brief History of Transfer Printed Tiles." Retrieved Fevereiro 2011.

Houst, Y. F. and F. H. Wittmann (2002). "Depth profiles carbonates formed during natural carbonation." Cement and concrete research 32: 1923-1930.

Konta, J. (1995). "Clay and man: Clay raw materials in the service of man." Applied Clay Science 10: 275 - 335.

Kopar, T., Ducman, Vilma (2007). "Low-vacuum SEM analyses of ceramic tiles with emphasis on glaze defects characterisation." Materials characterization 58: 1133-1137.

La Iglesia, A., V. González, V. López-acevedo and C. Viedma (1997). "Salt crystallization in porous construction materials I. Estimation of crystallization pressure." Journal of Crystal Growth 177: 111-118.

Lee, S., Y. J. Kim and H.-S. Moon (1999). "Phase Transformation Sequence from Kaolinite to Mullite Investigated by an Energy-Filtering Transmission Electron Microscope." Journal American Ceramic Society 82: 2841-2848.

Lepierre, C. (1899). Estudo chimico e technologico sobre cerâmica portugueza moderna. Imprensa nacional. Lisboa

Leão, M. (1999). A cerâmica em Vila Nova de Gaia. Editora Manuel Leão. Gaia

Lima, R. M. F. and J. A. M. Luz (2001). Análise granulométrica por técnicas que se baseiam na sedimentação gravitacional: Lei de Stokes. Revista Escola de Minas. Ouro Preto - Brasil, Scielo Brasil. 54, nº2.

Linnow, K., L. Halsberghe and M. Steiger (2006). "Analysis of calcium acetate efflorescences formed on ceramic tiles in a museum environment." Journal of Cultural Heritage 8: 44-52.

Linnow, K. and M. Steiger (2007). "Determination of equilibrium humidities using temperature and humidity controlled X-ray diffraction (RH-XRD)." Analytica Chimica Acta 583: 197-201.

Lubelli, B., T. G. Nijland and R. P. J. Hees (2010). "Self-healing of lime based mortars: microscopy observations on case studies." Netherlands

López-Azevedo, V., C. Viedma, V. Gonzales and A. La Iglesia (1997). "Salt crystallization in porous construction materials II. Mass transport and crystallization processes." Journal of Crystal Growth 182: 103-110.

M.M.Jordán, A. Boix, T.Sanfeliu and C. d. l. Fuente (1999). "Firing transformations of cretaceous clay used in manufacturing of ceramic tiles." Applied Clay Science 14: 225-234.

M.P.Riccardi, B.Messiga and P.Duminuco (1999). "An approach to the dynamics of clay firing." Applied Clay Science 15: 393-409.

M.S.Tite (2009). "The production technology of Italian maiolica: a reassessment." Journal of Archaeological Science 36: 2065-2080.

Magalhães, A. C. (2002). "Patologia de Rebocos Antigos." Caderno de Edifícios - LNEC 2.

Materials, T. A. S. f. t. (1945). C162 - Compilation of ASTM Standard Definitions. Philadelphia.

Micrometrics (1995). SediGraph 5100. Operation manual. Micrometrics.

- Mimoso, J. M. (2011). A research on manufacturing defects and decay by glaze loss in historical Portuguese azulejos. Laboratório Nacional de Engenharia Civil. Lisboa
- Mimoso, J. M. and L. Esteves (2011). Vocabulário Ilustrado da Degradação dos Azulejos Históricos, Laboratório Nacional de Engenharia Civil. Lisboa
- Molera, J., T. Pradell, N. Salvadó and M. Vendrell-Saz (2001). "Interactions between clay bodies and lead glazes." Journal of American Society 84: 1120-1128.
- Molera, J. and M. Vendrell-Saz (2001). "Chemical and Textural Characterization of Tin Glaze in Islamic Ceramics from Eastern Spain." Journal of Archaeological Science 28: 331-340.
- Molera, J. e. a. (1999). "Evidence of Tin Oxide Recrystallization in Opacified Lead Glazes." Journal of American Ceramic Society 82: 2871-2875.
- Monteiro, D. M. P. (2012). Ensaio de Envelhecimento a Sistemas Azulejares de Fachada. Master, Universidade de Aveiro.
- Nakamoto, K. (1970). Infrared Spectra of Inorganic and Coordination Compounds. New York.
- Navarro, J. M. (1991). El Vidrio. Fundación Centro Nacional del Vidrio. Madrid
- Padill, R., O. Schalm, K. Janssens and P. Van Espen (2005). "Microanalytical characterization of surface decoration in Majolica pottery." Analytica Chimica Acta 535: 201-211.
- Pardo, F. and e. al (2011). "Firing transformations of Chilean clays for manufacture of ceramic tile bodies." Applied Clay Science 51: 147-150.
- Pereira, S. M. (2011). Physical-chemical characterization of historic portuguese tiles. Laboratório Nacional de Engenharia Civil. Lisboa
- Pereira, Tiago André Reis (2008). Optimização das Características de Humedecimento e Secagem de Argamassas. Master, Universidade Nova de Lisboa.
- Portela, Ana Margarida (2004). "Devesas:As origens históricas da fábrica de cerâmica que mais marcou as fachadas de Ovar." Dunas 4: 61-72.

Prikryl, R., T. Lokajíček and Z. Weishauptová (2003). "Experimental weathering of marlstone from Prední Kopanina (Czech Republic)-historical building stone of Prague." Building and Environment 38: 1163-1171.

Prostes, P. (1907). Indústria Cerâmica. Livrarias Aillaud et Bertrand. Paris.

Qualidade, Instituto Português (2004). EN ISO 10545-3. Determination of water absorption of open porosity 10545-3.

Pereira, R.M. and J. Mimoso (2012). Salt degradation of historic Portuguese azulejos. Congresso Internacional Azulejar- Conservação de revestimentos azulejares em fachadas. Universidade de Aveiro.

Renau, R. G. (1994). Pastas y Vidriados en la fabricación de pavimentos y revestimientos cerámicos. Faenza Editrice Ibérica, S.L. Spain

Rigaku SuperQ Version 3.0 Reference Manual - XRD Theory, Rigaku.

Rigby, S. and K. Edler (2002). "The influence of mercury contact angle, surface tension, and retraction mechanism on the interpretation of mercury porosimetry data." Journal of Colloid and Interface Science 250: 175-190.

S.A.El-Defrawi, M.A.Serry and W.Weisweiler (1995). "Microchemistry and Microstructure of some glaze/tile interface in relation to their physical properties." Ceramics International 21: 69-75.

Sacavém, Museu (2009). Porta aberta às memórias. Sacavém

Sanjad, T., A. Rômulo Simões, M. Mendonça de Oliveira and W. A. d. M. Costa (2004). "Caracterização mineralógica de azulejos de Salvador e Belém dos séculos XVI, XVII e XIX." Revista Esc. Minas 57(4).

Santos, T. P., F. Vaz, M. Pinto and A. P. Carvalho (2012). "Porosity characterization of old Portuguese ceramic tiles." Construction and Building Materials 28: 104-110.

Scherer, G. W. (1999). "Crystallization in pores." Cement and concrete research 29: 1347-1358.

Scherer, G. W. (2000). "Reply to the discussion by S.Chatterji of the paper "Chrytallization in pores"." Cement and concrete research(30): 673-675.

Scherer, G. W. (2004). "Stress from crystallization of salts." Cement and concrete research 34: 1613-1624.

Segadães, A. M., M. A. Carvalho and H. C. Ferreira (2003). "Using phase diagrams to deal with moisture expansion." Ceramics International 29: 947-954.

Senna, J. (2008). "Characterization of clays used in ceramic manufacturing industry by reflectance spectroscopy: an experiment in the São Simão ball-clay deposit, Brazil." Applied Clay Science 41(2-1): 85-98.

Silva, C. P., Silva, M. F. and Angelica, R. S (2006). Azulejos históricos europeus produzidos no final do século XIX e início do século XX: caracterização mineralógica e química de biscoitos. XVII seminário de iniciação científica da UFPA. Brasil.

Sintra, Palácio Nacional (2013). "<http://pnsintra.imc-ip.pt/pt-PT/palacio/azulejos/ContentDetail.aspx>." Retrieved Janeiro 2011.

Soeiro, T., J. F. Alves, S. Lacerda and J. Oliveira (1995). A Cerâmica Portuense - Evolução Empresarial e Estruturas Edificadas. Portugalia.  
<http://ler.letras.up.pt/uploads/ficheiros/3834.pdf>. 16: 203 - 287.

Tabelas, p. c. (2010). "<http://betserpi-seguridadcontraincendio2.blogspot.pt/2010/06/materiales-solidos-poder-calorifico-en.html>." Retrieved Junho 2011.

Trindade, M. J. and e. al (2008). "Mineralogical transformations of calcareous rich clays with firing: A comparative study between calcite and dolomite rich clays from Algarve, Portugal." Applied Clay Science 42: 345-355.

Tschegg, C., T. Ntaflos and I. Hein (2009). "Thermally triggered two-stage reaction of carbonates and clay during ceramic firing-A case study on Bronze Age Cypriot ceramics." Applied Clay Science 43: 69-78.

Vasconcelos, Maria Cristina dos Santos (2008). Caulino: das origens às aplicações. Master. Universidade de Aveiro.

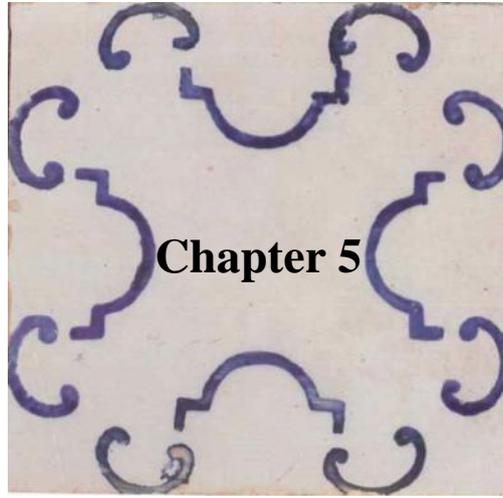
Veiga, R. and J. Aguiar (2002). "Revestimentos de paredes em edifícios antigos." Cadernos de edifícios - LNEC 2.

Velho, L., C. Gomes and C. Ramariz (1998). Minerais Industriais: geologia, propriedades, tratamentos, aplicações, especificações, produção e mercado. Universidade de Aveiro.

Veloso, A. J. d. B. (2009). Azulejos semi-industriais de fachada. I. Almasqué. Curso de história do azulejo, cinco séculos de presença em Portugal. Museu Nacional do Azulejo.

Viles, H. A. and A. S. Goudie (2007). "Rapid salt weathering in the coastal Namib desert: Implications for landscape development." Geomorphology 85: 49-62.





## **Conclusions**

---



## 5.1 Conclusions

The present work aimed at **developing ceramic bodies'** technical replicas **with physical and chemical characteristics similar to those of old ceramic bodies'**. The samples under study belong to the beginning of tile industrialization. They can easily be recognized from the tiles of former production periods, by their thickness (circa 9 mm while the tiles of previous century could reach 15 mm), by the fact that they are even, by the pressing moulds marks, by the greater homogeneity of the ceramic body (less impurities from the production process) and by the faster and reproducible decorative techniques which were used.

Twenty six different tile facades from Ovar were studied in order to perform a technical characterization of various samples. The studied tiles were removed from facades that undertook restoration processes due to their degraded condition. The samples were from A.A.Costa, J. Pereira Valente factories in the north of Portugal or unbranded tiles from unknown origin. Only one tile was from Sacavém production unit in the central region of Portugal. Ceramic body and glaze microstructure characterization were performed in order to determine constituent materials and create a scientific basis for tile replication.

The objectives proposed were achieved and important conclusions about the glazes were reached. Technical explanations about the quality of glaze ceramic body mechanical interaction were discussed and observations about the glaze/ceramic body interface were taken.

- **Characterization of ceramic bodies**

**For the ceramic bodies characterization the analytical techniques used were XRD, XRF, SEM, dilatometry, thermogravimetry, calcination tests, porosimetry, water absorption by immersion and water absorption due to capillary action. From the twenty six analysed tiles, twenty two were calcitic ceramic bodies and four were *pó de pedra*. XRD diffraction maxima of calcitic ceramic bodies results revealed that this kind of tiles are complex but have constant presence of six crystalline phases: quartz, mulite, anorthite, gehlenite, diopside and calcite. Two more phases appear randomly: portlandite and hematite. The complex mineralogical composition, together with the knowledge of the chemical elements of the calcitic bodies** leads to the belief that these bodies were probably produced with kaolinitic

clay (or a mixture of clay with kaolinite) quartz sand, calcite and talc, containing approximately 4% of iron oxide contamination and probable firing temperature between 1100°C and 1150°C. **These ceramic bodies have a large amount of pores between** 1µm and 0.05µm, 17.7 to 22.8% of water absorption percentage and 3.1 to 3.6 kg/(m<sup>2</sup>.h<sup>1/2</sup>) of water absorption coefficient due to capillarity action. Between all the calcitic samples no important differences could be found. There are normal fluctuations in the oxides' contents probably due to formula evolution, raw materials quality fluctuation or even due to formulation inaccuracy.

The studied *pó de pedra* ceramic bodies are very simple in XRD analysis as they only present three ceramic body crystalline phases: quartz, mullite and cristobalite. The ceramic body has larger pores than the calcitic tiles, presenting its modal value at 3.7 µm, a lower water absorption percentage (13.6%) and 2.6 kg/(m<sup>2</sup>.h<sup>1/2</sup>) of water absorption due to capillarity action, showing that these kind of ceramic bodies are completely different from the calcitic not only in what crystalline phases concerns but also in terms of water behaviour.

*Pó de pedra* tiles analyses were from J. Pereira and Sacavém production units. From XRF values it can be said that there is some similarity between them. The big difference between them may be seen in XRD. While in Sacavém's sample only mullite is present as high temperature phase, in J. Pereira's samples cristobalite and mullite diffraction maxima are present and more intense. From these results, it can be said that J.Pereira firing temperature of this type of tile was higher than Sacavém's.

It is known that J. Pereira Valente was a former A.A.Costa employee that built his own production unit. This means that J. Pereira Valente's calcitic ceramic bodies formulas were probably A.A.Costa state of the art at the time Valente left the factory, as one cannot see any noticeable difference between J. Pereira Valente and many of A.A.Costa calcitic ceramic bodies' tiles. The only difference that can be seen is a higher percentage of MgO in some of A.A.Costa tiles. Assuming it is true that J. Valente replicated the latest formula known by him as an A.A.Costa collaborator, it can be said that the content in MgO in A.A.Costa ceramic bodies formula decreased with time from at least 6.5% to 2.7%, taking into account the studied samples. Technically it is normal to accept that MgO content decreased with technical advance as talc is a very difficult raw material to work with due to its difficult mixing with other raw materials.

- Characterization of glazes

The glaze analyses were made by SEM/EDS and optical microscope. As expected for this kind of old tiles, all the analysed glazes are lead glazes. From all the samples, 19.2% are lead and tin glazes (opaque) with thicknesses ranging from 200 to 450  $\mu\text{m}$ . All the rest of the studied glazes are transparent lead glazes without engobe (23.1%) or with engobe (57.7%). The latter present a thickness of 100 to 200  $\mu\text{m}$  for the engobe and 200 to 300  $\mu\text{m}$  for the transparent glaze underneath. In the studied samples, the only glazes presenting no crazing were the lead/tin glazes revealing a good technical match. Crazing problems seem to have begun with the utilization of transparent glazes. In terms of chemical elements transparent glazes have more potassium and lead, but less calcium, sodium, aluminium and silica.

- Causes of tile pathology – crazing and glaze detachment

With the present study it was possible to formulate a technical explanation for the usual crazing in *pó de pedra* tiles, which was attributed to thermal expansion coefficient of the glaze and the ceramic bodies' incompatibility. Although only four *pó de pedra* samples were lab tested, many facades with *pó de pedra* tiles were observed and all tiles presented glaze crazing, revealing how common the problem is. The study of this technical flaw may give indications on technical difficulties of past production methods and techniques.

The lower use of *pó de pedra* tiles in facades is apparently controversial as *pó de pedra* should be a cheaper tile as the very expensive tin oxide was not needed in its glaze. The fact that few *pó de pedra* tiles were in fact used may be linked to two factors: lack of mastery of this production technique which presented some important flaws, such as glaze crazing, or unexpected high production costs due to the raw materials purity and higher firing temperature needed.

During the samples microstructure study by SEM/EDS, the question of how thick the glaze/ceramic body interface should be to assure the tile endurance to glaze detachment was raised.

The present work allowed a very interesting observation made by analysing glaze/ceramic body interfaces showing that tiles with no observed interface can withstand in facades for tens of years demonstrating no special fragility when compared with tiles with measurable and significant interfaces. The big difference, however, is noticeable when

restoration processes are needed, like glaze stabilization in tiles with some glaze detachment. In this case, the glaze easy “peel off” is a challenge to who has the restoration responsibility.

These results reveal that glaze detachment must be linked with other technical aspects than glaze/ceramic body interface thickness.

In pursuit of the possible technical glaze detachment causes in the studied samples by XRD, FTIR and SEM/EDS evidences point out that the main determinant factor are volume and pore size of the ceramic body. The higher the open porosity and its volume, the greater the capacity of the ceramic body to be filled by saline solutions from the water that rises through the structure of the building and passes through the materials that are beneath the tile. When the saline solution reaches its saturation point the porous network provides cristalization conditions, formation of salt crystals occurs; with time great quantities of salt are disseminated through the ceramic body, promoting destructive stresses.

In the analysed samples facts point out that portlandite/calcite salts from the mortar, are one of the responsible salts for glaze and ceramic body structure degradation.

- Execution of ceramic body replicas

For the replicas’ investigation, portuguese raw materials were selected considering geological proximity to the studied ancient production center or due to their comercial accessibility and ability for ceramic industry utilization. Replicas’ production process was performed with the techniques believed to be used in the past, although their firing was made in electrical furnace instead of flame firing.

Calcitic ceramic bodies’ replicas were achieved using 33% of ball clay, 11% of kaolin, 10% of quartz sand, 35% of lime and 11% of talc, with the composite mixture with modal diameter of 4  $\mu\text{m}$ . The pressure used to make samples was 546 bar, and they were fired in a 19h 30min heating curve with 1120° C ring temperature.

Technical replicas of the *pó de pedra* tiles were achieved with a mixture of 58.5% of kaolin and 41.5% of quartz sand. The raw materials were ground until 6  $\mu\text{m}$  of modal diameter particle size and the mixture was pressed at 780 bars. The sintering of the ceramic bodies was carried out at 1210° C at a heating rate of 1° C/minute, with a 2 hours soaking at maximum temperature (1235° C ring temperature).

## 5.2 Future work

To enable deeper knowledge on 19<sup>th</sup> century tiles a vast universe of different production units and production regions should be considered for study, as there is lack of written information left by the tile producers or scholars of the time. As future work, the technical characterization of tiles that becomes available through restoration processes or demolitions, from all Portuguese production units from the beginning of the industrialization period, is an ambitious but possible aim.

Glaze replicas should also be made so as to together with the ceramic body replicas, be studied by weathering tests. Probably some questions on decay problems could be answered.

Some technical aspects should be carefully studied, as the difficulty in consolidating the glaze in tiles with no measurable glaze/ceramic body interface, the behaviour of the replicas applied in facades and a study of tile ageing versus its porosity.